

## Technical Report Documentation Page

**1. REPORT No.**

632100

**2. GOVERNMENT ACCESSION No.****3. RECIPIENT'S CATALOG No.****4. TITLE AND SUBTITLE**

Secondary Compression In Embankment Foundations

**5. REPORT DATE**

July 1971

**6. PERFORMING ORGANIZATION****7. AUTHOR(S)**

Su, Hon-Hsieh and Prysock, R.H.

**8. PERFORMING ORGANIZATION REPORT No.**

632100

**9. PERFORMING ORGANIZATION NAME AND ADDRESS**

State of California  
Department of Public Works  
Division of Highways  
Materials and Research Department

**10. WORK UNIT No.****11. CONTRACT OR GRANT No.****12. SPONSORING AGENCY NAME AND ADDRESS****13. TYPE OF REPORT & PERIOD COVERED**

Final Report

**14. SPONSORING AGENCY CODE****15. SUPPLEMENTARY NOTES****16. ABSTRACT**

Long Term settlements of highway embankments due to secondary compression in compression foundation soils are investigated. Laboratory consideration tests are performed and field settlement data are reviewed. In the laboratory investigation, it is found that the rate of secondary compression is independent of void ratio or pressure-increment ratio in a normally consolidated clay and is greatly reduced in an over-consolidated clay. Modified theories of consolidation considering both primary and secondary compressions are studied for their applicability in settlement analysis. It is found that the applicability of these methods in predicting the field time-- settlement relationship depends solely on how closely the field loading conditions are simulated in the laboratory. Comparisons of field settlement data and laboratory consolidation data indicate that an accurate evaluation of field conditions is as important as, if not more than, the choice of method of settlement analysis. However, it is found that the rate of settlement due to secondary compression may be predicted from laboratory study. A close reproduction of field loading conditions is required to predict the overall time-settlement relationship including both primary and secondary compressions.

**17. KEYWORDS**

Secondary compression, primary compression, consolidation, settlement, rate of settlement, pressure-increment ratio, normally consolidated clay, overconsolidated clay, peat, Bay mud, embankment foundation

**18. No. OF PAGES:**

164

**19. DRI WEBSITE LINK**

<http://www.dot.ca.gov/hq/research/researchreports/1971/71-12.pdf>

**20. FILE NAME**

71-12.pdf

# HIGHWAY RESEARCH REPORT

## SECONDARY COMPRESSION IN EMBANKMENT FOUNDATIONS

71-12

**STATE OF CALIFORNIA**

**BUSINESS AND TRANSPORTATION AGENCY**

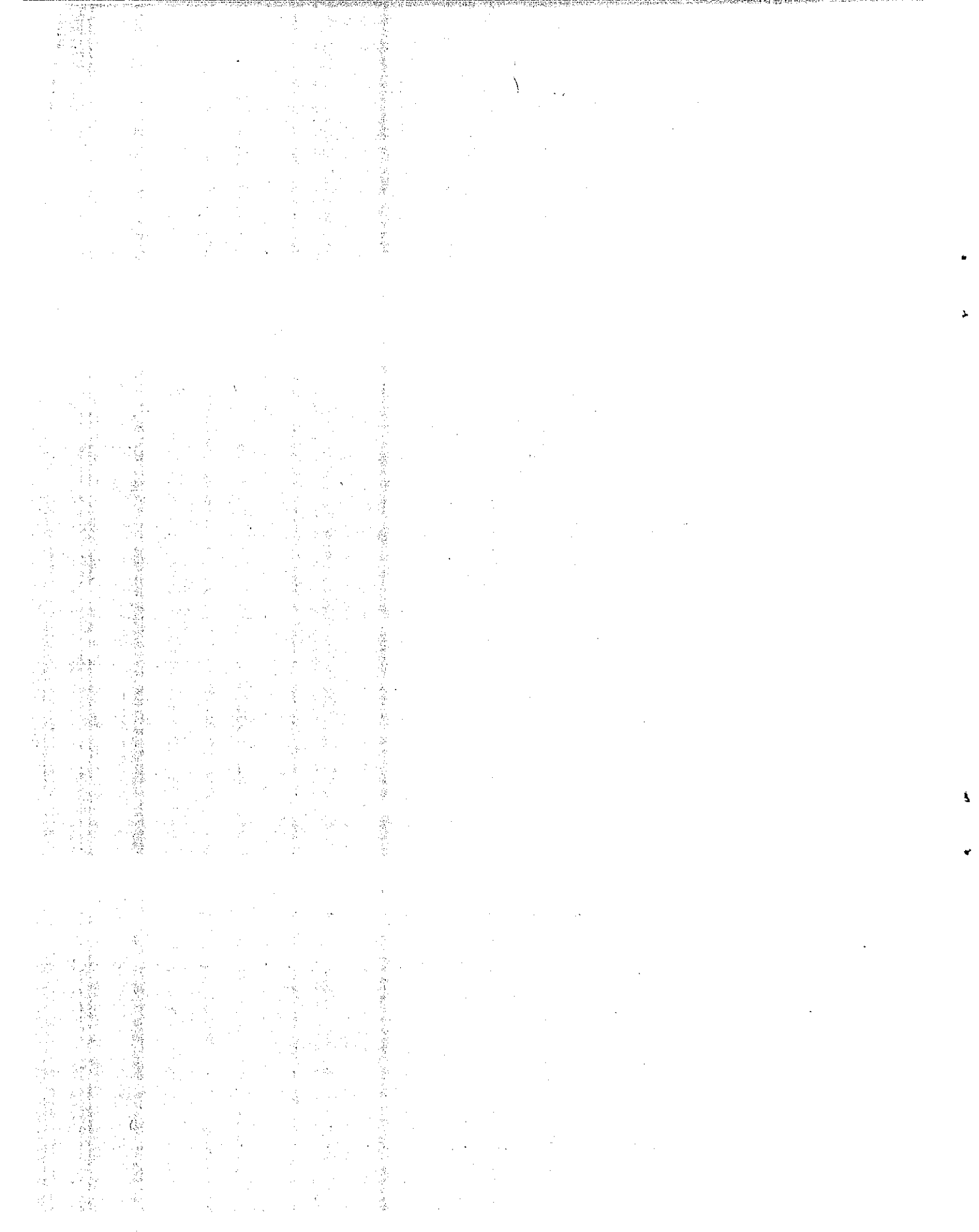
**DEPARTMENT OF PUBLIC WORKS**

**DIVISION OF HIGHWAYS**

**MATERIALS AND RESEARCH DEPARTMENT**

**RESEARCH REPORT**

**NO. M & R 632100**



DEPARTMENT OF PUBLIC WORKS

**DIVISION OF HIGHWAYS**

MATERIALS AND RESEARCH DEPARTMENT  
5900 FOLSOM BLVD., SACRAMENTO 95819



July 1971  
Final Report  
M & R No. 632100

Mr. J. A. Legarra  
State Highway Engineer

Dear Sir:

Submitted herewith is a research report titled:

SECONDARY COMPRESSION

IN

EMBANKMENT FOUNDATIONS

Report by

HON-HSIEH SU  
Associate Professor of Civil Engineering  
Sacramento State College

And

R. H. PRYSOCK  
Associate Materials and Research Engineer

Very truly yours,

A handwritten signature in cursive script, appearing to read "John L. Beaton".

JOHN L. BEATON  
Materials and Research Engineer

1944

1945

1946

1947

1948

1949

1950

1951

1952

1953

1954

1955

1956

1957

1958

1959

1960

1961

1962

1963

1964

1965

1966

1967

1968

1969

1970

1971

1972

1973

1974

1975

1976

1977

1978

1979

1980

1981

1982

1983

1984

1985

1986

1987

1988

1989

1990

1991

1992

1993

1994

1995

1996

1997

1998

1999

2000

2001

2002

2003

2004

2005

2006

2007

2008

2009

2010

2011

2012

2013

2014

2015

2016

2017

2018

2019

2020

2021

2022

2023

2024

2025

1926

1927

1928

1929

1930

1931

1932

1933

1934

1935

1936

1937

1938

1939

1940

1941

1942

1943

1944

1945

1946

1947

1948

1949

1950

1951

1952

1953

1954

1955

1956

1957

1958

1959

1960

1961

1962

1963

1964

1965

1966

1967

1968

1969

1970

1971

1972

1973

1974

1975

1976

1977

1978

1979

1980

1981

1982

1983

1984

1985

1986

1987

1988

1989

1990

1991

1992

1993

1994

1995

1996

1997

1998

1999

2000

2001

2002

2003

2004

2005

2006

2007

2008

2009

2010

2011

2012

2013

2014

2015

2016

2017

2018

2019

2020

2021

2022

2023

2024

2025

1906

1907

1908

1909

1910

1911

1912

1913

1914

1915

1916

1917

1918

1919

1920

1921

1922

1923

1924

1925

1926

1927

1928

1929

1930

1931

1932

1933

1934

1935

1936

1937

1938

1939

1940

1941

1942

1943

1944

1945

1946

1947

1948

1949

1950

1951

1952

1953

1954

1955

1956

1957

1958

1959

1960

1961

1962

1963

1964

1965

1966

1967

1968

1969

1970

1971

1972

1973

1974

1975

1976

1977

1978

1979

1980

1981

1982

1983

1984

1985

1986

1987

1988

1989

1990

1991

1992

1993

1994

1995

1996

1997

1998

1999

2000

2001

2002

2003

2004

2005

2006

2007

2008

2009

2010

2011

2012

2013

2014

2015

2016

2017

2018

2019

2020

2021

2022

2023

2024

2025

REFERENCE: Su, Hon-Hsieh and Prysock, R. H., "Secondary Compression in Embankment Foundations," State of California, Department of Public Works, Division of Highways, Materials and Research Department, Research Report No. 632100, July 1971.

ABSTRACT: Long Term settlements of highway embankments due to secondary compression in compressible foundation soils are investigated. Laboratory consolidation tests are performed and field settlement data are reviewed. In the laboratory investigation, it is found that the rate of secondary compression is independent of void ratio or pressure-increment ratio in a normally consolidated clay and is greatly reduced in an overconsolidated clay. Modified theories of consolidation considering both primary and secondary compressions are studied for their applicability in settlement analysis. It is found that the applicability of these methods in predicting the field time-settlement relationship depends solely on how closely the field loading conditions are simulated in the laboratory. Comparisons of field settlement data and laboratory consolidation data indicate that an accurate evaluation of field conditions is as important as, if not more than, the choice of method of settlement analysis. However, it is found that the rate of settlement due to secondary compression may be predicted from laboratory study. A close reproduction of field loading conditions is required to predict the overall time-settlement relationship including both primary and secondary compressions.

KEY WORDS: Secondary compression, primary compression, consolidation, settlement, rate of settlement, pressure-increment ratio, normally consolidated clay, overconsolidated clay, peat, Bay mud, embankment foundation.

... ..  
... ..  
... ..

... ..  
... ..  
... ..  
... ..  
... ..

... ..  
... ..  
... ..  
... ..

... ..  
... ..  
... ..  
... ..  
... ..

... ..  
... ..  
... ..  
... ..  
... ..

... ..  
... ..  
... ..  
... ..

... ..  
... ..  
... ..  
... ..

... ..  
... ..  
... ..  
... ..

... ..  
... ..  
... ..

## ACKNOWLEDGEMENTS

The writers wish to extend thanks to T. W. Smith, under whose general supervision this research project was carried out; W. F. Kleiman and B. Zeiler who supplied field data; D. S. Onodera and Darrell Knight who performed and supervised the laboratory testing; R. A. Anderson for his assistance in obtaining reference materials, and to N. Morikawa for his help in computer analysis.

The work reported herein was authorized under the work program HPR-1(7), D-3-35, in cooperation with the Federal Highway Administration, U.S. Department of Transportation.

The opinions, findings, and conclusions expressed in this publication are those of the authors and not necessarily those of the Federal Highway Administration.

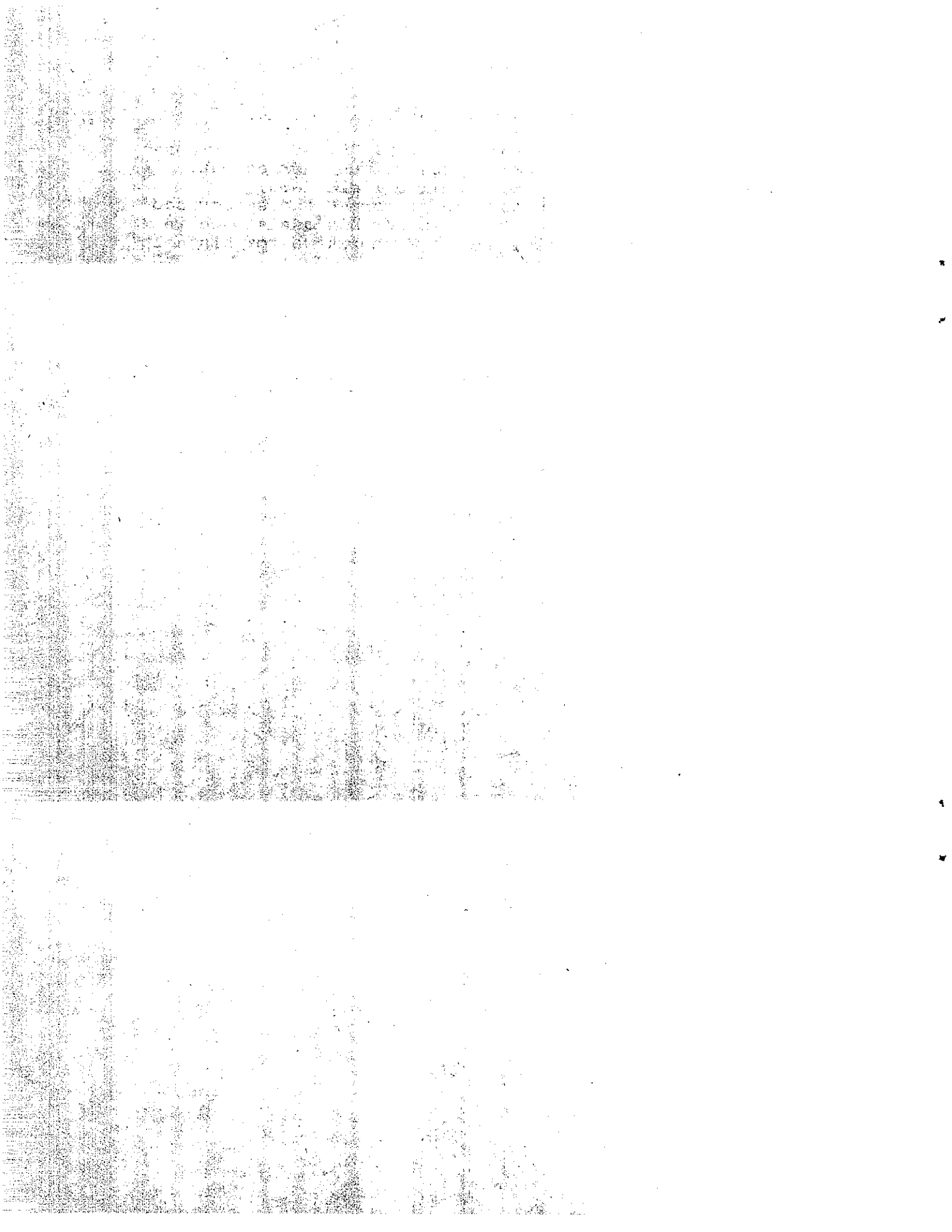


## TABLE OF CONTENTS

|                                                          | <u>Page</u> |
|----------------------------------------------------------|-------------|
| ABSTRACT -----                                           | i           |
| ACKNOWLEDGEMENTS -----                                   | ii          |
| TABLE OF CONTENTS                                        |             |
| List of Figures                                          |             |
| List of Tables                                           |             |
| Chapter 1 INTRODUCTION -----                             | 1           |
| Chapter 2 CONCLUSIONS AND IMPLEMENTATION -----           | 4           |
| Chapter 3 REVIEW OF LITERATURE -----                     | 7           |
| Chapter 4 LABORATORY INVESTIGATION -----                 | 11          |
| 4.1. Definitions -----                                   | 11          |
| 4.2. Testing Program -----                               | 13          |
| 4.3. Analysis of Test Results -----                      | 14          |
| 4.3.1 The Time-Compression Relationship -----            | 14          |
| 4.3.2 Coefficient of Secondary Compression -----         | 14          |
| 4.3.3 Effect of Overconsolidation Ratio -----            | 15          |
| 4.3.4 Effect of Pressure - Increment Ratio -----         | 15          |
| 4.4. Summary -----                                       | 17          |
| Chapter 5 METHODS OF SETTLEMENT CALCULATION -----        | 18          |
| 5.1. Settlement by Terzaghi's Theory -----               | 18          |
| 5.1.1 Magnitude of Settlement -----                      | 18          |
| 5.1.2 Rate of Settlement -----                           | 20          |
| 5.2. Some Refined Methods of Time-Settlement Calculation | 21          |
| 5.2.1 Wahls' Method -----                                | 22          |
| 5.2.2 Hansen's Method -----                              | 23          |
| 5.3. Summary -----                                       | 24          |

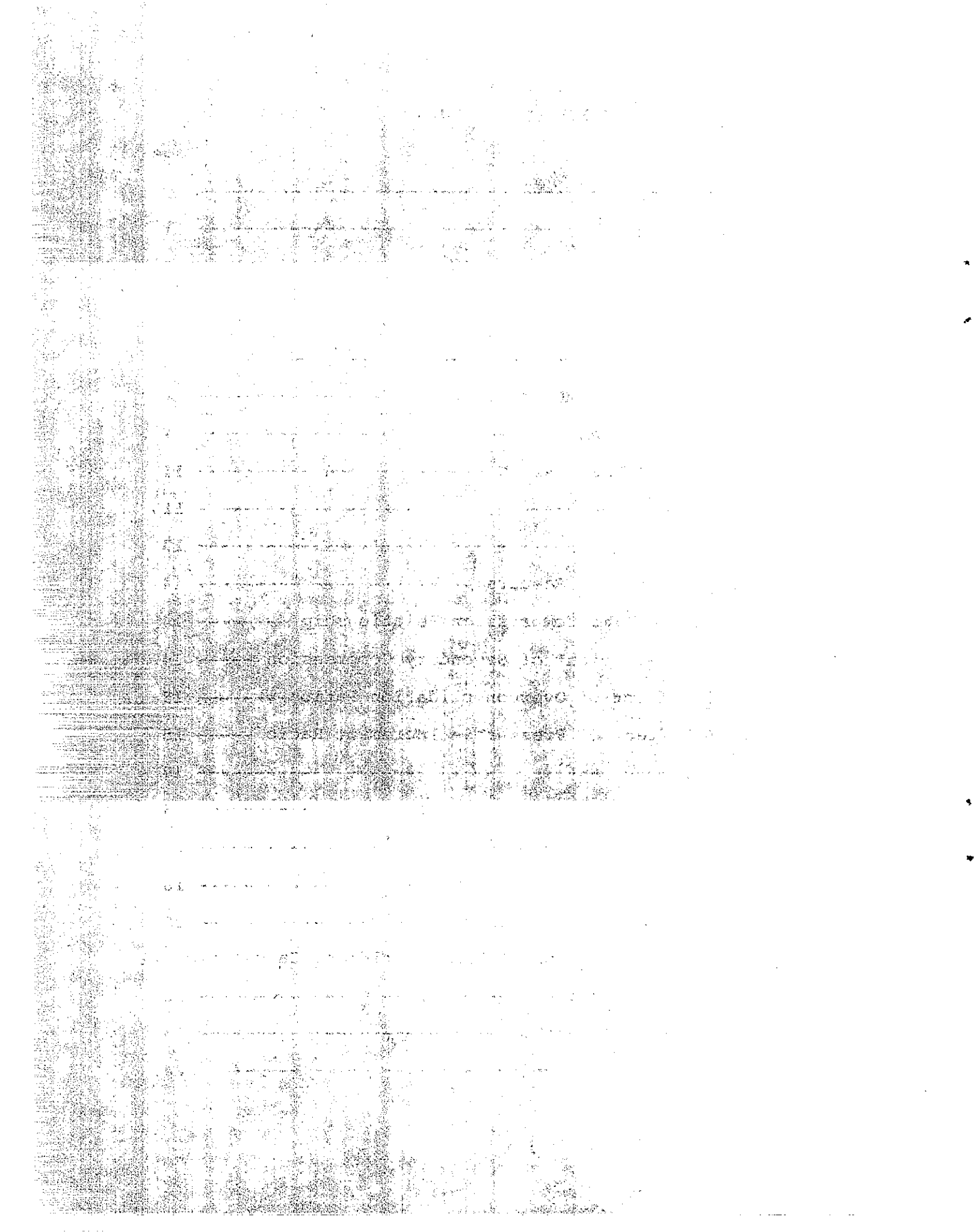
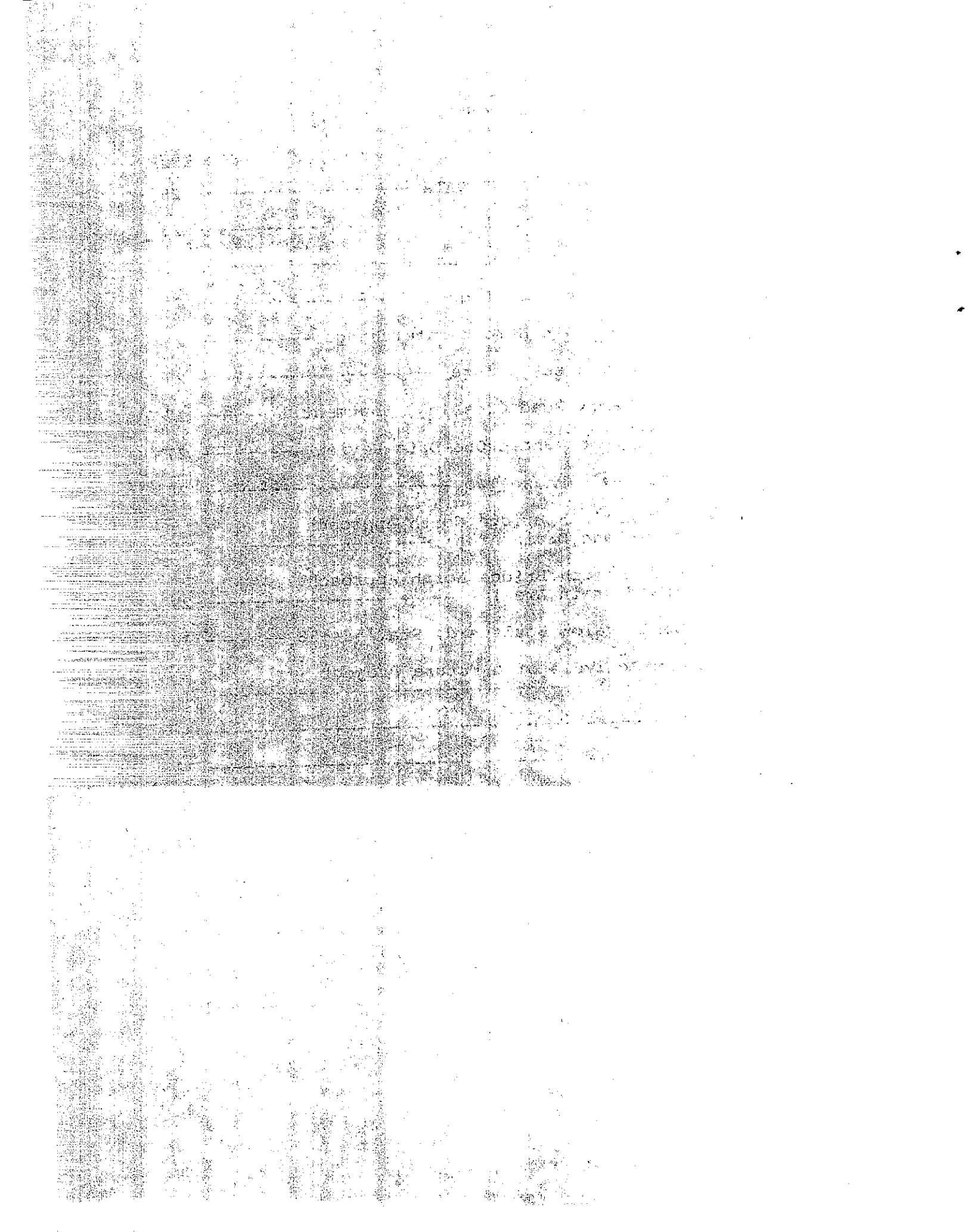


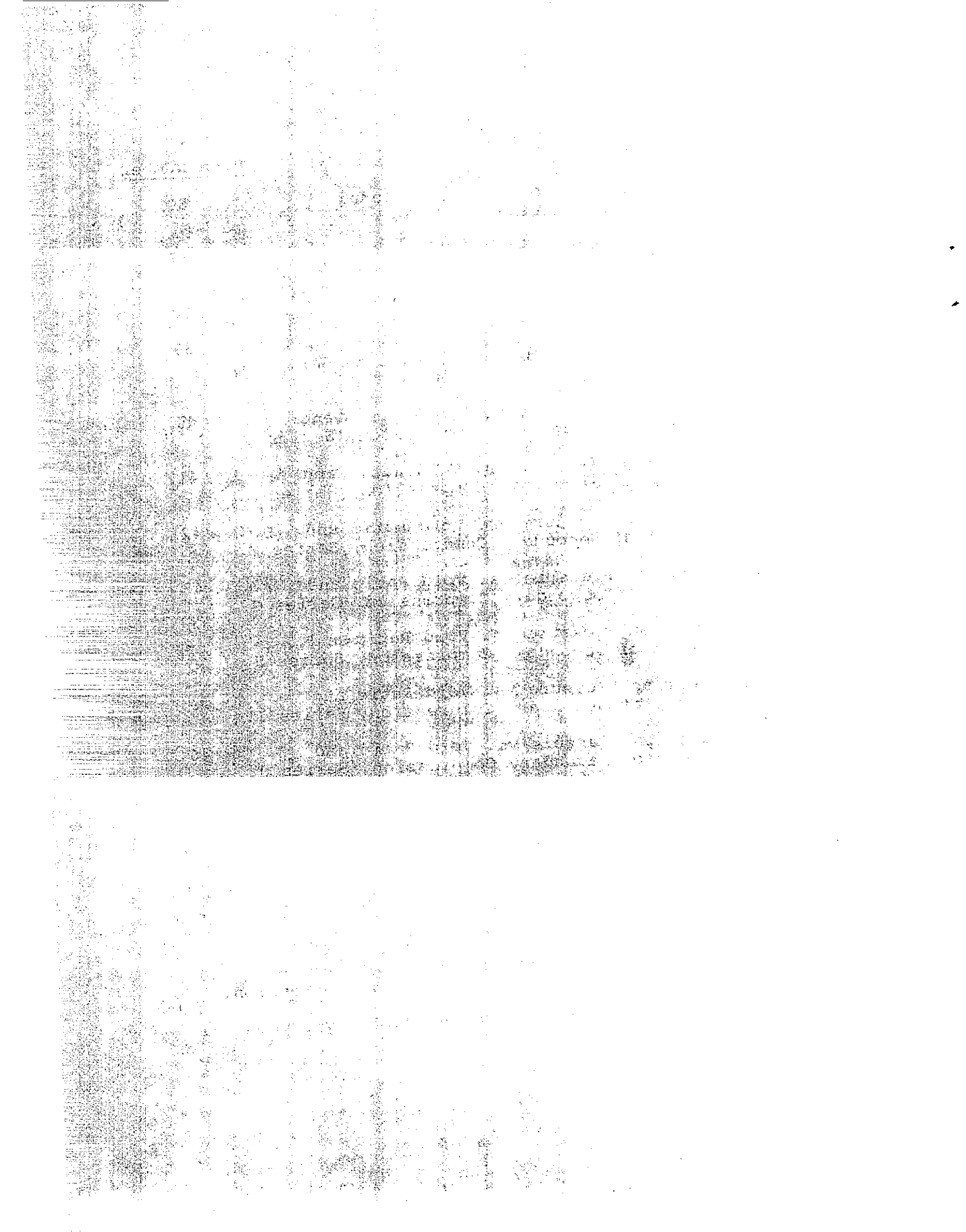
TABLE OF CONTENTS (con't.)

|                                                                              | <u>Page</u> |
|------------------------------------------------------------------------------|-------------|
| Chapter 6 STUDY OF FIELD SETTLEMENT DATA -----                               | 25          |
| 6.1. Project Review - First Phase -----                                      | 25          |
| 6.1.1 San Diequito River Basin -----                                         | 25          |
| 6.1.2 Los Penasquitos Lagoon -----                                           | 26          |
| 6.1.3 Arcata - 4th Street Interchange -----                                  | 26          |
| 6.1.4 Lindsay Creek Bridge -----                                             | 27          |
| 6.1.5 San Ramon Road Crossing, Abutment 1 -----                              | 27          |
| 6.1.6 Summary of Phase One Data Review -----                                 | 27          |
| 6.2. Project Review - Phase Two -----                                        | 28          |
| 6.2.1 Old Antioch Bridge North Approach<br>(Non-Sand Drain Area) -----       | 28          |
| 6.2.2 Old Antioch Bridge North Approach<br>(Sand Drain Area) -----           | 29          |
| 6.2.3 West Avalon Boulevard, Sta. 584+58 -----                               | 30          |
| 6.3. Settlement Analysis of a Future Project<br>(Wahls' Method) -----        | 31          |
| 6.4. Summary -----                                                           | 32          |
| REFERENCES -----                                                             | 33          |
| APPENDICES -----                                                             | 73          |
| A. Summary of Consolidation Test Results -----                               | 73          |
| B. Comparison of Laboratory Data with Field Settlement<br>Measurements ----- | 93          |
| C. Wahls' Method of Time-Settlement Calculation -----                        | 96          |
| D. Hansen's Method of Time-Settlement Calculation -----                      | 102         |
| E. Computer Program HONZ -----                                               | 105         |



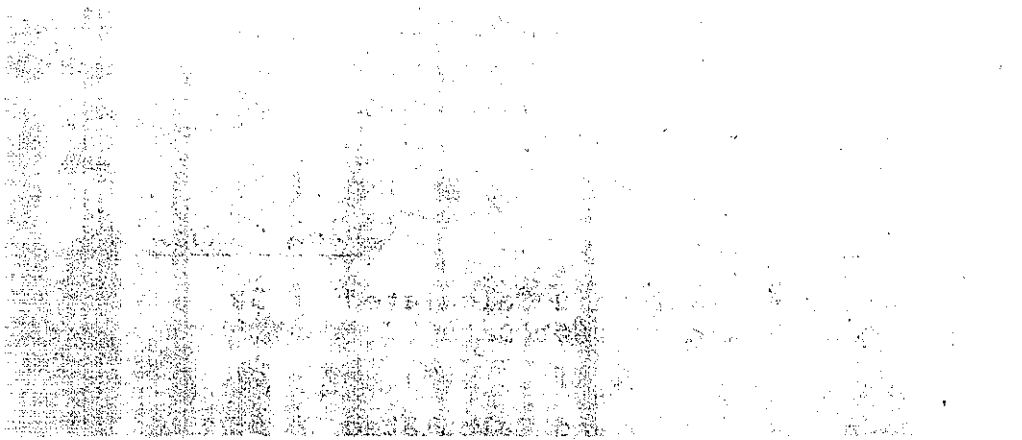
## LIST OF FIGURES

| <u>Figure<br/>Number</u> | <u>Title</u>                                                                                     | <u>Page Number</u> |
|--------------------------|--------------------------------------------------------------------------------------------------|--------------------|
| 1                        | Simplified Models for One-Dimensional Theory of Consolidation.                                   | 36                 |
| 2                        | Effect of Pressure-Increment Ratio on the Shape of Time-Compression Curves.                      | 37                 |
| 3                        | Typical Time-Compression Curves.                                                                 | 38                 |
| 4a                       | Consolidation Pressure vs. Void Ratio and Coefficient of Secondary Compression, Series A, B.     | 39                 |
| 4b                       | Consolidation Pressure vs. Void Ratio and Coefficient of Secondary Compression, Series D.        | 40                 |
| 4c                       | Consolidation Pressure vs. Void Ratio and Coefficient of Secondary Compression, Series E.        | 41                 |
| 4d                       | Consolidation Pressure vs. Void Ratio and Coefficient of Secondary Compression, Series F.        | 42                 |
| 4e                       | Consolidation Pressure vs. Void Ratio and Coefficient of Secondary Compression, Series G.        | 43                 |
| 4f                       | Consolidation Pressure vs. Void Ratio and Coefficient of Secondary Compression, Series H.        | 44                 |
| 4g                       | Consolidation Pressure vs. Void Ratio and Coefficient of Secondary Compression, Series I.        | 45                 |
| 4h                       | Consolidation Pressure vs. Void Ratio and Coefficient of Secondary Compression, Series J.        | 46                 |
| 5                        | Coefficient of Secondary Compression vs. Void Ratio.                                             | 47                 |
| 6                        | Relationship Between Overconsolidation Ratio and Coefficient of Secondary Compression.           | 48                 |
| 7                        | Relationship Between Pressure-Increment Ratio and Coefficient of Secondary Compression.          | 49                 |
| 8                        | Relationship Between Pressure-Increment Ratio and the Ratio of Secondary to Primary Compression. | 50                 |
| 9                        | Calculated Coefficient of Consolidation vs. Void Ratio.                                          | 51                 |



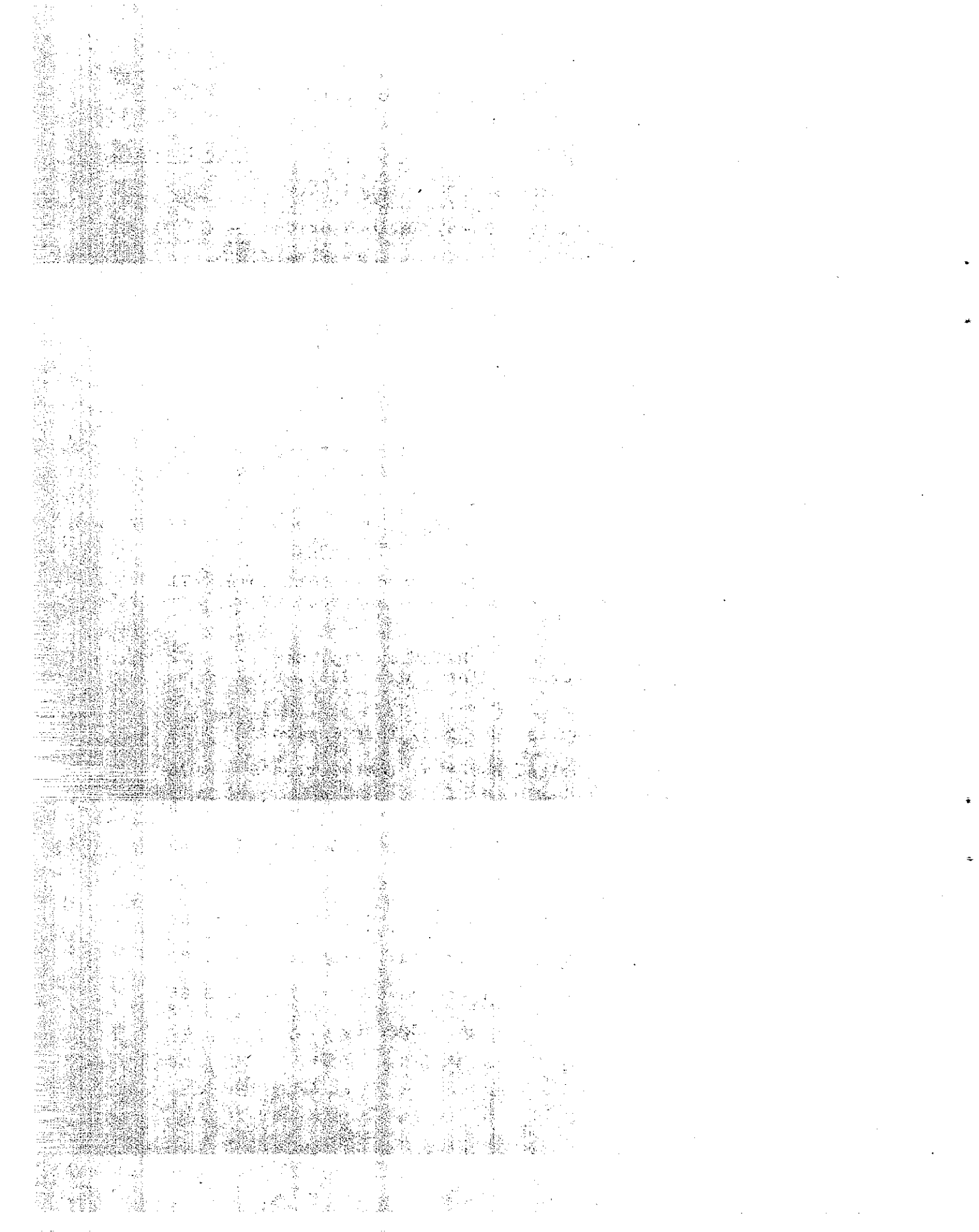
LIST OF FIGURES (con't.)

| <u>Figure<br/>Number</u> | <u>Title</u>                                                                                                                                                                                             | <u>Page Number</u> |
|--------------------------|----------------------------------------------------------------------------------------------------------------------------------------------------------------------------------------------------------|--------------------|
| 10                       | Relationship Between Void Ratio and Calculated Permeability from Consolidation Test Data (Bay Mud).                                                                                                      | 52                 |
| 11                       | Relationship Between Void Ratio and Calculated Permeability from Consolidation Test Data (Peat Soil).                                                                                                    | 53                 |
| 12                       | Void Ratio vs. Log Pressure Curve as Related to Length of Load Increment.                                                                                                                                | 54                 |
| 13                       | Terzaghi's Method of Calculating Time-Compression Relationship.                                                                                                                                          | 55                 |
| 14                       | Sample Settlement Analysis - Wahls' Method (Silty Clay).                                                                                                                                                 | 56                 |
| 15                       | Sample Settlement Analysis - Wahls' Method (Bay Mud).                                                                                                                                                    | 57                 |
| 16                       | Comparison of Methods of Calculating Time-Compression Relationship.                                                                                                                                      | 58                 |
| 17a                      | Settlements of San Diequito River Basin, Sta. "SD" 1278+50.                                                                                                                                              | 59                 |
| 17b                      | Settlements at Los Penasquitos Lagoon, Sta. "SD" 1095.                                                                                                                                                   | 60                 |
| 17c                      | Settlements at Arcata - 4th St. Interchange, Sta. 88+50.                                                                                                                                                 | 61                 |
| 17d                      | Settlements at Lindsay Creek Bridge, Sta. 197+50.                                                                                                                                                        | 62                 |
| 17e                      | Settlements at San Ramon Road Overcrossing, Abutment No. 1.                                                                                                                                              | 63                 |
| 18a                      | Comparison of Measured and Calculated Rate of Settlement in Peaty Soil, Using Wahls' Method (Sta. 70+82, Non-Sand Drain Area, Antioch Bridge North Approach, Pressure-Increment Ratio equal to one).     | 64                 |
| 18b                      | Comparison of Measured and Calculated Rate of Settlement in Peaty Soil, Using Wahls' Method (Sta. 70+82, Non-Sand Drain Area, Antioch Bridge North Approach, Pressure-Increment Ratio greater than one). | 65                 |



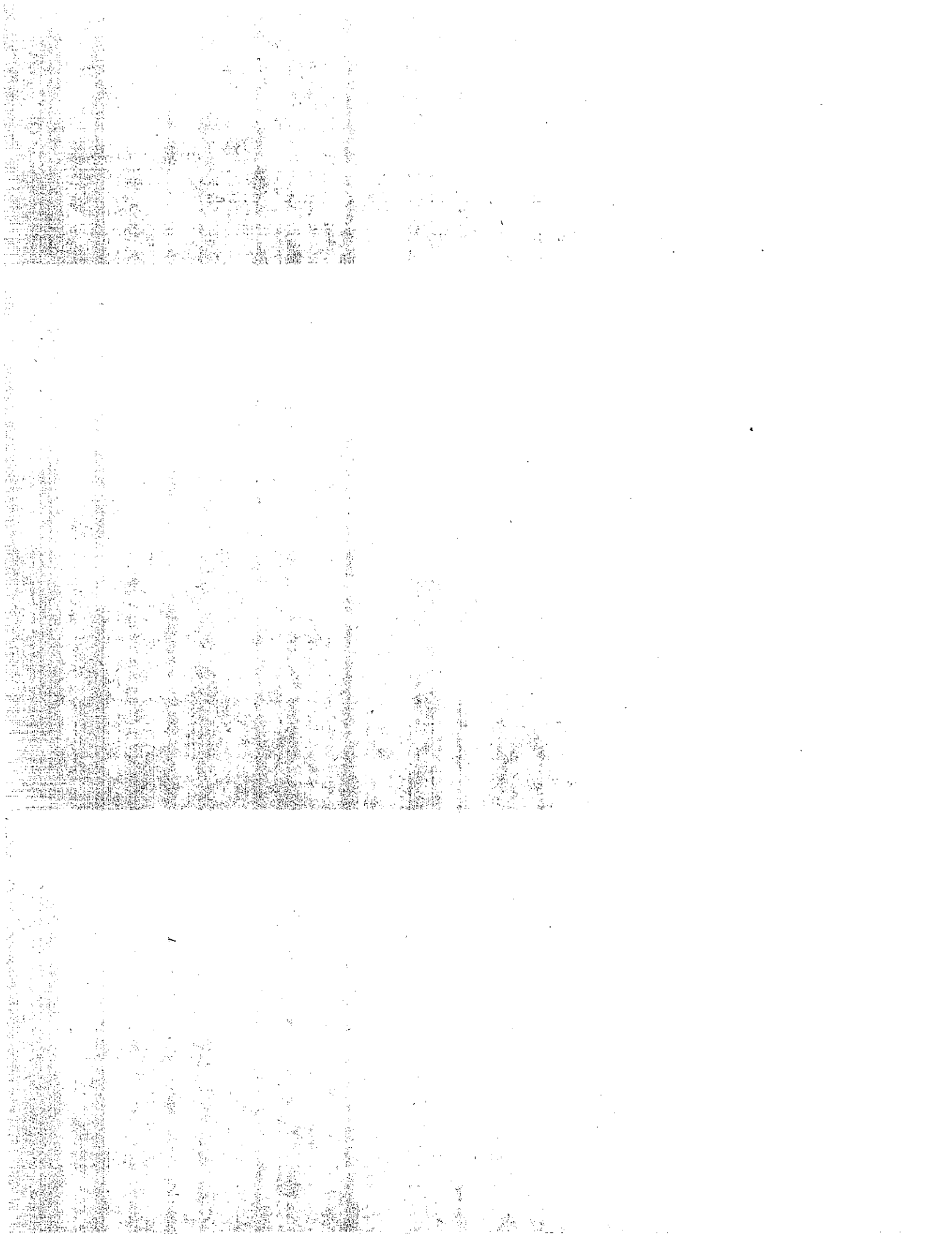
LIST OF FIGURES (con't.)

| <u>Figure Number</u> | <u>Title</u>                                                                                                                                                   | <u>Page Number</u> |
|----------------------|----------------------------------------------------------------------------------------------------------------------------------------------------------------|--------------------|
| 19                   | Comparison of Measured and Calculated Rate of Settlement of Peaty Soil Using Wahls' Method (Sta. 80+10, Sand Drain Area, Antioch Bridge North Approach).       | 66                 |
| 20a                  | Comparison of Calculated and Measured Rate of Settlement in Silty Clay, Using Wahls' Method ( $\frac{\Delta P}{P_0} = 1$ ), West Avalon Blvd. Sta. 584+58.     | 67                 |
| 20b                  | Comparison of Calculated and Measured Rate of Settlement in Silty Clay, Using Wahls' Method ( $\frac{\Delta P}{P_0}$ variable), West Avalon Blvd. Sta. 584+58. | 68                 |
| 21a                  | Laboratory Consolidation Data Used in Settlement Prediction of New Antioch Bridge Approach (Peat, $w = 185\%$ ).                                               | 69                 |
| 21b                  | Predicted Time-Settlement Relationship, New Antioch Bridge Approach (Peat, $w = 185\%$ ).                                                                      | 70                 |
| 22a                  | Laboratory Consolidation Data Used in Settlement Prediction of New Antioch Bridge Approach (Peat, $w = 520\%$ ).                                               | 71                 |
| 22b                  | Predicted Time-Settlement Relationship, New Antioch Bridge Approach (Peat, $w = 520\%$ ).                                                                      | 72                 |
| A-1                  | Consolidation Test Results, Bay Mud, Test Series A.                                                                                                            | 74                 |
| A-2                  | Consolidation Test Results, Bay Mud, Test Series B.                                                                                                            | 76                 |
| A-3                  | Consolidation Test Results, Silty Clay, Test Series C.                                                                                                         | 78                 |
| A-4                  | Consolidation Test Results, Bay Mud, Test Series D.                                                                                                            | 80                 |
| A-5                  | Consolidation Test Results, Bay Mud, Test Series E.                                                                                                            | 82                 |
| A-6                  | Consolidation Test Results, Peat, Test Series F.                                                                                                               | 84                 |
| A-7                  | Consolidation Test Results, Peaty Clay, Test Series G.                                                                                                         | 86                 |
| A-8                  | Consolidation Test Results, Clayey Peat, Test Series H.                                                                                                        | 88                 |
| A-9                  | Consolidation Test Results, Peat and Peaty Clay, Test Series I.                                                                                                | 90                 |



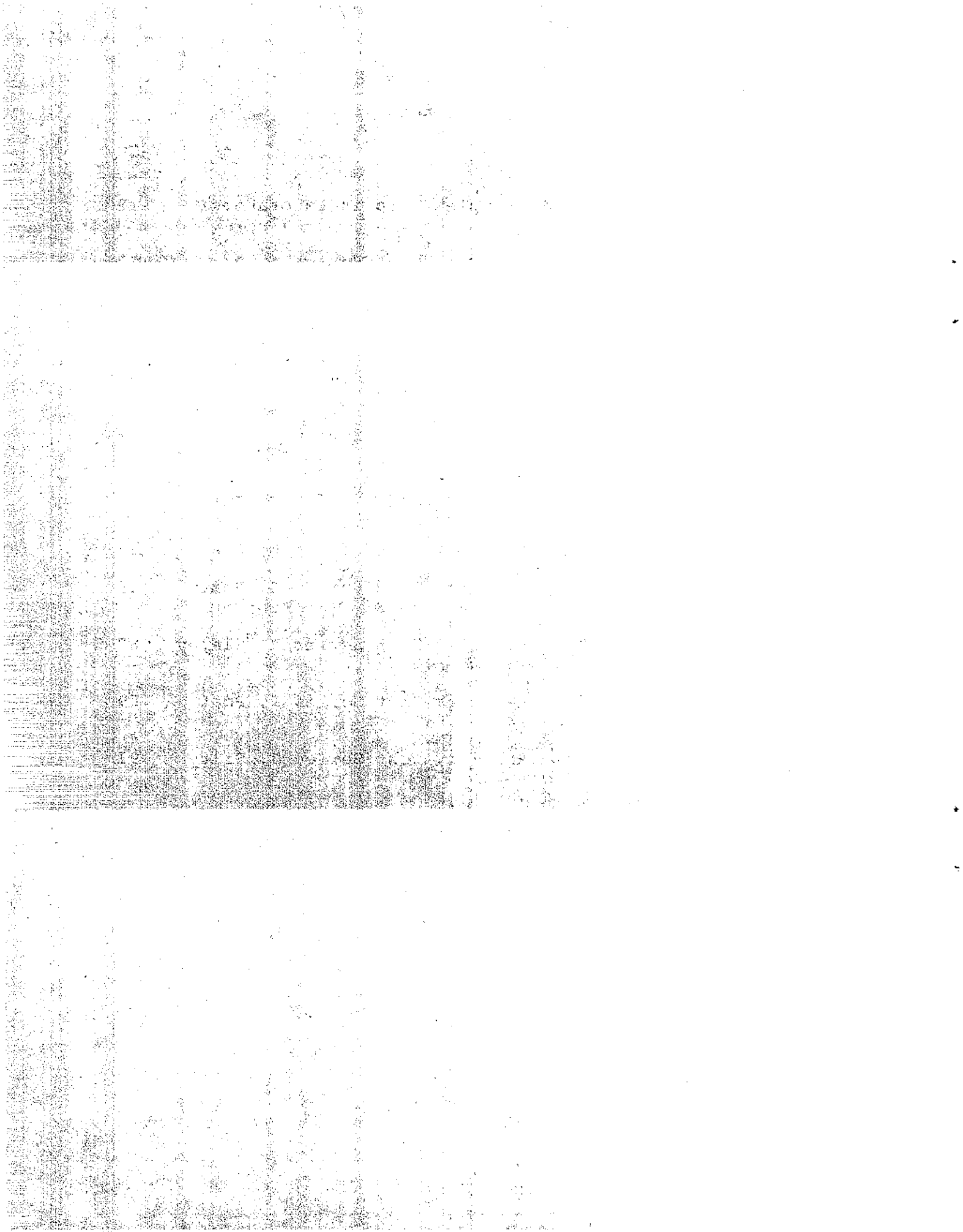
LIST OF FIGURES (con't.)

| <u>Figure Number</u> | <u>Title</u>                                                                              | <u>Page Number</u> |
|----------------------|-------------------------------------------------------------------------------------------|--------------------|
| A-10                 | Consolidation Test Results, Silty Clay, Test Series J.                                    | 92                 |
| C-1                  | Rheological Model in Wahls' Method.                                                       | 97                 |
| D-1                  | Time-Compression Plot in Hansen's Method.                                                 | 103                |
| E-1                  | Laboratory Time-Compression Curve for Wahls' Method<br>Computer Analysis.                 | 106                |
| E-2                  | Field Time-Settlement Relationship Calculated Using<br>Wahls' Method, Data in Figure E-1. | 108                |



LIST OF TABLES

| <u>Table<br/>Number</u> | <u>Title</u>                                                    | <u>Page<br/>Number</u> |
|-------------------------|-----------------------------------------------------------------|------------------------|
| 1                       | Description of Soil Samples Used in Laboratory Investigation.   | 12                     |
| A-1                     | Consolidation Test Results, Test Series A, Bay Mud.             | 73                     |
| A-2                     | Consolidation Test Results, Test Series B, Bay Mud.             | 75                     |
| A-3                     | Consolidation Test Results, Test Series C, Silty Clay.          | 77                     |
| A-4                     | Consolidation Test Results, Test Series D, Bay Mud.             | 79                     |
| A-5                     | Consolidation Test Results, Test Series E, Bay Mud.             | 81                     |
| A-6                     | Consolidation Test Results, Test Series F, Peat.                | 83                     |
| A-7                     | Consolidation Test Results, Test Series G, Peaty Clay.          | 85                     |
| A-8                     | Consolidation Test Results, Test Series H, Clayey Peat.         | 87                     |
| A-9                     | Consolidation Test Results, Test Series I, Peat and Peaty Clay. | 89                     |
| A-10                    | Consolidation Test Results, Test Series J, Silty Clay.          | 91                     |
| B-1                     | San Dieguito River Basin, Sta. "SD" 1278+50.                    | 93                     |
| B-2                     | Los Penasquitos Lagoon, Sta. "SD" 1095.                         | 93                     |
| B-3                     | Arcata - 4th Street Interchange, Sta. 23+25.                    | 94                     |
| B-4                     | Lindsay Creek Bridge, Sta. 197+50.                              | 94                     |
| B-5                     | San Ramon Road Overcrossing, Abutment 1.                        | 95                     |



## CHAPTER 1

### INTRODUCTION

The term settlement in soil mechanics is applied to the vertical displacements of structures resulting from stresses induced in the foundation soils by the imposed loads of the structures. It is generally accepted that settlements of structures resting on compressible saturated clays can be separated into the following three components:

1. An immediate settlement due to elastic deformations taking place at constant volume.
2. A settlement due to primary consolidation wherein volume change is controlled by the change in effective stresses as a result of the dissipation of excess pore water pressure.
3. A settlement due to the so-called secondary compression wherein volume change continues after excess pore water pressures are essentially dissipated.

Basically, these settlements occur in the order listed although some secondary compression does take place during primary consolidation. The relative importance of these components depends on several factors and a complete separation of components is not yet possible. For the majority of soil deposits, the amount of settlement due to secondary compression may be negligible compared to that resulting from primary compression, but for some highly compressible soils and organic deposits it may be a large portion of the total settlement.

Conventional settlement analyses based on Terzaghi's theory of one-dimensional consolidation do not consider either initial or secondary compression. The effects of these two compression components must be considered separately if they are to be included in the overall settlement analysis. For many earth structures, especially roadway embankments, foundation soils are analyzed only for primary compression. Normally, the analysis involves a series of laboratory consolidation tests on undisturbed soil samples based on Terzaghi's theory and a calculation of an ultimate settlement using the resulting laboratory  $e$ - $\log p$  curves. The rate of settlement is then predicted from laboratory coefficients of consolidation and field drainage conditions. However, even when field exploration and laboratory investigations are carefully performed, and a reasonably accurate evaluation of field stress distribution is possible, settlements predicted by this procedure do not always agree with actual settlements, the difference frequently being substantial. The uncertainty associated with predicted settlements is therefore a

subject of concern during design and construction stages since design considerations and construction schedules are often dependent on amount and rate of expected settlement.

It is presently unclear whether discrepancies between predicted and observed behavior are caused by the more or less normal limitations and inaccuracies in the several phases of the overall foundation investigations, or by a more basic factor or quantity that is not receiving sufficient consideration during the investigation. For example, in a laboratory consolidation test the process of compression is purely one-dimensional with a Poisson's ratio of zero. Therefore, it may be expected that field settlements predicted from laboratory data will deviate, at least to some extent, from actual field settlements unless the immediate settlement that occurs without pore pressure dissipation is considered under three-dimensional configurations. This aspect of the field settlement problem was investigated elsewhere by Skempton and Bjerrum (23), Janbu (14), and Davis and Poulos (9). Similarly, since secondary compression is not considered in Terzaghi's theory, it is somewhat unreasonable to expect predicted settlements to agree with measured settlements where secondary compression is present.

In an attempt to resolve some of the cloudy aspects of embankment settlement analysis, secondary compression was selected as a central topic for study based largely on the following considerations:

1. Secondary compression is neglected in most road embankment foundation investigations although it is one of the components contributing to total compression.

2. Secondary compression occurs both during and after completion of primary compression. Therefore, the effects of secondary compression on the time-settlement relationship obtained from a theory that was originally developed only for primary compression may be appreciable.

3. Discrepancies between predicted and measured settlements cover the entire range of the time-settlement diagram (that is, both short- and long-term). It is in this same range that secondary compression occurs.

The purpose of the project reported herein was to investigate the effects of secondary compression on settlements of selected highway embankments constructed over compressible soils in California. Specifically, the primary objectives were:

1. to determine representative contributions by secondary compression to total measured settlements, and
2. to develop or modify an existing method for predicting secondary compression.

It was also hoped that the investigation would result in improvements in current techniques for predicting primary compression settlements. Through normal use of findings and improved methods, expected benefits would include:

1. more accurate predictions of magnitude and rate of settlements, both short- and long-term,
2. more accuracy in establishing waiting periods subsequent to embankment construction but prior to placement of pavement structural sections, and
3. more accuracy in the initial specification of, and subsequent changes in, loading rates when controlled loading is required.

## CHAPTER 2

### CONCLUSIONS AND IMPLEMENTATION

The investigation reported herein has resulted in the following conclusions:

- (1) Secondary compression is a long term phenomenon the rate of which is approximately linear in a semi-logarithmic time-compression plot. This phenomenon has been observed in the laboratory and in the field but its field measurement is often complicated by the complex nature of layered soil deposits of different consolidation characteristics and drainage conditions. For example, in multi-layered deposits some of the layers with difficult drainage conditions may still be in the primary stage of compression while others have already reached the secondary stage. Measured settlements, therefore, reflect the combined effects of all the complicating factors that influence and govern the consolidation process.
- (2) The coefficient of secondary compression in a normally consolidated clay is found to increase with increase in void ratio, but is found to be independent of total effective pressure and pressure-increment ratio. In an overconsolidated clay, this coefficient is much less than for a normally consolidated clay. Therefore, in a settlement analysis involving secondary compression, it is important to determine the overconsolidation ratio of compressible clay layers. For a normally consolidated clay, since the coefficient of secondary compression is independent of pressure-increment ratio, the total amount of compression resulting from a relatively small load increment may be largely due to secondary compression. On the other hand, in an overconsolidated clay with a small load increment, the settlement due to secondary compression is usually very small.
- (3) The ratio of secondary to primary compression is a function of the pressure-increment ratio. An increase in pressure-increment ratio rapidly reduces the secondary to primary compression ratio. This conclusion follows directly from the observation that the coefficient of secondary compression is independent of pressure-increment ratio in a normally consolidated clay. Therefore, the relative importance of secondary to primary compression depends on the actual loading conditions. This implies that unless laboratory consolidation tests simulate field loading conditions it is not possible to predict accurately the field consolidation process involving both primary and secondary compressions. This implication is important since in a standard consolidation test the pressure-increment ratio is always unity in the normally consolidated range of loads while the actual pressure-increment ratio in situ may be several times greater or smaller than one.

- (4) The standard consolidation test procedure is generally satisfactory to evaluate the void ratio versus logarithm of pressure relationship even if a considerable amount of secondary compression is present. Since the total amount of settlement is usually predicted from this e-log p curve, this implies that a pressure-increment ratio of one as commonly used may still yield satisfactory results in predicting the magnitude of settlement regardless of field loading conditions. However, an accurate rate of secondary compression may be obtained only if sufficient time is allowed in a consolidation test to delineate the secondary tail of a time-compression curve.
- (5) Wahls' method of calculating the time-compression relationship of simultaneous primary and secondary compressions was found to yield a more satisfactory result in predicting the field time-settlement relationship than the conventional method based on Terzaghi's theory. However, since the soil parameters used in Wahls' method are evaluated from laboratory tests, the accuracy of this method cannot exceed that of the laboratory test data. Comparisons of field measurements of settlements, laboratory consolidation data, and predicted time-settlement relationships indicate that the evaluation of field conditions (especially drainage) is as important as (if not more than) the choice of the method of settlement calculation.

Based on the projects reviewed in this investigation it appears that secondary compression normally does not contribute an appreciable amount to the total settlement of roadway embankments. However, it was found that secondary compression affects the time-settlement relationship as predicted by conventional methods and may be the principal cause of observed discrepancies between predicted and measured settlement rates. It was also found that the actual pressure-increment ratio is an important factor in determining settlement rate.

To account for the effects of secondary compression and pressure-increment ratio, an improved procedure for predicting time-settlement relationships was adopted and consists largely of the method developed by Wahls. Use of this method as compared to current practice is more time consuming, requires carefully planned laboratory tests and possibly more tests, and well planned and executed field investigations, but results in a more accurate time-settlement relationship. It is expected that the method will be of most benefit for those situations involving large settlements since, in these cases, substantial differences between predicted and measured settlements during or shortly after construction could result if erroneous time-settlement relationships were obtained by current procedures. In this respect, the improved procedure will be a useful supplemental tool for

analyzing difficult foundation settlement problems. It should be emphasized, however, that the method was developed for compressible clays that exhibit a laboratory time-compression curve of Type I described in Chapter 3 and cannot be used for a Type II curve.

Findings from this investigation have been used in predicting a time-settlement relationship for the New Antioch Bridge Approach Fill to be founded on peats and peaty clay. The embankment will be monitored as a routine operation during and after construction and data will be used to assess the procedure adopted. Further implementation will be by the Materials and Research Department during future embankment foundation investigations.

## CHAPTER 3

### REVIEW OF LITERATURE

The first theory of one-dimensional consolidation of a homogeneous, saturated soil stratum was presented by Terzaghi (31) in 1925. In this so-called hydrodynamic theory of consolidation, the rate of compression is governed solely by the rate of pore water drainage. As can be seen in the simplified hydromechanical model in Figure 1a, the applied force is first taken up by the pore water and then transferred gradually to the soil skeleton (represented by Spring  $S_1$ ) as drainage of pore water takes place. The compression ceases when the effective force in the spring is equal to the applied force.

Laboratory one-dimensional consolidation tests and field settlement observations clearly show that Terzaghi's theory does not fully explain the consolidation characteristics of clays. The actual time-compression curves often indicate a definite continuation of compression, although at a decreasing rate, long after complete dissipation of excess pore water pressure. This phenomenon is termed "plastic time lag" by Taylor (28) and in general is referred to as "secondary compression" to distinguish it from "primary compression" which is that portion of compression predicted by Terzaghi's theory of hydrodynamic consolidation. While efforts to separate secondary compression from primary compression in the entire consolidation process have been made (see, for example, Casagrande (6,7)), it is now acknowledged that a new or modified concept is required to satisfactorily explain the observed consolidation characteristics of clay soils.

Taylor and Merchant (29) proposed a modification to Terzaghi's basic model which was further modified by Taylor (3), as shown in Figure 1b. It is apparent from this model, in which secondary compression characteristics are represented by a dash pot, that primary and secondary compressions develop simultaneously and cease simultaneously. Moreover, the ultimate compression will never exceed that predicted by Terzaghi's theory which is the compression of the spring. To eliminate the restriction that the total compression in Taylor's model can never exceed that predicted by Terzaghi's theory, Tan (27) proposed a model (Figure 1c) with two springs in which secondary compression will continue until spring  $S_2$  carries all the load,  $\Delta p$ , while spring  $S_1$ , which is equivalent to spring  $S_1$  in Taylor's modified model of Figure 1b, represents primary compression.

The causes of secondary compression were attributed by Terzaghi (32) and Taylor (29) to the readjustment of grain particles delayed by the viscous resistance in the bound clay-water system. Tan (27) proposed a theory that secondary compression is caused by

jumping of bonds formed by the clay particles. This jump may be from one rough spot to the next, or it may be from one particle to the next. Zeevaert (36) and DeJong (10) proposed another mechanism of consolidation that includes secondary compression by considering the structure of clay soil to consist of packets or domains interwoven by a system of coarse channels and macropores. In this mechanism the primary stage of consolidation is the dissipation of pore pressures in the macropores which is essentially the process of Terzaghi's theory. However, as the stress is transferred to the micro-structures in the packets, the water in the micropores in the packets will start to drain into the macropores with extremely low permeability involved, resulting in secondary compression.

While the exact causes and mechanisms of secondary compression have not been fully explained, a number of investigators have studied the secondary time effects of consolidation in quantitative terms. Buisman (3), in 1936, proposed a semi-empirical equation derived from long term consolidation data to estimate secondary settlements. It was in his paper that the linearity of secondary compression with respect to logarithm of time was first proposed. Various rheological models of consolidation, mostly modifications of the basic models discussed previously, have been proposed to obtain mathematical expressions for calculating secondary compression. These models include those proposed by Lo (21), Wahls (33), Leonards and Altschaeffl (19), Hansen (11), Barden (1,2) and Tan (27). However, since these are curve fitting methods developed from laboratory compression test data, the parameters used in the various mathematical formulas must be determined from laboratory time-compression curves.

Numerous field experiences related to long term settlements have been reported. Among them are Burn (4,5), Cedergren and Weber (8), Horn (12), Kern (15), Kleiman (16), Smith, Hirsch and Kleiman (24), Spangler (25,26), Walker (34) and Weber (36). In many cases where settlement calculations were made using the conventional Terzaghi's theory, it has been observed that while the magnitude of total settlement can be estimated with reasonable accuracy, the rate of settlement generally deviates substantially from that predicted. In the secondary compression region of the time-compression curve where Terzaghi's theory does not apply, the empirical relationship proposed by Buisman (3) has been widely used. According to reports by Horn and Lambe (13), and Walker (34), it appears that Buisman's method can be used to satisfactorily estimate the rate of field secondary compression from long term laboratory consolidation tests.

Laboratory investigations to study experimentally the secondary time effects of consolidation have been reviewed by Leonards and Ramiah (20), and Ladd and Preston (17). It was pointed out by Leonards, et al (18,19) and Wahls (33) that the pressure-increment

ratio, defined as the ratio of the incremental pressure being applied on the specimen to the total effective pressure prior to the incremental pressure application, significantly affects the shape of the time compression curve. When the pressure-increment ratio is large, the time-compression curve is characterized by Terzaghi's theory, and the Casagrande construction delineates the dial readings corresponding to 100% primary compression to a good approximation even when the magnitude of the secondary compression is large. (Type I curve in Figure 2b). On the other hand, when the pressure-increment ratio is small, Terzaghi's theory cannot predict, even approximately, the rate of pore pressure dissipation and the curve fitting methods for calculating the coefficient of consolidation are no longer applicable. (Type II curve in Figure 2a). Some intermediate curve may exist for intermediate pressure-increment ratios and at very large times.

Leonards and Girault (18) report that the relative magnitude of secondary compression as reflected by the ratio of secondary to primary compression, drops rapidly as the pressure-increment ratio increases. However, when the coefficient of secondary compression is defined as the slope of the secondary compression curve in semi-log plot, Wahls (33) found that the magnitude of this coefficient is independent of the pressure-increment ratio but is dependent on void ratio.

Newland and Allely (22) tested both undisturbed and remolded Whangamarino clay and found that the coefficient of secondary compression is independent of the pressure-increment ratio, thickness of sample, total consolidation pressure, and duration of previous increment. Barden (2) also showed that the secondary creep rate is not governed by either the sample thickness or the duration of the last increment. However, according to Terzaghi's theory, the time required for development of the characteristic secondary portion of the time-compression curve still depends on the time required for completion of primary compression which is proportional to the square of the sample thickness.

Leonards, et al (18,20), Ladd and Preston (17), and Wahls (33) reported the effects of over consolidation ratio on the rate of secondary compression. A typical behavior appears to be that the rate of secondary compression increases rapidly as the field preconsolidation pressure is approached and then stays approximately constant in the normally consolidated load range.

In summary, secondary compression has been observed in both field and laboratory consolidation of compressible soils. While the causes and mechanisms of this phenomenon are not completely known, it is generally agreed that secondary compression can be studied in the laboratory and field behavior can be approximately predicted from laboratory study. Little information is available

comparing predicted and measured secondary compression settlements and there is no widely accepted method of predicting secondary compression in the field. It is believed to be possible, however, based on present knowledge derived from theories and laboratory investigations, and by analyzing available long term field settlement data, to arrive at reasonably accurate means of predicting secondary compression.

## CHAPTER 4

### LABORATORY INVESTIGATION

To evaluate the relative importance of some known factors affecting secondary compression and the appropriateness of standard testing procedures when secondary compression is of concern, a laboratory testing program consisting of ten series of special tests was conducted. Index properties of the soils tested are listed in Table 1.

Series A, B, D and E samples were soft to firm silty clays, known locally as Bay Muds, preconsolidated in-situ to pressures of 0.4 to 0.5 tons per square foot. Series F, G, H and I samples were peats with water contents ranging from 60 to 500 percent. Series C and J samples were firm, silty clays preconsolidated to approximately 1.5 tons per square foot.

#### 4.1 Definitions

The following definitions are of key terms used in this chapter.

1. Coefficient of Secondary Compression,  $C_{\alpha}$ . The coefficient of secondary compression is defined as the percent compression of the specimen per logarithmic cycle in a compression vs. logarithm of time curve. It may be written as

$$C_{\alpha} = \frac{\Delta H}{H_0} \times \frac{100}{\log_{10} t}$$

in which  $C_{\alpha}$  is the coefficient of secondary compression,  $\Delta H$  is the differential compression in the linear range of secondary compression for a time interval  $t$ , and  $H_0$  is the initial height of specimen.

2. Pressure-Increment Ratio,  $\Delta P/P_0$ . This is defined as the ratio of the incremental pressure being applied to the specimen to the maximum past effective pressure on the specimen. In a standard consolidation test, this ratio is one in the normally consolidated range of loads and less than one for loads less than the precompression pressure. This ratio should not be confused with the pressure-increment ratio normally used to describe the standard laboratory procedure of doubling the load with each increment, and which has no connection at all with the preconsolidation pressure of the specimen.

3. Overconsolidation Ratio, OCR. The overconsolidation ratio is defined as the ratio of the maximum past effective pressure on the specimen to the existing effective pressure. In a standard consolidation test, this ratio is commonly 1.0 in the

Table 1

## Description of Soil Samples Used in Laboratory Investigation

| Test Series | Soil Type | Particle Size |             | Liquid Limit (%) | Plastic Limit (%) | Natural Water Content (%) |
|-------------|-----------|---------------|-------------|------------------|-------------------|---------------------------|
|             |           | % < 5 $\mu$   | % < 1 $\mu$ |                  |                   |                           |
| A           | CH        | 42            | 27          | 77               | 37                | 64                        |
| B           | CH        | 40            | 27          | 85               | 36                | 70                        |
| C           | CH        | 69            | 31          | 58               | 31                | 45                        |
| D           | CH        | 55            | 31          | 69               | 33                | 68                        |
| E           | CH        | 52            | 31          | 66               | 32                | 70                        |
| F           | OH        | 60            | 20          | -                | -                 | 190                       |
| G           | OH        | 48            | 16          | -                | -                 | 70                        |
| H           | OH        | 57            | 20          | -                | -                 | 80                        |
| I           | OH        | 60            | 25          | 150~200          | 75~110            | 130~420                   |
| J           | CH        | 58            | 40          | 56               | 32                | 43                        |

normally consolidated range of loads. However, in an over-consolidated range the value of OCR is always greater than unity.

4. Normally Consolidated Load Range. That portion of the total range of test loads in which all loads are greater than the preconsolidation pressure of the specimen being tested.

#### 4.2 Testing Program

In test series A, B and C, the duration of each load increment was varied to cover a range from the standard one day to a maximum of seven days. This was done in order to evaluate more accurately the rate of secondary compression and to study the effect of previous load increment duration on secondary compression. In the normally consolidated region of loads, the pressure-increment ratio was varied to study its effects on the rate of secondary compression, ratio of secondary to primary compression, and time required for completion of primary compression. This was based on the fact that, in a standard consolidation test, a pressure-increment ratio of one is routinely used, while in actual construction loading the in-situ pressure-increment ratio may be several times greater or smaller than unity, depending on the depth of the compressible soil layer, and the applied structural load.

Series D and E tests were designed to study the effects of pressure-increment ratio and overconsolidation ratio on secondary compression. In a normally consolidated range, pressure-increment ratios greater than, equal to, and less than unity were used in these test series. In an overconsolidated range, where  $\frac{\Delta P}{P_0}$  is always less than one, the value of  $\frac{\Delta P}{P_0}$  was also varied.

Series F, G, H and I tests were designed to study the secondary compression characteristics of peaty clays. The materials range from highly compressible fibrous peat to silty clay containing organic matter. Except for repeating the testing programs designed for Series A, B and C on these peaty clays, some of the test results were intended for use in time-settlement analysis. These samples were obtained from near the north Antioch Bridge approach fill where approximately 13 years of field settlement data are available. Comparison of measured settlement data with those calculated from the present investigation was intended.

Samples used in Series J tests were obtained from near the West Avalon Boulevard Bridge in Los Angeles from which site approximately ten years of settlement data are available. Since it was intended to use these test results for time-settlement analysis, pressure-increment ratios were varied to simulate the field loading conditions.

Typical time-compression curves for these tests are presented in Figures A-1 through A-10. The e-log p curves are presented in Figures 4a through 4h and also Figures A-1 through A-5. The test data and consolidation parameters are tabulated in Tables A-1 through A-10.

## 4.3 Analysis of Test Results

### 4.3.1 The Time-Compression Relationship

By definition, secondary compression is the long-term compression after all the excess pore pressures have dissipated. Therefore, sufficient time must be allowed in a consolidation test for evaluation of this secondary characteristic. In Figure 3, two typical time-compression curves are presented. It may be noted that for Series C sample, the standard one-day increment test is sufficient to develop the secondary time-compression relationship. However, for the more compressible Bay Mud sample of Series A, approximately three days are needed to clearly define the secondary compression.

The linear relationship of log time versus compression in the secondary compression range as suggested by Buisman (3) is generally confirmed for the soils tested as shown in Figures A-1 through A-10. The shape of the time-compression curve depends on the pressure-increment ratio. When the value of  $\frac{\Delta P}{P_a}$  is small (less than one), the curve resembles that of Type II curve in Figure 2 where the separation of primary and secondary compressions is difficult. As the value of  $\frac{\Delta P}{P_a}$  is increased, the amount of primary compression increases while secondary compression stays at approximately the same magnitude. Therefore, the shape of the time-compression curve becomes that of Type I curve in Figure 2 where Casagrande's method may be used to separate the primary and secondary compressions.

### 4.3.2 Coefficient of Secondary Compression

In most of the consolidation tests in the present investigation, sufficient time was allowed for evaluation of the coefficient of secondary compression. Detailed test results for each increment of load are presented in Table A-1 through A-10. As discussed in Chapter 3, previous investigators have found that the magnitude of secondary compression increases rapidly as the pre-compression pressure is approached. In the normally consolidated range, however, the magnitude of this coefficient is found to remain approximately constant. Typical results from the present investigation are plotted in Figures 4a through 4h. It may be seen that as the effective pressure is increased the coefficient of secondary compression increases rapidly with the maximum rate of increase at or near the pre-compression pressure. As the effective pressure is further increased, the coefficient of secondary compression reaches its peak at an effective pressure approximately twice the precompression pressure and then generally stays at or decreases to a somewhat constant value. This behavior is consistent in recompression cycles as shown in Figure 4b. For example, in Specimen #4, Test Series D, the sample was consolidated to 2 TSF and then

rebounded to 1/16 TSF before the second loading cycle was applied. Consistent behavior in the value of the coefficient of secondary compression as described above was exhibited in both cycles of consolidation.

In Figure 5, the coefficient of secondary compression for Bay Mud in the normally consolidated range is plotted against the average void ratio. A regression analysis of the data showed that the correlation between plotted quantities was not statistically significant.

#### 4.3.3 Effect of Overconsolidation Ratio

The foregoing analysis suggests that the coefficient of secondary compression is affected by the overconsolidation ratio and the pressure-increment ratio. In Figure 6, the relationship between the overconsolidation ratio and coefficient of secondary compression during recompression cycles of Series D tests is presented. The rate of secondary compression appears to increase with a decrease in overconsolidation ratio. Also, as may be noted from Figures 4a through 4h, the coefficient of secondary compression generally reaches its peak at or near the precompression pressure and may decrease to or stay at an approximately constant value as the effective stress is further increased.

#### 4.3.4 Effects of Pressure-Increment Ratio

In Figure 7, the relationship between pressure-increment ratio and coefficient of secondary compression is shown using Series E test data and Series D data from Figure 6. In an overconsolidated range of loads, the coefficient of secondary compression increases rapidly with increase in pressure-increment ratio when the precompression pressure is approached and being exceeded. However, in the normally consolidated load range, this pressure-increment ratio seems to have little or no effect on the rate of secondary compression. It is quite significant that at a pressure-increment ratio of 0.125, the value of  $C_{\alpha}$  for a normally consolidated clay is approximately four times greater than that of the same clay when it is overconsolidated. On the other hand, within the normally consolidated range, an increase of pressure-increment ratio from 0.125 to 3 does not appear to affect the rate of secondary compression at all.

In a standard consolidation test, the incremental pressure applied on the specimen is usually taken as equal to the total effective pressure that exists prior to loading. This means that the pressure-increment ratio as defined in this report is commonly 1.0 within the normally consolidated range and is less than 1.0 within the recompression range. However, depending on the depth of the compressible clay layer, and the magnitude of the total pressure being applied, the actual pressure-increment ratio in field construction loading may be many times greater

or smaller than unity. If the pressure-increment ratio is small, then the time compression curve may generally be represented by Type II curve in Figure 2. The shape of this Type II curve is dominated by secondary compression since primary compression is only a small portion of the total compression. An increase in pressure-increment ratio causes an increase in primary compression while secondary compression stays approximately constant. Therefore, Type I curve in Figure 2 is generally obtained for higher pressure-increment ratios.

The relationship between pressure-increment ratio and ratio of secondary to primary compression is shown in Figure 8. Secondary compression,  $R_s$  and primary compression,  $R_{100}$  were separated using Casagrande's method. The value of  $R_s/R_{100}$  decreases sharply as the ratio  $\frac{\Delta P}{P_0}$  increases up to one. The compression ratio continues to decrease although at a much slower rate, as  $\frac{\Delta P}{P_0}$  increases beyond a value of one. For peaty clay, as shown in Figure 8b, the secondary compression decreases from 80% to less than 20% of the primary compression as  $\frac{\Delta P}{P_0}$  increases from 0.5 to 4. This is significant in that it shows the relative importance of secondary to primary compression depending on the magnitude of field loading. The fact that a pressure-increment ratio of one happens to be approximately where the maximum rate of change in  $R_s/R_{100}$  occurs in Figure 8 may be an explanation of why field settlement rates often deviate from those predicted.

To investigate more closely the effect of pressure-increment ratio, the value of  $t_{100}$  was obtained using Casagrande's method whenever possible to calculate the coefficient of consolidation,  $C_v$ . These calculated values of  $C_v$  for Bay Mud Samples are plotted against void ratio in Figure 9. The data for overconsolidated clay shown on the right hand side of Figure 9 were obtained in the laboratory during the second cycle recompression of consolidation test Series D. It is seen that when the pressure-increment ratio is one or greater, no apparent effect on the value of  $C_v$  can be detected. However, for pressure-increment ratios of less than one, a large variation in  $C_v$  is noted. From Figure 9, higher  $C_v$  values are seen for overconsolidated clay and generally lower  $C_v$  values are obtained for normally consolidated clay when the pressure-increment ratio is less than one. It is recognized that at least a portion of this variation in  $C_v$  is due to the difficulty and inaccuracy in separating primary and secondary compressions at small pressure-increment ratios.

In Figures 10 and 11, permeability constants calculated from laboratory consolidation data are plotted against void ratio. It is noted that in Figure 10, calculated permeability constants deviate from the average values significantly for small values of  $\frac{\Delta P}{P_0}$  in normally consolidated clay. On the other hand, in the overconsolidated range, the calculated permeability constants for small  $\frac{\Delta P}{P_0}$  values agree reasonably well with the average values as shown in Figures 10 and 11. This suggests that, in a normally consolidated clay with a small pressure-increment ratio, the

time-compression curve is dominated by secondary compression (Type II curve in Figure 2). The accuracy in evaluating the value of  $C_v$  or permeability constant is therefore greatly reduced.

#### 4.4 Summary

Based on limited laboratory investigations as discussed above, it was found that the rate of secondary compression is approximately linear in a semi-logarithmic time-compression plot. The time required to reach this secondary stage in a time-compression curve is a function of the material and the standard one-day increment consolidation test may not be sufficient time for some of the more compressible soils. The coefficient was found to increase only slightly with increase in void ratio in a normally consolidated clay. Generally speaking, the magnitude of secondary compression is relatively small in overconsolidated clay but increases rapidly when the precompression pressure is approached. This phenomenon is related to pressure-increment ratio. In an overconsolidated clay, the coefficient of secondary compression increases with an increase in pressure-increment ratio. In a normally consolidated clay, however, the coefficient of secondary compression was found to be independent of pressure-increment ratio.

The pressure-increment ratio was also found to have a profound effect on the ratio of secondary to primary compression and, as a result, on the overall shape of the time-compression curve. Therefore, if the laboratory time-compression data are to be used in predicting a field time-settlement relationship, the laboratory loading schedule should closely reflect the stresses applied to the soil in situ. The laboratory  $e$ -log  $p$  curves obtained in this investigation show little or no effect produced by change in pressure-increment ratio. Since the magnitude of settlement is ordinarily predicted from this  $e$ -log  $p$  curve, the standard procedure of using a pressure-increment ratio of one in a consolidation test appears to produce no significant error in a settlement analysis as far as the total settlement is concerned.

## CHAPTER 5

### METHODS OF SETTLEMENT CALCULATION

This chapter describes in abbreviated detail first, how amount and rate of settlement are calculated using Terzaghi's theory, and then two refined methods that account for secondary compression as well as primary compression.

#### 5.1 Settlement by Terzaghi's Theory

##### 5.1.1 Magnitude of Settlement

It is assumed that the total settlement of a structure resting on a compressible soil may be separated into the three components previously defined, namely, immediate settlement, primary compression, and secondary compression. Total settlement can therefore be represented by the equation

$$S_f = S_i + S_c + S_s$$

where  $S_f$  = the final total settlement

$S_i$  = immediate settlement calculated from theory of elasticity by considering Poisson's ratio to have some value other than zero.

$S_c$  = total compression due to primary consolidation calculated from one-dimensional theory of consolidation.

$S_s$  = secondary compression determined from laboratory consolidation tests.

Assuming that secondary compression takes place only after primary compression is complete, or that secondary compression may be initially neglected, the total settlement,  $S_t$ , at time  $t$  after load application, is

$$S_t = S_i + US_c$$

where  $U$  is the degree of consolidation at time  $t$  as evaluated from Terzaghi's theory. If the geometrical configuration is such that  $S_i$  may also be neglected (such as a fill extending over a horizontal area sufficiently large to result in one-dimensional compression only of underlying soils), then the above equation can be further simplified to

$$S_t = US_c$$

which is the equation commonly used in a simplified settlement calculation based only on Terzaghi's theory. Since  $S_c$  is equal to  $S_t$  at  $U = 100$  percent, the magnitude of  $S_c$  represents the total expected settlement and is computed from consolidation test data by the equation

$$S_c = \frac{h}{1+e_1} \Delta e$$

in which  $h$  is the total thickness of the compressible soil layer,  $e_1$  is the initial void ratio before load application, and  $\Delta e$  is the total void ratio change due to the net increase of pressure in the soil layer as a result of the load application. The quantity  $\Delta e$  is usually obtained by interpolation from the void ratio versus logarithm of pressure ( $e - \log p$ ) curve constructed from consolidation test data from representative, undisturbed soil samples.

According to the above assumption that secondary compression takes place only after primary compression is complete,  $S_t$  includes no part of the secondary compression. However, in a standard laboratory consolidation test of one-day duration per load increment, usually no attempt is made to separate the secondary compression from the primary compression in calculation and plotting of the void ratio versus pressure relationship. As a result, the calculated total settlement,  $S_t$  or  $S_c$ , in fact does include some part of the secondary compression since secondary compression occurs both during and after primary compression. This is a direct contradiction of theory and practice in that the secondary compression neglected in the theory is usually included, at least partly, in calculated settlement. It is of interest to note that this procedure inadvertently results in improving the agreement between predicted and actual settlement. The conventional method of settlement calculation as cited above is widely accepted as being sufficiently accurate with regard to magnitude of total settlement. In Figure 12, void ratio versus log pressure curves are plotted to show the differences between compressions at the end of one-day load increments, five-day load increments, and primary compressions. It may be seen that even for a peat which shows a significant amount of secondary compression, the one-day increment test can generally account for a large part of the secondary compression. Obviously, the difference between predicted settlement and actual settlement will increase with an increase in either or both the rate of secondary compression and the ratio of secondary to primary compression. As pointed out in the preceding chapter, since the ratio of secondary to primary compression is affected by the pressure-increment ratio, the actual field stress application should be considered in conducting laboratory consolidation tests. In practice, since the actual field stress application is not always known during

the design stage, and also since the field stress distribution varies both vertically and laterally, the laboratory consolidation tests should be designed to cover the probable range of field stress variations. Furthermore, for soils having large coefficients of secondary compression and low permeabilities, the duration of laboratory consolidation tests should be extended to include a sufficient amount of secondary compression so that the long-term prediction of settlement may be realistic.

### 5.1.2 Rate of Settlement

It is generally recognized that the prediction of settlement rate is far more difficult than the prediction of amount of settlement. This may be due largely to the complex nature of soil deposits and the difficulty in identifying the various soil layers and their field drainage conditions. Also, the presence of secondary compression will cause the time-compression relationship to deviate from that predicted by the hydrodynamic theory of consolidation.

The conventional method of predicting the time-compression relationship using Terzaghi's theory may be described as follows. It can be shown that Terzaghi's theory would yield a solution to a consolidation process of the form

$$U (\%) = f (T)$$

where the percent consolidation,  $U$ , is expressed as a function of a dimensionless time factor,  $T$ . The value of  $T$  depends on the initial distribution of pore water pressure with respect to depth and may be related to other parameters as

$$T = \frac{C_v}{H^2} t$$

in which  $H$  is the longest drainage path,  $t$  is the time required for a corresponding percent consolidation  $U$ , and  $C_v$  is the coefficient of consolidation whose value depends on the permeability constant  $k$ , average void ratio  $e$ , coefficient of compressibility  $a_v$ , unit weight of water  $\gamma_w$ , and may be expressed as

$$C_v = \frac{k(1+e)}{a_v \gamma_w}$$

When the value of  $C_v$  is determined from a laboratory consolidation test on undisturbed soil sample, the above equations may be used to calculate the time required for hydrodynamic consolidation to take place at various stages of  $U$  in a laboratory specimen as follows:

$$t_s = \frac{TH_s^2}{C_v}$$

where  $H_s$  is the longest specimen drainage path,  $t_s$  is the time required for the laboratory specimen to consolidate to a given  $U$ , and  $T$  is the time factor for a given  $U$ . The corresponding time in the field,  $t_f$ , for the same degree of consolidation,  $U$ , may then be calculated from

$$t_f = \left(\frac{H_f}{H_s}\right)^2 t_s$$

where  $H_f$  is the longest field drainage path. Since the relationship between  $U$  and  $T$  is known in Terzaghi's theory, the above procedure is rather simple for practical usage.

In actual investigations of field consolidation, problems such as erratic soil profile, variation of material in a soil layer, uncertainty in field drainage conditions (including drainage in the horizontal direction), time-dependent loading, etc., must be considered. Even with the absence of these complicating factors, the predicted time-settlement relationship will not agree with the actual time-settlement curve in that the calculated curve must always be asymptotic to the horizontal at 100 percent consolidation as a direct result of the basic assumption in Terzaghi's theory. This difference will become more pronounced with an increase in the rate of secondary compression. Figure 13 contains a laboratory time-compression curve and two similar curves calculated by the conventional method using parameters obtained from the laboratory time-compression curve. It may be noted that when only primary compression is considered, the calculated time-compression curve agrees fairly well with the laboratory curve for nearly 90 percent of the primary compression. The secondary compression is then completely neglected. This is likely to occur when a standard one-day increment consolidation test is used for a soil that exhibits fairly large secondary compression. On the other hand, if a long term consolidation test is performed and the total compression is taken as a basis for predicting the time-compression relationship, then Figure 13 indicates that while the total final compression will be more accurately predicted, the calculated time-compression relationship will deviate from that measured. The difference will increase with an increase in the ratio of secondary to primary compression.

## 5.2 Some Refined Methods of Time-Settlement Calculation

In the preceding discussion, the discrepancies between actual and predicted compressions are clearly shown. These discrepancies will continue to exist as long as the conventional method of settlement calculation based on Terzaghi's theory is being applied to a soil in which secondary compression plays a significant role. Various rheological models of consolidation have been proposed as

modifications to Terzaghi's theory to include the behavior of soil exhibiting secondary compression. Mathematical expressions derived from these models generally show more closely the true consolidation characteristics of soil exhibiting secondary compressions. However, since the parameters used in these mathematical expressions must be obtained from the laboratory time-compression curves, these refined methods may be viewed, in a sense, only as curve fitting methods. The methods proposed by Wahls (33) and Hansen (11) will be discussed here.

### 5.2.1 Wahls' Method

Wahls (33) proposed a mathematical model wherein both primary and secondary compressions start at the same time in the overall consolidation process, but at different rates. At the end of primary compression, the relationship between void ratio changes is

$$\Delta e_{100} = \Delta e_{\text{primary}} + \Delta e_{\text{secondary}}$$

where  $\Delta e_{100}$  is the total void ratio change at the end of primary compression. Beyond this point all additional change in void ratio must be due to secondary compression only. Wahls' equation for calculating the total compression at any time is as follows:

$$R_t = R_1 + R_2 = A_p \Delta P f(T) + C_{\alpha} h(T)$$

where  $R_t$  = total compression at time  $t$ .

$$R_1 = A_p \Delta P f(T) = \text{primary compression.}$$

$A_p$  = constant representing the compressibility of soil based on hydrodynamic theory of consolidation.

$\Delta P$  = pressure increment.

$f(T)$  = a function of the time factor  $T$  that contributes to primary compression.

$$R_2 = C_{\alpha} h(T) = \text{secondary compression.}$$

$C_{\alpha}$  = coefficient of secondary compression.

$h(T)$  = a function of the time factor  $T$  that contributes to secondary compression.

The time-compression relationship represented by the above equation can be calculated by an empirical procedure developed by Wahls, the details of which are presented in Appendices C and E. Since the soil parameters  $A_p$  and  $C_{\alpha}$  must be determined from laboratory test data, the accuracy of the field time-settlement

relationship predicted from this method is solely governed by the time-compression relationship obtained in the laboratory consolidation test.

Two hypothetical time-settlement relationships predicted from laboratory tests using different pressure-increment ratios are shown in Figures 14 and 15. It should be noted that when the total settlement is given the time-settlement relationship is largely a function of the shape of the laboratory consolidation curve. Generally, a higher pressure-increment ratio results in settlement occurring faster than those with smaller pressure-increments ratios. Since the laboratory time-compression curve depends on the pressure-increment ratio, it may be concluded that the field loading condition must be closely reproduced in the laboratory before this method can be applied to predict the field time-settlement relationship. Also shown in Figures 14 and 15 are time-settlement curves calculated from Terzaghi's theory. These curves were calculated using a pressure-increment ratio of one and assuming the same amount of total settlement. It may be noted that since no secondary compression is predicted by Terzaghi's theory, latter parts of settlements are shown to occur earlier than predicted from Wahls' method. It is also noted that the settlement curves calculated by Wahls' method using pressure-increment ratios greater than one will predict even faster settlements, especially in the range of primary compression. When Wahls' method is used for curve fitting of laboratory test data, there is excellent agreement between measured and calculated curves in the secondary compression range, as shown in Figure 16.

### 5.2.2 Hansen's Method

Hansen's method (11) is an approximate mathematical expression for calculating the time-compression relationship based on laboratory consolidation curves and involving a series of approximations. Hansen also considered that both primary and secondary compressions start simultaneously but with different rates. His mathematical expression for the total compression at any time  $t$  after application of load is

$$E_t = \frac{E_s}{\sqrt[6]{\frac{H^6}{C_s^3 \left(t \log_{10} \frac{t+5t_s}{5t_s}\right)^3 + \frac{1}{\left(\log_{10} \frac{t+t_s}{t_s}\right)^6}}}}$$

where  $E_t$  = total compression at time  $t$  expressed as percent of the total thickness of soil layer.

$H$  = longest drainage path of soil layer.

$E_s$ ,  $C_s$ ,  $t_s$  are characteristic soil constants determined from laboratory time-compression curves.

Hansen's method is also basically a curve fitting method whose accuracy and applicability depend on the laboratory data. Examples of applying Hansen's method in calculating the time-compression relationship are also shown in Figure 16. When the characteristic constants are easily determined, the agreement between laboratory measured and calculated curves is reasonably good. To apply this method in predicting the field time-settlement relationship, the field conditions must be closely reproduced in the laboratory since the basic assumption in this method is that the consolidation characteristics exhibited in the laboratory are representative of field behavior. A brief description of Hansen's method is presented in Appendix D.

### 5.3 Summary

In a conventional settlement analysis where laboratory test results are used and Terzaghi's theory is assumed to apply, and the total compression for each load increment is used for calculating the void ratio versus pressure relationship, the predicted time-settlement relationship will generally deviate from that established by field measurements. The difference increases with rate and amount of secondary compression.

Improved methods of calculating the time-settlement relationship such as Wahls' and Hansen's methods are available. These methods account for secondary compression by combining it with primary compression. When these methods are used in calculating the laboratory time compression relationship, generally a better agreement may be obtained between predicted and measured field settlements. However, it must be observed that these methods are primarily curve fitting methods based on the assumption that laboratory characteristics are representative of field behavior. Factors such as field drainage conditions, representativeness of specimen and field loading conditions must be considered. Since a time-settlement curve is affected by pressure-increment ratio, the accuracy of predicted settlement rate may be improved by simulating the in-situ loading conditions in laboratory consolidation tests. This requires a clear identification of the location of compressible clay layers and their drainage conditions since the field pressure-increment ratio varies with depth.

## CHAPTER 6

### STUDY OF FIELD SETTLEMENT DATA

Records of eight field projects were reviewed to compare measured settlements with predicted settlements and to ascertain the contributions by secondary compression to the total observed settlements.

In the first phase of the review, five projects, all constructed at least 6 years ago, were selected and the time-settlement relationships predicted from Terzaghi's theory were compared with measured settlements. An attempt was made to compare coefficients of secondary compression determined from plots of field data with those determined from original laboratory test data.

A second review phase was conducted to compare measured settlements with time-settlement relationships predicted by Wahls' method. Since this method requires tests of sufficient duration to clearly establish the secondary portion of the time-compression curve and varying pressure-increment ratios to simulate field loading conditions, three projects at two locations were selected from which samples were easily obtainable. Two of the projects were constructed several years ago and were sampled during this investigation whereas the third was in the design state at the time of this study and samples were already available in the laboratory. Tests on samples from this second phase of the field data review were discussed in Chapter 4 and comprised Test Series F-J.

#### 6.1 Project Review - First Phase

##### 6.1.1 San Diequito River Basin

The San Diequito River Basin is filled with typical marsh land soils of soft silts and clays extending to a depth of 30 feet or more and is about 6400 feet wide where it is crossed by the roadway. Over these soft soils, an embankment with a maximum height of 90 feet was constructed in 1962 at a controlled rate of three feet per week. The resulting settlement for a 5 year period is shown in Figure 17a for Station 1278+50 where the embankment height is 61 feet. The plot of field data indicates that practically all the settlements due to primary compression ceased about one year after completion of the embankment. The plot also shows that subsequent settlement, presumably due to secondary compression, continues at a rate of about 0.52 percent per log cycle. This rate agrees very well with the average rate of 0.56 percent per cycle determined from old test data which are summarized in Table B-1.

In estimating the time-settlement relationship from laboratory data, it was assumed that compression within layers 1 and 4 would be instantaneous. Two time-settlement curves were then developed using Terzaghi's theory and considering different drainage conditions within layers 2 and 3 as shown in Figure 17a.

It is noted that the measured settlements occurred much faster than those predicted. One of the possible sources of error is the difference between field and laboratory loading conditions. The field loading is linear with a pressure-increment ratio varying with depth but generally much greater than one. Thus the ratio of primary to secondary compression is increased which results in a change in shape of the time-compression curve. As previously discussed, settlement under such conditions occurs faster than that predicted from a standard consolidation test with a pressure-increment ratio of one or less. Another possible source of error is that field drainage conditions may be quite different from that assumed. Also, the permeability constant and coefficient of consolidation, evaluated from laboratory tests, may be different under different loading conditions as shown previously in the laboratory investigation. All these factors may contribute to the inaccurate prediction of the time-settlement relationship.

#### 6.1.2 Los Penasquitos Lagoon

Subsoil conditions at this site consist of about 15 feet of soft compressible soil underlain by dense sand. As shown in Table B-2, the consolidation data indicate an average coefficient of secondary compression of 0.40 percent per log cycle of time compared to 1.20 percent from field measurements. However, field measurements were discontinued prematurely on this project and hence reliable secondary compression data were not obtained. The actual rate of field secondary compression probably would have been determined to be less than 1.20 percent if settlement measurements had been continued for a longer period.

The theoretical time-settlement curve based on Terzaghi's theory in Figure 17b shows that predicted settlement occurs faster than measured settlement. Again, differences in the loading and drainage conditions may exist between laboratory and field although the agreement between predicted and measured settlements seems to be reasonably good.

#### 6.1.3 Arcata - 4th Street Interchange

At this project site, 18 feet of compressible soils exist between depths of 15 and 33 feet. Figure 17c shows that the measured settlement occurred faster than was predicted from theory. This may suggest a better field drainage condition than that assumed in the calculation. It is also likely that

primary compression was still going on when field measurements were discontinued as indicated by Figure 17c. The coefficient of secondary compression from previous laboratory tests is 0.58 percent as shown in Table B-3.

#### 6.1.4 Lindsay Creek Bridge

Subsurface soil conditions at this project site were rather complex with alternate layers of compressible silty clays and less compressible silts to a depth of approximately 40 feet. Previous laboratory data indicate a fairly small coefficient of secondary compression of 0.2 percent compared to the value of 0.32 percent obtained from field measurements (Table B-4). The time-settlement relationships, measured and predicted from Terzaghi's theory, are shown in Figure 17d. The assumptions of elastic settlements for layers 1 and 3, and single drainage condition for layers 2 and 4 were made in the theoretical calculation of settlement. The agreement between predicted and measured field settlements appears to be reasonable for both primary and secondary compressions, but the measured settlement occurred faster than was predicted.

#### 6.1.5 San Ramon Road Crossing, Abutment 1

Settlement records are available for this project at Stations 27+70 and 28+90. The foundation soils at these locations consist of soft silts and clays extending to a depth of approximately 40 feet. The measured and predicted time-settlement curves are shown in Figure 17e. Again, the actual settlements occur at a faster rate than predicted, indicating a possible inaccuracy in the assumed field drainage conditions. As presented in Table B-5, the predicted coefficients of secondary compression are 0.20 and 0.25 percent, respectively, compared to measured values of 0.30 and 0.44 percent. However, the field condition is complicated by the removal of surcharge at about one year after loading which may have affected the measured rate of secondary compression.

#### 6.1.6 Summary of Phase One Data Review

From the above review of settlement and laboratory data from five embankments, it appears that a reasonable agreement generally exists between field and predicted coefficients of secondary compression. Some of the factors affecting the accuracy of predicted secondary compression are the difficulty in identifying the soil layers exhibiting secondary compression, complicated field drainage conditions, insufficient time allowed in laboratory consolidation tests, and the difference between field and laboratory loading conditions. Factors that affect field settlement data, and consequently the agreement between predicted and measured settlements, are non-linear embankment

loading, removal of surcharge load, and the immediate settlements that occur during construction. Also, the field pressure-increment ratio may be so large that some degree of plastic deformation may occur either locally or on a fairly large scale during construction. This type of creep continues for some time after construction and is measured as part of the settlement.

## 6.2 Project Review - Second Phase

Two projects for which long term field settlement data are available were selected for analysis of their time-settlement relationships using Wahls' method. The first project is the Antioch Bridge north approach fill which is constructed on thick, highly compressible peats. The second project is at West Avalon Boulevard in Los Angeles where the embankment is underlain by 54 feet of rather uniform silty clay. Laboratory consolidation tests designed to simulate the field loading conditions were performed on samples taken from these two sites. The results of these settlement analyses are described below.

### 6.2.1 Old Antioch Bridge North Approach (Non-Sand Drain Area), Station 70+82

At this location, the roadway embankment, 8.7 feet high, is underlain by 27 feet of compressible peat which is underlain by 40 feet of soft peaty clay. The amount of settlement 13 years after construction is 7 feet out of an estimated ultimate settlement of 8.5 feet. From the measured time-settlement curve, it appears that about 50 percent of the total settlement is due to secondary compression.

In time-settlement calculations using laboratory test data, single drainage was assumed for both peat and soft peaty clay layers. To show the effect of pressure-increment ratio on the time-settlement relationship, an analysis was made first using Wahls' method and laboratory data obtained from a pressure-increment ratio of one for both layers. Time-settlement curves were obtained separately for each layer and then added to obtain the total curve as shown in Figure 18a. It may be seen that the general time-settlement relationship agrees reasonably well with field measured settlement. However, when the actual field loading condition is considered, it becomes apparent that the top layer of peat was subjected to a much higher pressure-increment ratio (about 2.75) than that of the lower peaty clay layer (0.8). To account for this difference in pressure-increment ratio, a second time settlement calculation was made, again using Wahls' method but with a laboratory time-compression curve obtained from a pressure-increment ratio of 2.5 for the top peat layer. For the bottom layer, the previous time-compression curve for a pressure-increment ratio of unity was

used. The results are plotted in Figure 18b. It may be noted that the change in pressure-increment ratio for the top layer results in a shift of the total time-settlement curve toward the left, or a faster occurrence of settlement. Furthermore, it is observed that the new curve will improve the accuracy of the calculated time-settlement relationship. Moreover, the general trend that field settlements frequently occur faster than those predicted may be explained by this effect of pressure-increment ratio of time-settlement curves.

In both Figures 18a and 18b, the time-settlement curve calculated from Terzaghi's theory is also shown. This curve was obtained by considering two layers separately and then superimposing to obtain the total time-compression. However, since the total settlement of 8.5 feet at this location is used as the 100% consolidation in Terzaghi's method, the calculated curve results in settlements occurring much faster than those measured. Another point to note about this curve is that it appears to show secondary compression taking place which should not exist in a curve predicted from Terzaghi's theory. The portion of the curve appearing as a secondary tail is actually the settlement due to primary compression of the bottom peaty clay layer lagging in time due to lower permeability and longer drainage path. When subsurface conditions are rather complicated, such as by the existence of extremely low permeability layers interspersed with strata of higher permeabilities, or by difficult drainage conditions in general, the above observation indicates that it is possible to confuse primary compression for secondary compression.

#### 6.2.2 Old Antioch Bridge North Approach (Sand Drain Area)

A location where vertical sand drains were used to facilitate the consolidation process was also selected for time-settlement analysis. As shown in Figure 19, the compressible soils extend to a depth of 56 feet and consist of 26 feet of peat, 15 feet of clayey peat, and 15 feet of soft peaty clay. The amount of settlement 13 years after construction under 15.4 feet of embankment is 14.2 feet and it is estimated that the ultimate settlement will reach 15.2 feet. The vertical sand drains are spaced 10 feet on center and extend to a depth of approximately 40 feet.

In the analysis using Wahls' method, the time-settlements of the three layers were calculated separately based on different laboratory time-compression curves available. The time-settlements for the top two layers were obtained using a coefficient of consolidation calculated from the horizontal permeability constant determined from field permeability tests, and a coefficient of compressibility determined in the laboratory. The time-settlement for the bottom clay layer was obtained using a coefficient of

consolidation obtained from a laboratory consolidation test since the field drainage of this layer is in the vertical direction. The total time-settlement curve was obtained by adding the curves for the three layers. It is seen from Figure 19 that the calculated total time-settlement agrees reasonably well with the measured settlement despite the fact that the pressure-increment ratios used in the laboratory tests were smaller than those in the field. It is expected that the agreement would be somewhat improved with closer simulation of field loading conditions in the laboratory.

### 6.2.3 West Avalon Boulevard, Station 584+58

Approximately ten years of settlement measurements are available at this location. The total embankment height was 29 feet from which a 10-foot surcharge was removed three months after placement of the fill. In Figure 20, this removal of surcharge is seen to have affected the time-settlement curve only temporarily after which the settlement continued at approximately the same rate in semi-log time-compression plot. The amount of settlement after 10 years is about 4 feet and the estimated ultimate settlement is 4.75 feet.

The subsurface exploration and subsequent laboratory tests showed that the compressible soil under the fill is a medium stiff silty clay of medium to high plasticity to a depth of 54 feet underlain by medium dense sand. A time-settlement analysis was performed using Wahls' method after dividing the 54-foot layer into three 18-foot layers. The analysis was made first with a constant pressure-increment ratio of unity and then with a varying pressure-increment ratio. A time-settlement curve was also calculated from Terzaghi's theory assuming an ultimate settlement of 4.75 feet.

In Figure 20a, time-settlement curves are shown for each layer and for total settlement calculated from laboratory consolidation test data using a constant pressure-increment ratio of one. The agreement between the calculated and measured settlements is rather poor. This is probably due to the fact that the laboratory curves, based on a pressure-increment ratio of one, are not representative of field loading conditions. In Figure 20b, time-settlement curves are shown using laboratory data for pressure-increment ratios of 3.5, 2.0, and 1.67 for top, middle, and bottom layers respectively. The total curve in this case agrees fairly well with the measured time-settlement relationship.

From the results obtained in this example of comparing the calculated and measured time-settlement relationships, it may be noted that the pressure-increment ratio plays an important role in the accuracy of the settlement rate prediction. Wahls' method is generally more favorable compared to the conventional method

based on Terzaghi's theory in predicting the overall time-settlement relationship. Also, it should be noted that the field time-settlement curve sometimes may be misleading in that it shows generally an early completion of primary compression and a much greater ratio of secondary to primary compression than actually exists. This is due to the fact that the apparent secondary portion of the measured settlement is actually primary compression of layers with difficult drainage conditions lagging in time.

### 6.3 Settlement Analysis of A Future Project (Wahls' Method)

Based on the favorable comparison between the field measured settlement data and the calculated time-settlement relationship as described in the preceding section, it was decided to use Wahls' method of time-settlement analysis for a highway embankment currently in the design state. The project chosen is the New Antioch Bridge North Approach located just a few hundred feet west of the existing approach fill. The subsurface material consists of an average of 12 feet of peat overlaying silty sand or silty clay. The water content of the peat ranges from about 100% to over 500%. The proposed embankment is from 3 feet to 5 feet in height.

Assuming that the peat underlying the proposed embankment is of the same type as that under the existing embankment, and that their consolidation characteristics are similar, two sets of time-settlement calculations were performed. The consolidation test data of peat at a water content of 185% are shown in Figure 21a. Two time-compression curves representative of pressure-increment ratios approximately equivalent to 3 feet and 5 feet of embankment were developed from test data. The time-settlement relationships based on Wahls' method were calculated from these two time-compression curves and are shown in Figure 21b. It was assumed that settlement would result solely from consolidation of the peat layer and that double drainage conditions would exist. Appropriate corrections may be made should the field conditions deviate significantly from those assumed. In Figures 22a and 22b, similar laboratory consolidation data and calculated time-settlement relationships are shown for a peat layer with a water content of 520%.

It was hoped that the water contents of 185% and 520% used in this analysis would cover the range of moisture variation in the peat so that intermediate conditions may be evaluated by interpolation. In Figures 21a and 22a, the time-compression curves are from those available (Test Series F) and the actual field pressure-increment ratio may be slightly different from those used in the laboratory. However, it is believed that a quantitative comparison of these predicted settlements and actual field settlements are possible by taking into account the variation in water content, pressure-

increment ratio, thickness of clay, and drainage condition between assumed and actual conditions.

#### 6.4 Summary

Field drainage conditions and pressure-increment ratios are important factors in predicting time-settlement relationships. A measured time-settlement curve represents the overall picture of combined primary and secondary compressions in various layers of soils with different consolidation characteristics, different stress conditions, and different drainage conditions. The conventional method of time-settlement analysis based on Terzaghi's theory and the standard consolidation test usually involves oversimplified assumptions regarding these factors. When secondary compression is important, the discrepancy between measured rate of settlement and calculated rate of settlement using the conventional method may be large.

When the conventional method based on Terzaghi's theory is used in calculating the rate of settlement, the accuracy is largely affected by the presence of secondary compression. When secondary compression is important, calculated settlements generally occur faster than field settlements because no secondary settlement is considered in the theory. On the other hand, when secondary compression is relatively small compared to primary compression, calculated settlements generally lag in time. This is due, at least partly, to the difference between field and laboratory pressure-increment ratios, the field value usually being greater than that used in the laboratory.

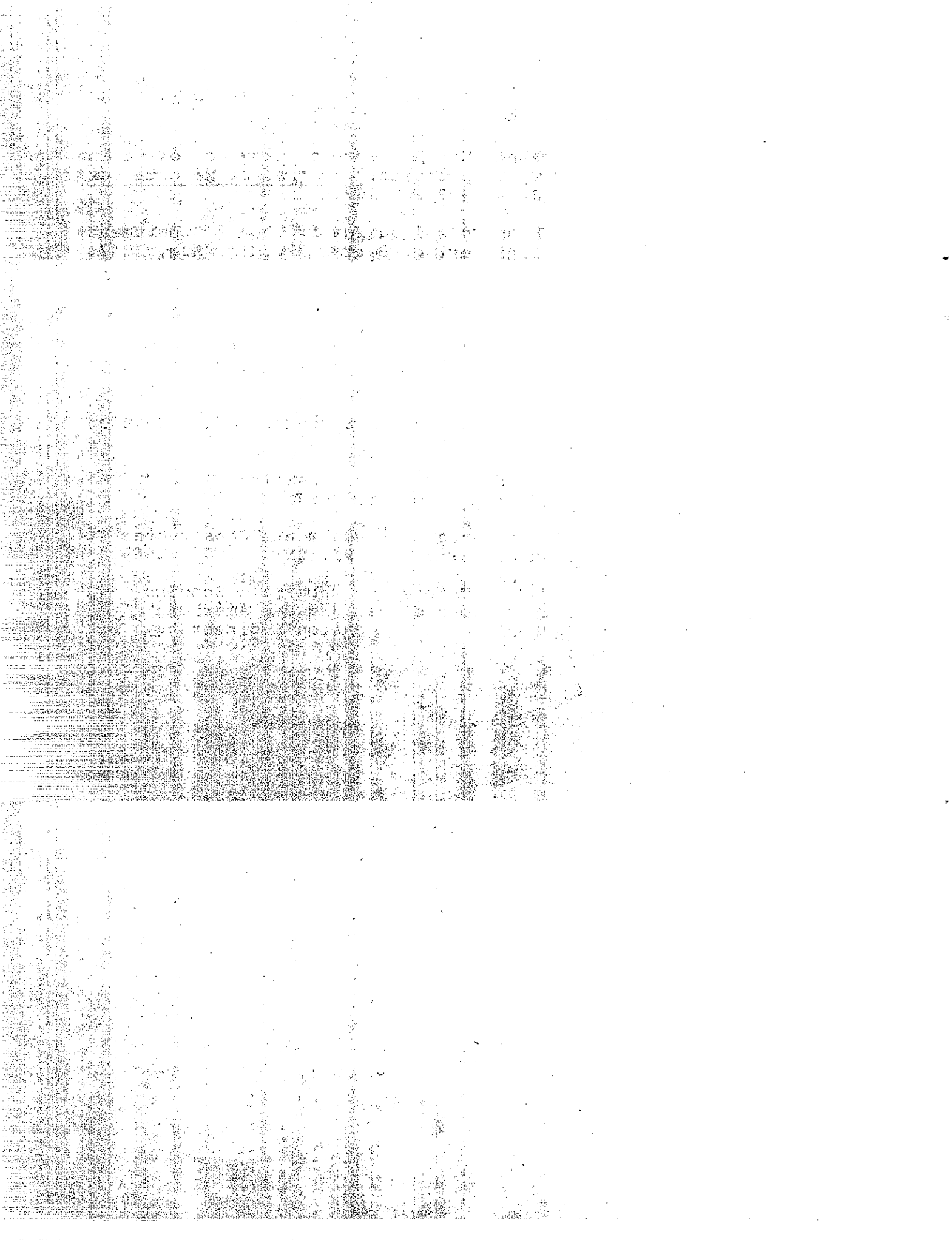
Wahls' method is based on simultaneous primary and secondary compressions and, therefore, will generally result in a better agreement between predicted and measured time-settlement curves than can be obtained by the conventional method. Results from the use of Wahls' method can be further improved if field loading conditions are closely simulated in a carefully designed laboratory test program.

## REFERENCES

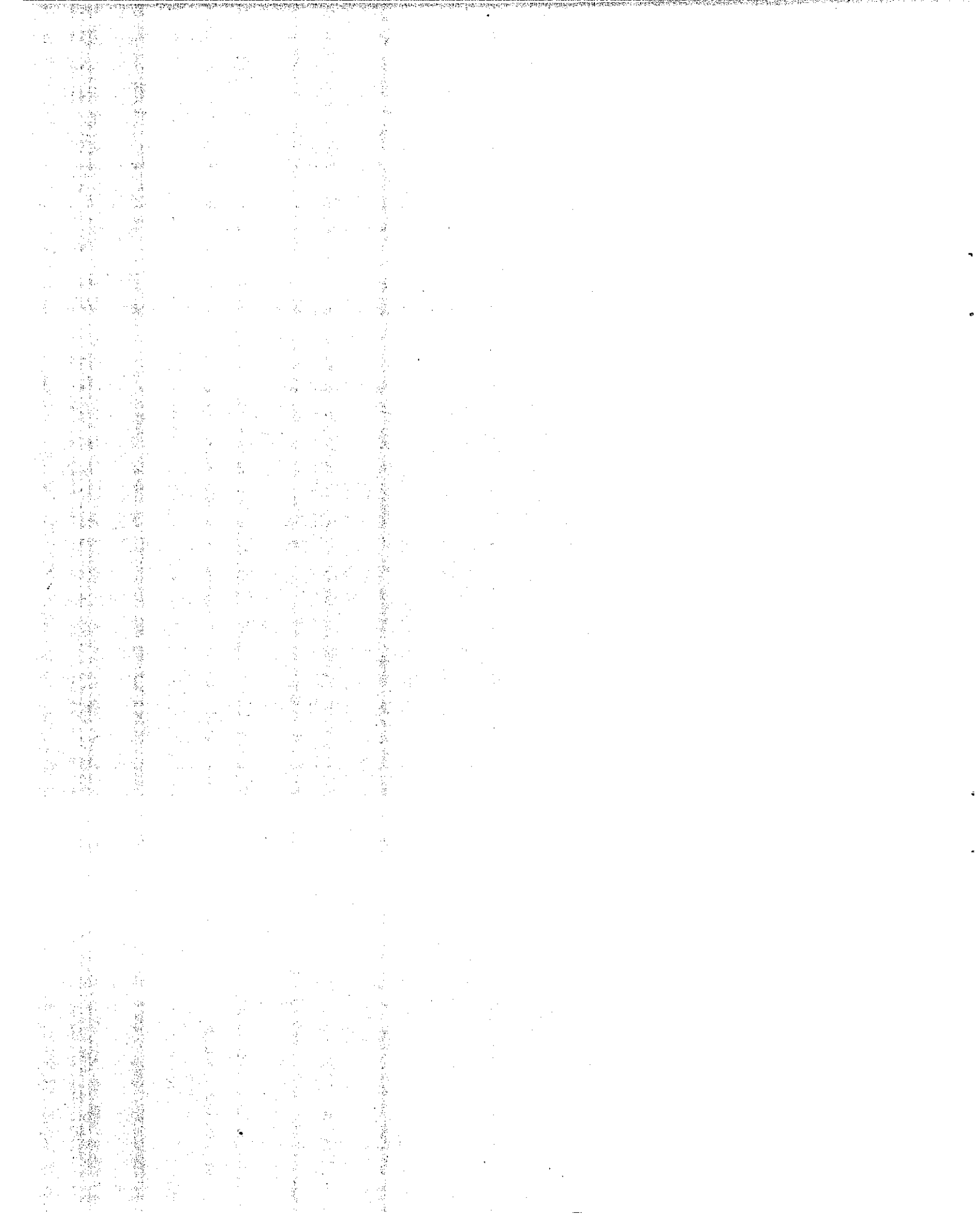
- (1) Barden, L. "Primary and Secondary Consolidation of Clay and Peat." Geotechnique, Vol. 18, March 1968, p. 1.
- (2) Barden, L. "Time Dependent Deformation of Normally Consolidated Clays and Peats." Journal, SMFD, ASCE, SMI, January 1969, p. 1.
- (3) Buisman, A.S.K. "Results of Long Duration Settlement Tests." Proceedings, 1st International Conference on Soil Mechanics and Foundation Engineering, Vol. 1, p. 103, 1936.
- (4) Burn, K. N. "Settlement of A High Embankment and Overpass Structures in Ottawa." Canadian Geotechnical Journal, Vol. 6, p. 33, 1969.
- (5) Burn, K. N. and Hamilton, J. J. "Settlement of an Embankment on Leda Clay." Canadian Geotechnical Journal, Vol. 5, No. 1, Feb. 1968, p. 16.
- (6) Casagrande, A. "The Structure of Clay and its Importance in Foundation Engineering." Journal, Boston Society of Civil Engineers, April 1932.
- (7) Casagrande, A. and Fadum, R. E. "Application of Soil Mechanics in Designing Building Foundations." Transactions, ASCE, 1944.
- (8) Cedergren, H. R. and Weber, W. G. "Subsidence of California Highways." ASTM, STP No. 322, p. 248, 1962.
- (9) Davis, E. H. and Poulos, H. G. "The Use of Elastic Theory for Settlement Prediction Under Three-Dimensional Conditions." Geotechnique, Vol. 18, No. 1, March 1968, p. 67.
- (10) DeJong, J. "Consolidation Models Consisting of an Assembly of Viscous Elements or a Cavity Channel Network." Geotechnique, Vol. 18, June 1968.
- (11) Hansen, J. B. "A Model Law for Simultaneous Primary and Secondary Consolidation." Proceedings, 5th International Conference on Soil Mechanics and Foundation Engineering, Vol. 1, p. 133, 1961.
- (12) Horn, H. M. and Lambe, T. W. "Settlements of Buildings on MIT Campus." Journal, SMFD, ASCE, Vol. 90, SM5, p. 181, 1964.
- (13) Horn, H. M., and Lambe, T. W. "Closure on Discussion, Settlements of Buildings on MIT Campus." Journal, SMFD, ASCE, Vol. 92, May 1966, p. 149.

- (14) Janbu, N. "Soil Compressibility as Determined by Oedometer and Triaxial Tests." Proceedings, European Conference on SMFE, Vol. 1, p. 19, 1963.
- (15) Kern, P. "Discussion on Settlements of Buildings on MIT Campus." Journal, SMFD, ASCE, Vol. 91, SM5, Sept. 1965, p. 95.
- (16) Kleiman, W. F. "Use of Surcharge in Highway Construction." Journal, SMFD, ASCE, Vol. 90, SM5, Sept. 1964, p. 331.
- (17) Ladd, C. C. and Preston, W. E. "On the Secondary Compression of Saturated Clays." Soils Publication, No. 181. MIT, 1965.
- (18) Leonards, G. A., and Girault, P. "A Study of the One-dimensional Consolidation Test." Proceedings, 5th International Conference on Soil Mechanics and Foundation Engineering, Vol. 1, p. 213, 1961.
- (19) Leonards, G. A. and Altschaeffl, A. G. "Compressibility of Clays." Journal, SMFD, ASCE, Vol. 90, SM5, 1964, p. 133.
- (20) Leonards, G. A. and Ramiah, B. K. "Time Effects in the Consolidation of Clays." ASTM, STP, No. 254, 1959, p 116.
- (21) Lo, K. Y. "Secondary Compression of Clays." Journal, SMFD, ASCE, Aug. 1961, SM4, p. 61.
- (22) Newland, P. L. and Allely, B. H. "A Study of the Consolidation Characteristics of a Clay." Geotechnique, Vol. 10, No. 2, p. 62, 1960.
- (23) Skempton, A. W. and Bjerrum, L. "A Contribution to the Settlement Analysis of Foundations on Clay." Geotechnique, Vol. 7, Dec. 1957, p. 168.
- (24) Smith, T. W., Hirsch, A. D. and Kleiman, W. F. "Long Range Settlement Study at Bridge Approaches." Interim Report, Highway Research Report, Materials and Research Department, California State, Division of Highways, 1968.
- (25) Spangler, M. G. and Griebing, A. L. "Foundation Settlements in the Ft. Randall Dam Embankment." Highway Research Board, Bulletin 173, p. 1.
- (26) Spangler, M. G. "Further Measurements of Foundation Settlements in the Ft. Randall Dam Embankment." Highway Research Record, No. 223, p. 60.
- (27) Tan, T. K. "Secondary Time Effects and Consolidation of Clays." Academia Sinica, Institute of Civil Engineering and Architecture Harbin, China, June 1957.

- (28) Taylor, D. W. Fundamentals of Soil Mechanics, John Wiley and Sons, Inc., New York, 1948.
- (29) Taylor, D. W. and Merchant, W. "A Theory of Clay Consolidation Accounting for Secondary Compression." Journal of Mathematics and Physics, Vol. 19, July 1940, p. 167.
- (30) Taylor, D. W. "Research on Consolidation of Clay." Department of Civil and Sanitary Engineering. Serial 82, MIT, Aug. 1942.
- (31) Terzaghi, K. "Erdbaumechanik auf bodenphysikalischer Grundlage." Leipzig, Denticke, 1925.
- (32) Terzaghi, K. "Undisturbed Clay Samples and Undisturbed Clays." Journal, Boston Society of Civil Engineers, Vol. 28, No. 3, July 1941.
- (33) Wahls, H. E. "Analysis of Primary and Secondary Consolidation." Journal, SMFD, ASCE, SM6, Dec. 1962, p. 207.
- (34) Walker, L. K. "Secondary Settlement in Sensitive Clays." Canadian Geotechnical Journal, Vol. 6, 1969.
- (35) Weber, W. G., Jr., "Performance of Embankments Constructed Over Peat." Journal, SMFD, ASCE, Vol. 95, SM1, p. 53, 1969.
- (36) Zeevaert, L. "Consolidation Theory for Materials Showing Intergranular Viscosity." Proceedings, 3rd Pan American Conference on Soil Mechanics and Foundation Engineering, Vol. 1, p. 89, 1967.







**FIGURES**

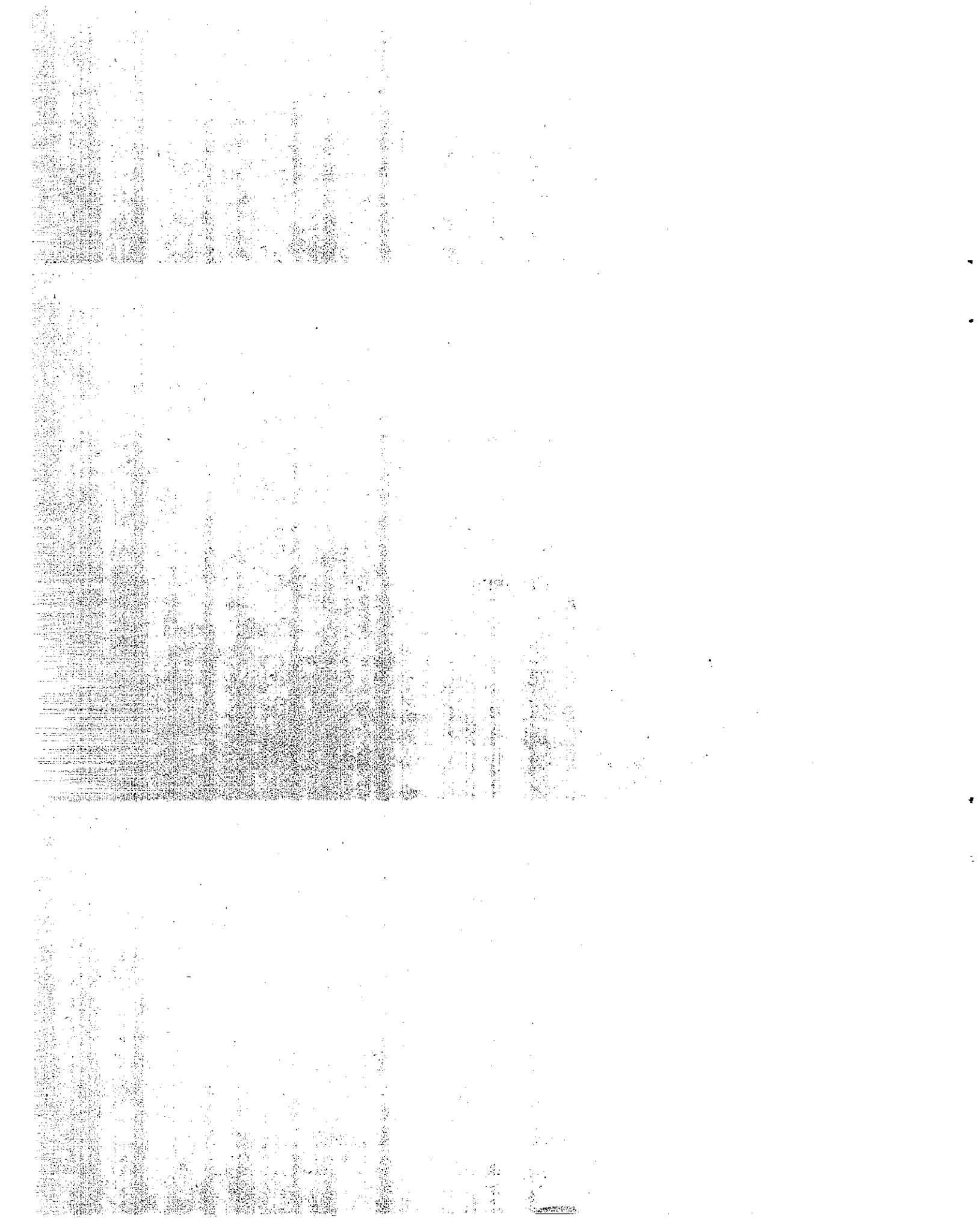
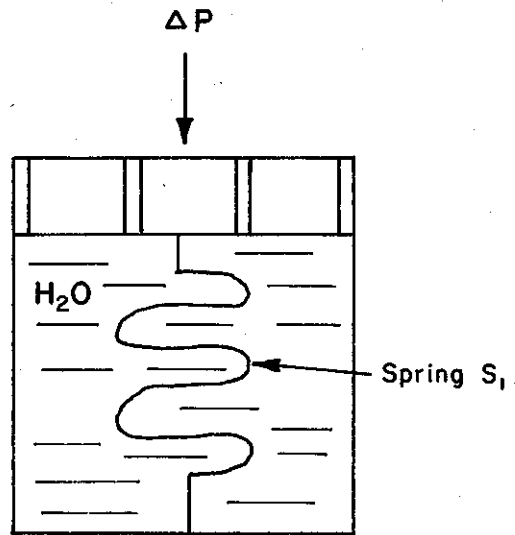
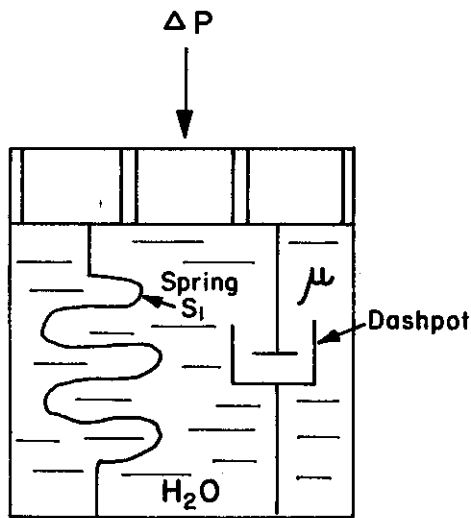


Figure 1

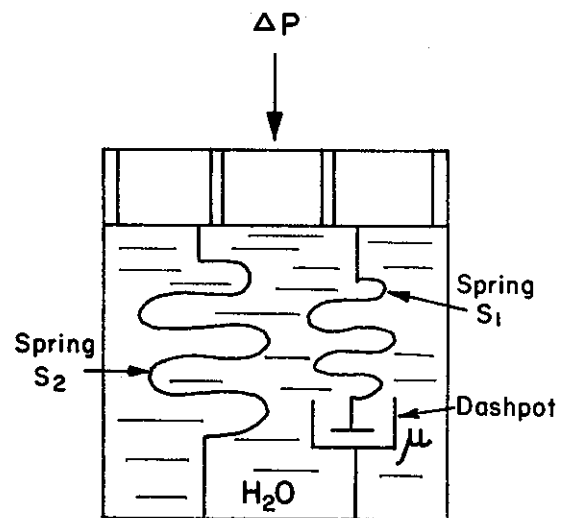
# SIMPLIFIED MODELS FOR ONE-DIMENSIONAL THEORY OF CONSOLIDATION



a. TERZAGHI'S BASIC MODEL



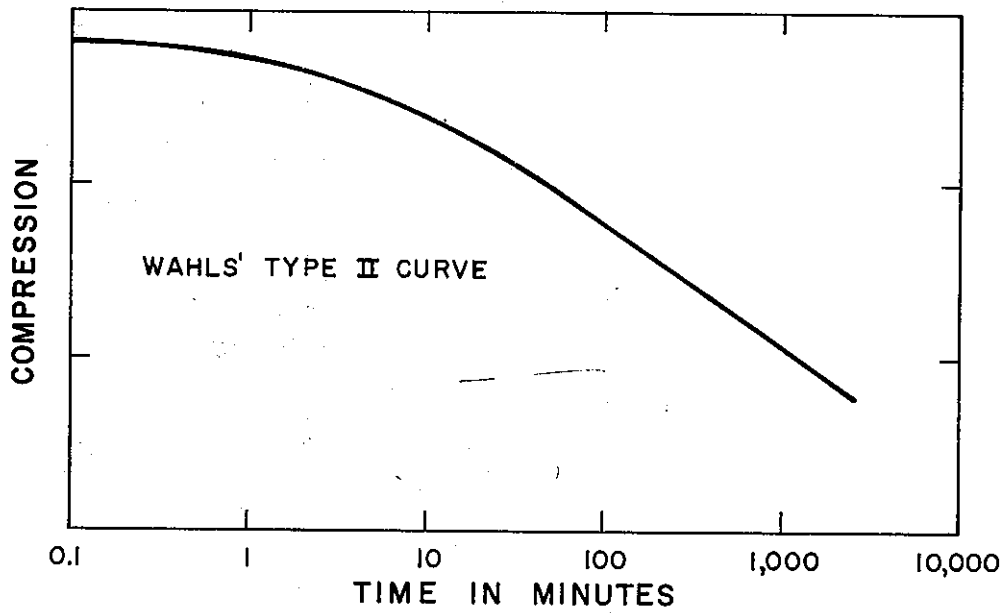
b. TAYLOR'S MODIFIED MODEL



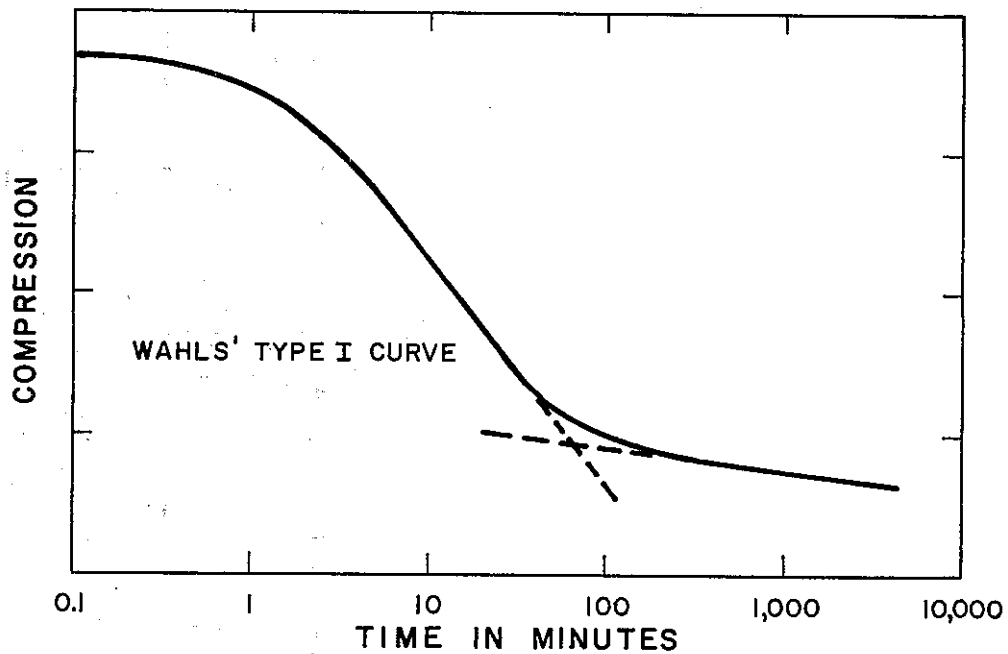
c. TAN'S RHEOLOGIC MODEL

Figure 2

EFFECT OF PRESSURE-INCREMENT RATIO ON THE SHAPE OF TIME-COMPRESSION CURVES



a. TIME-COMPRESSION CURVE WHEN  $\Delta P/P_0$  IS SMALL



b. TIME COMPRESSION CURVE WHEN  $\Delta P/P_0$  IS LARGE

Figure 3

### TYPICAL TIME - COMPRESSION CURVES

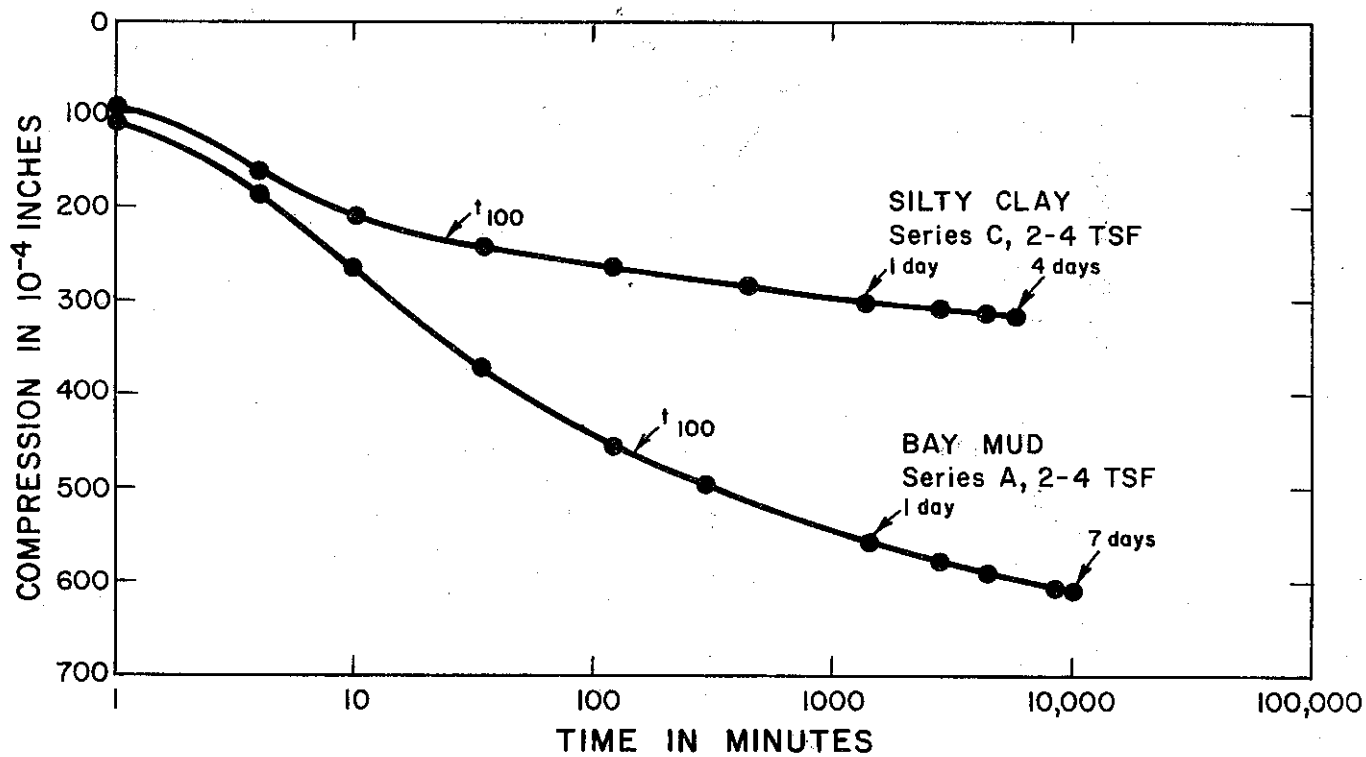


Figure 4a

CONSOLIDATION PRESSURE VS VOID RATIO  
AND COEFFICIENT OF SECONDARY COMPRESSION

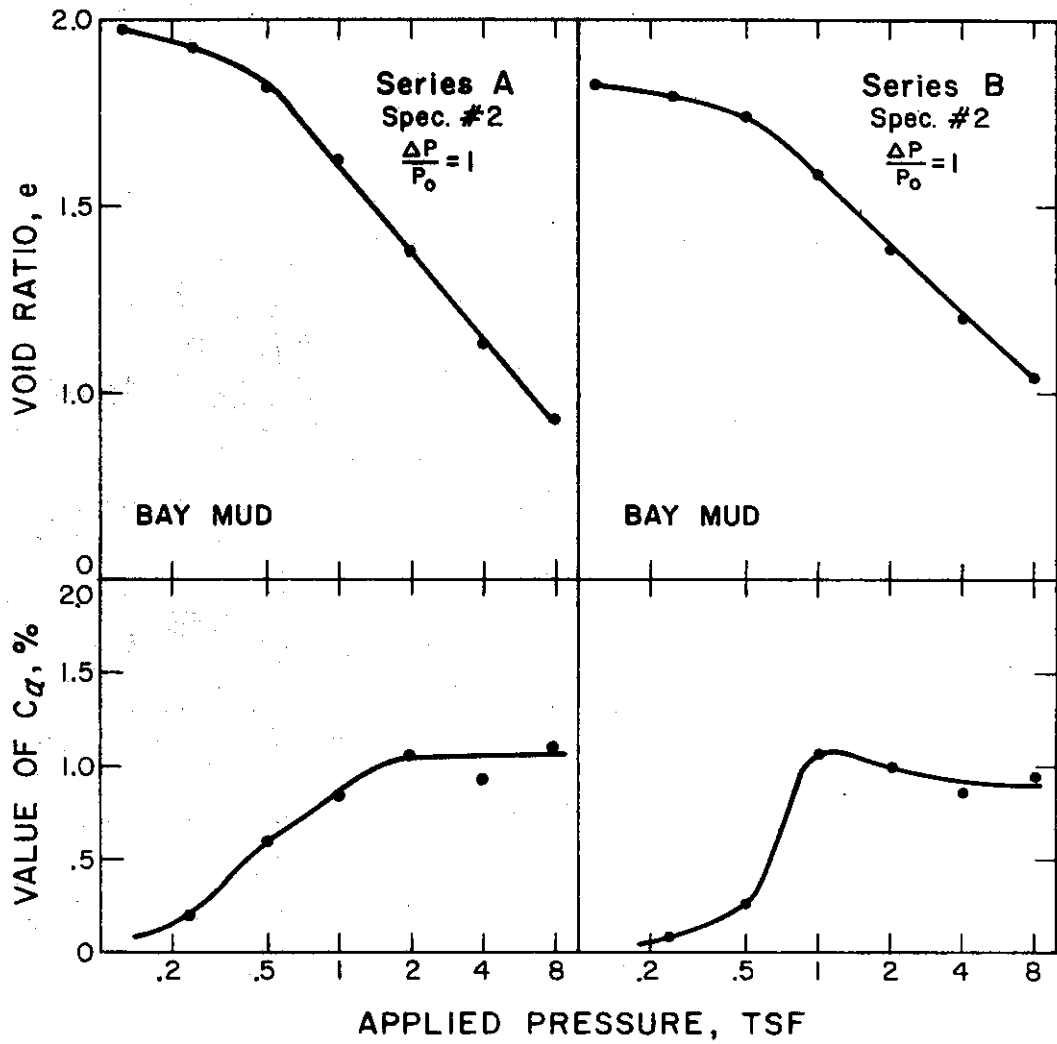
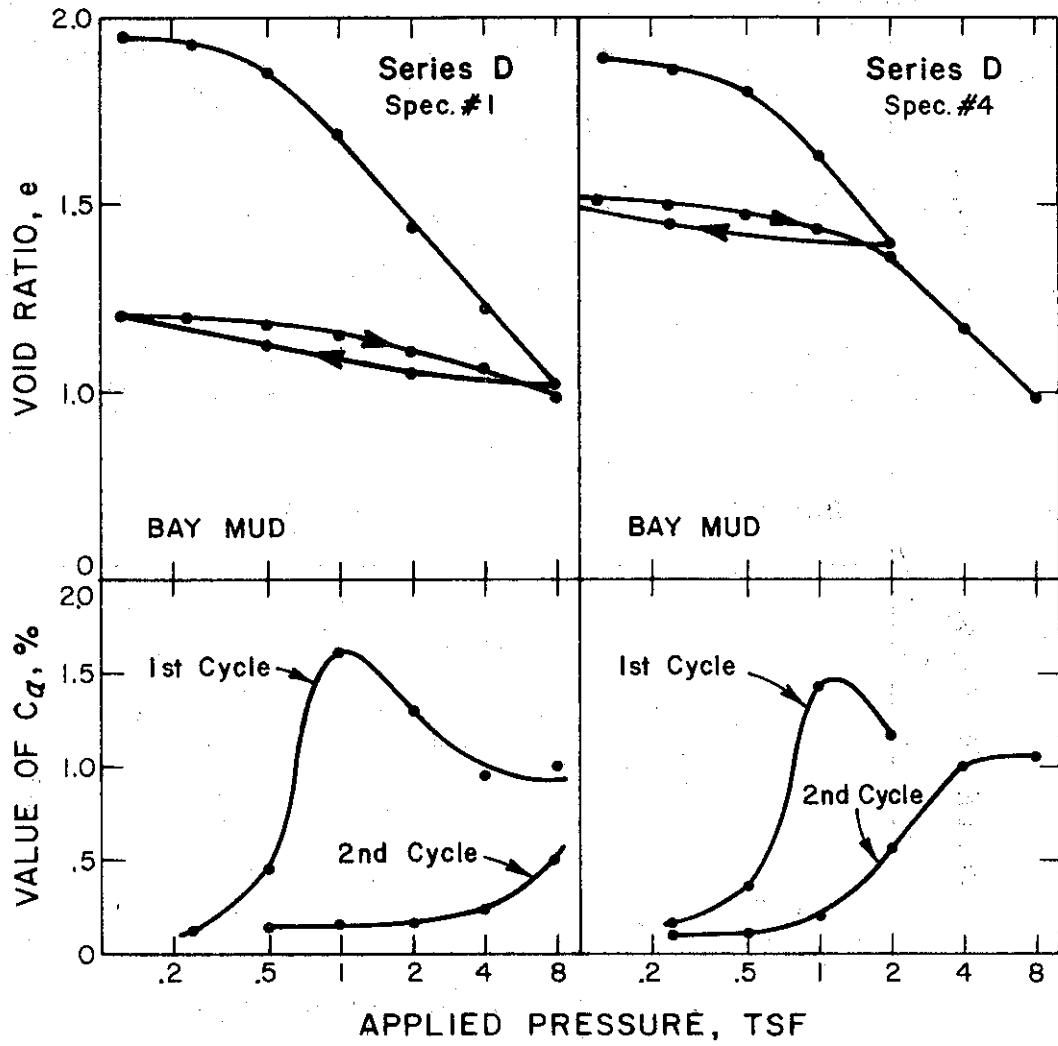


Figure 4b

### CONSOLIDATION PRESSURE VS VOID RATIO AND COEFFICIENT OF SECONDARY COMPRESSION



CONSOLIDATION PRESSURE VS VOID RATIO  
AND COEFFICIENT OF SECONDARY COMPRESSION

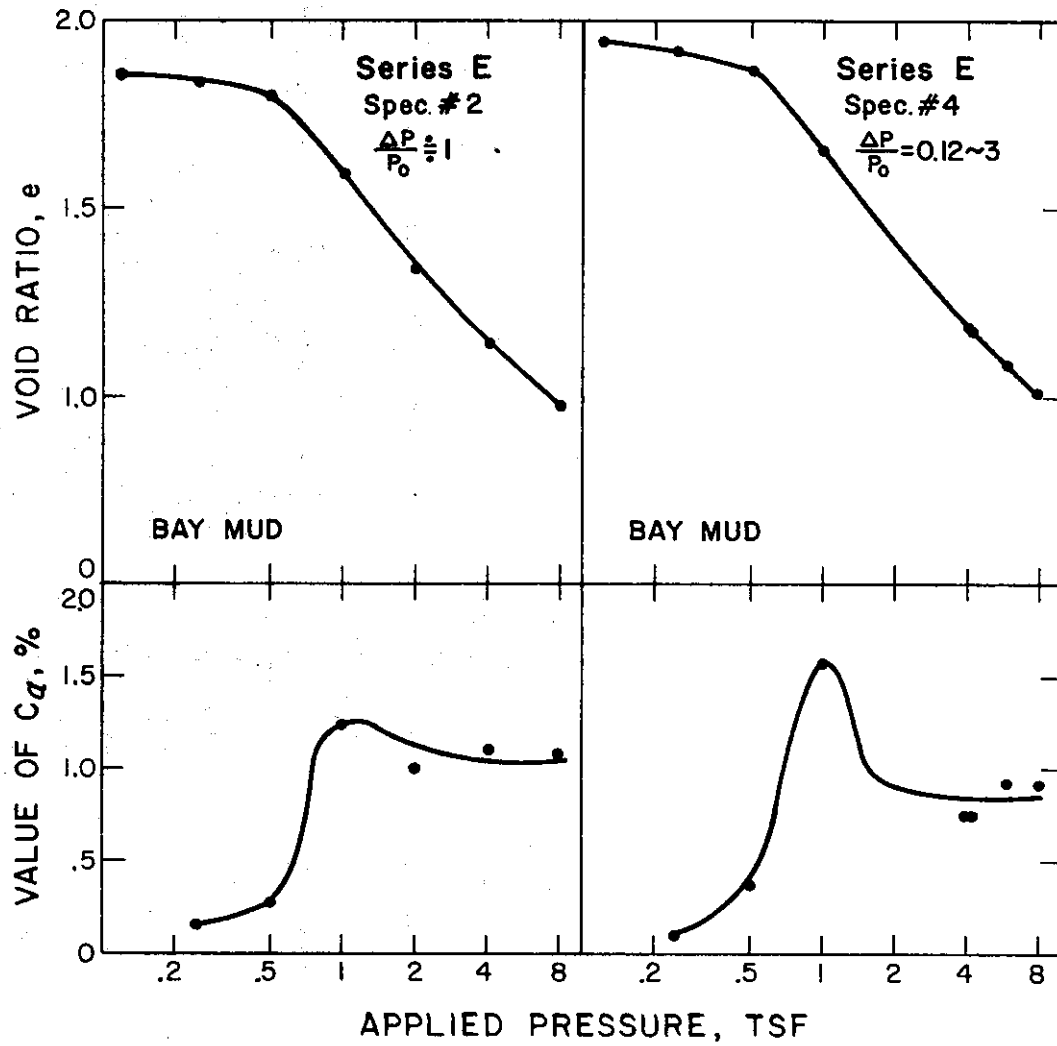


Figure 4d

### CONSOLIDATION PRESSURE VS VOID RATIO AND COEFFICIENT OF SECONDARY COMPRESSION

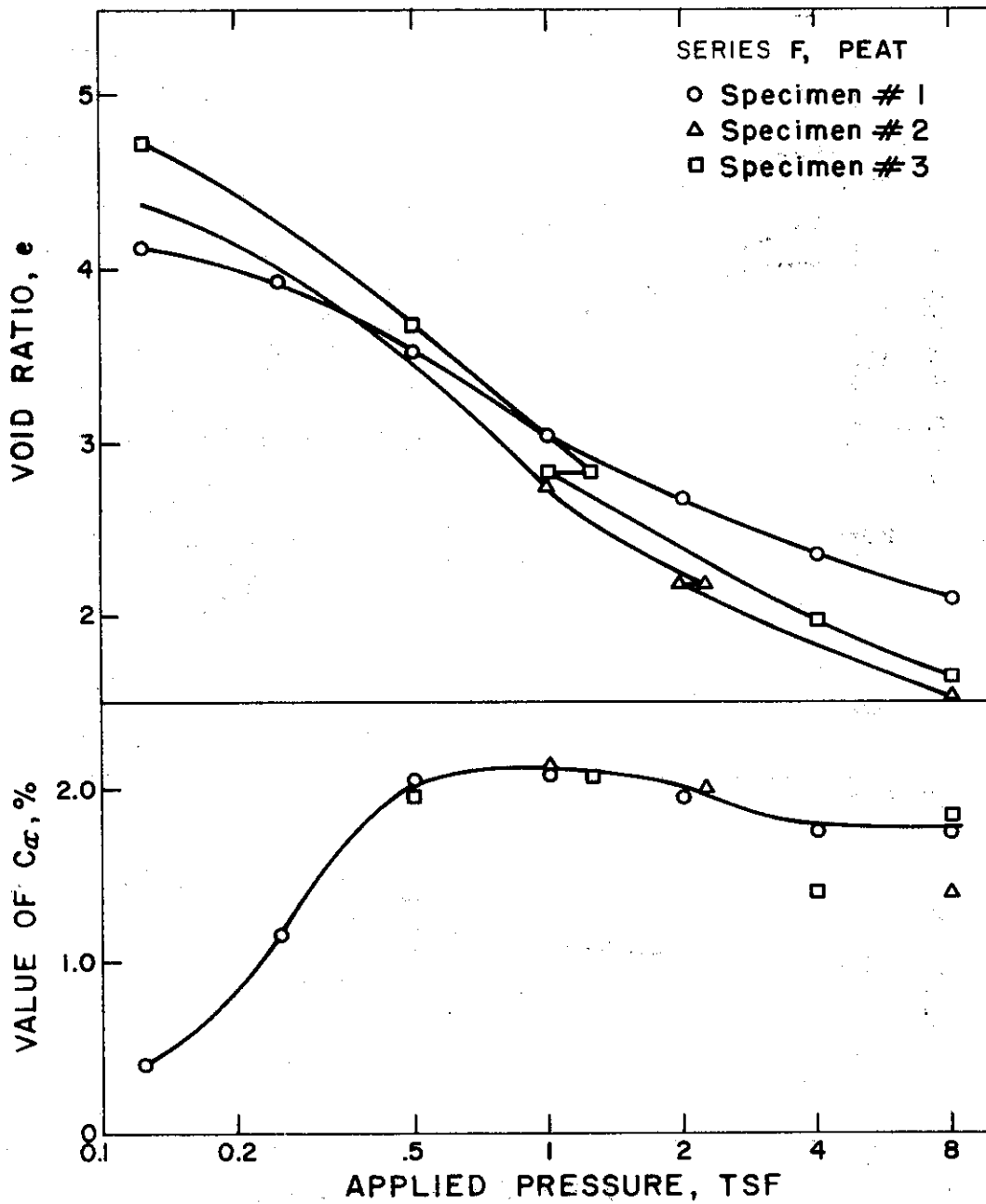


Figure 4 e

### CONSOLIDATION PRESSURE VS VOID RATIO AND COEFFICIENT OF SECONDARY COMPRESSION

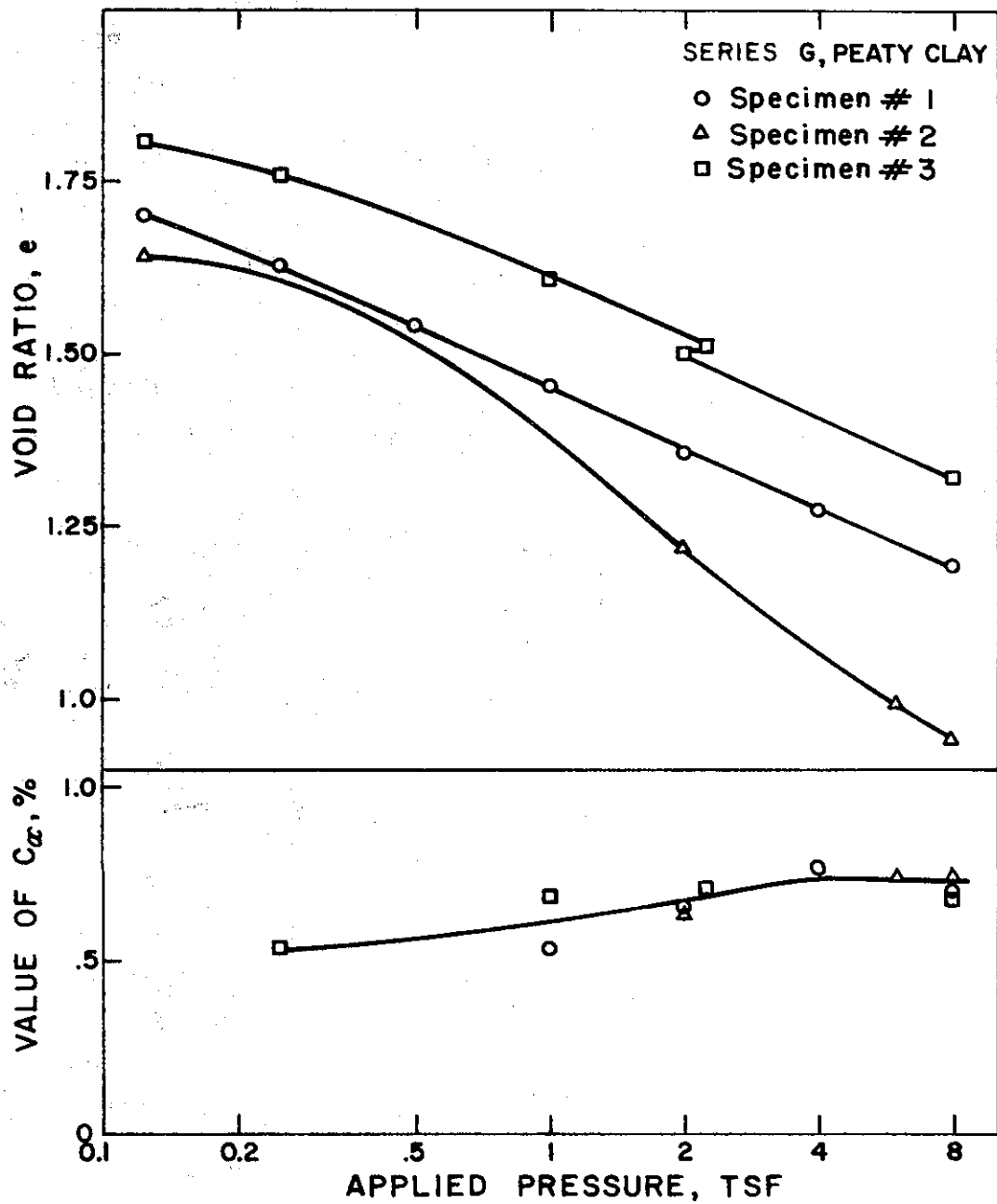


Figure 4 f

### CONSOLIDATION PRESSURE VS VOID RATIO AND COEFFICIENT OF SECONDARY COMPRESSION

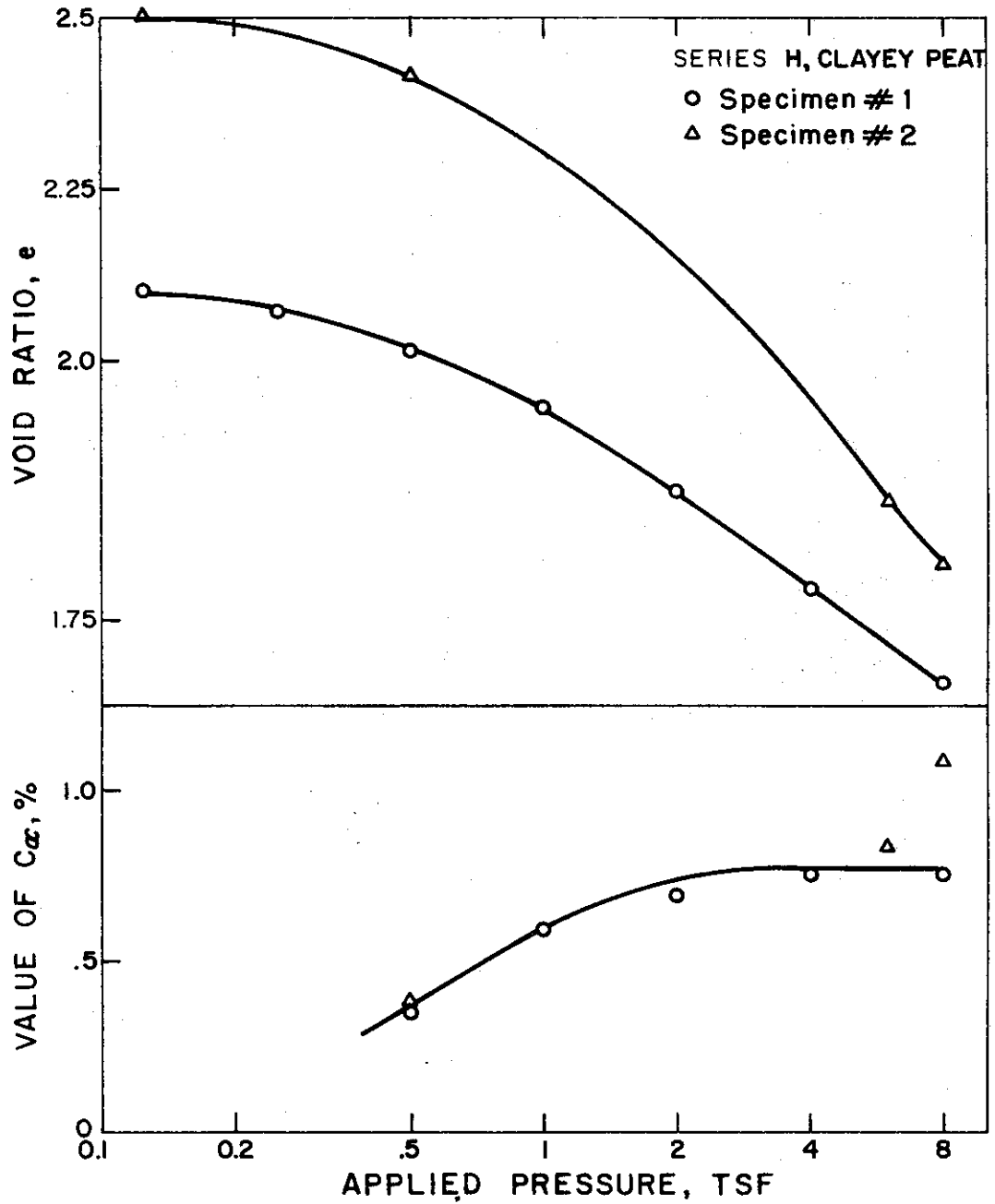


Figure 4g

CONSOLIDATION PRESSURE VS VOID RATIO  
AND COEFFICIENT OF SECONDARY COMPRESSION

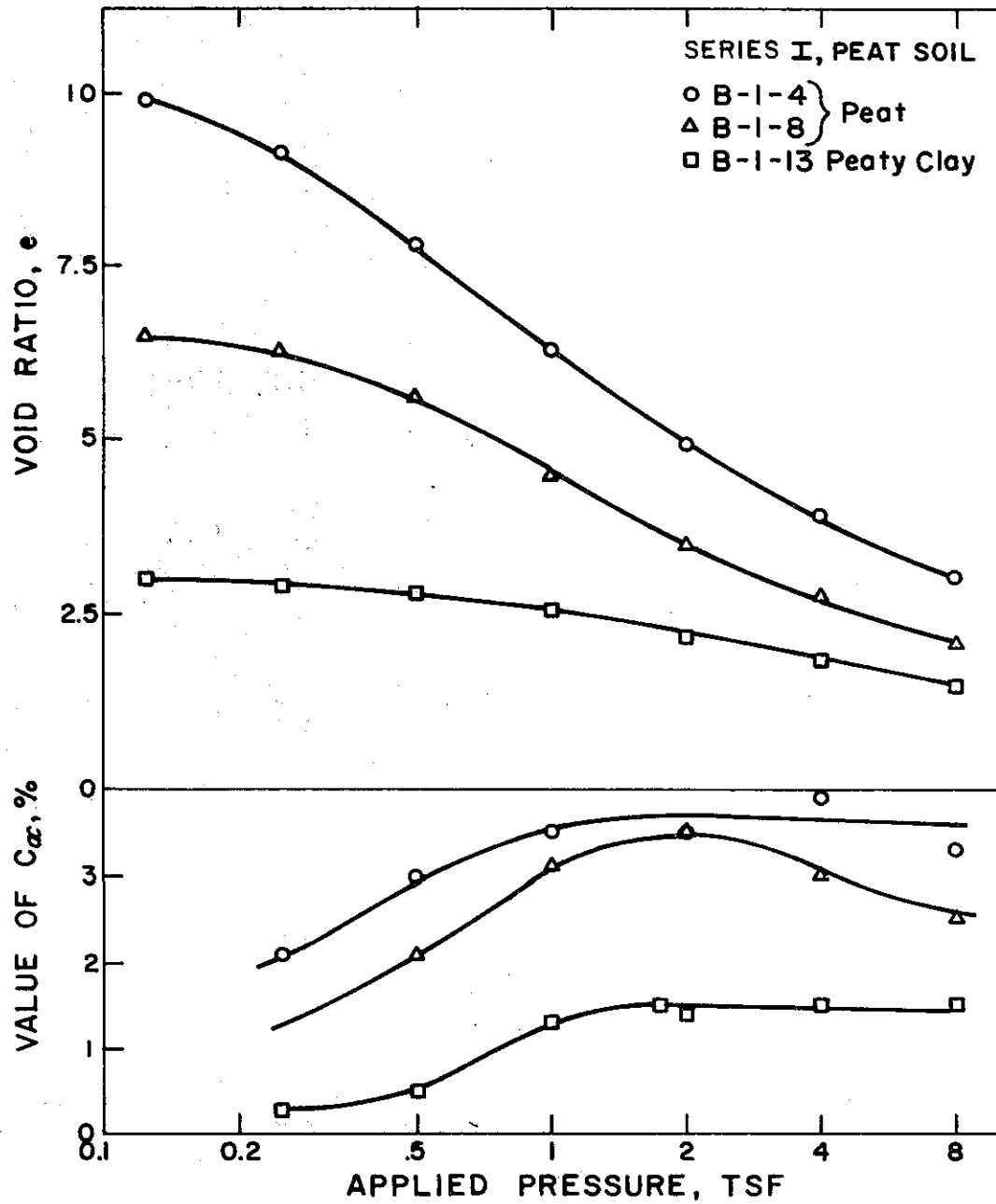


Figure 4h

CONSOLIDATION PRESSURE VS VOID RATIO  
AND COEFFICIENT OF SECONDARY COMPRESSION

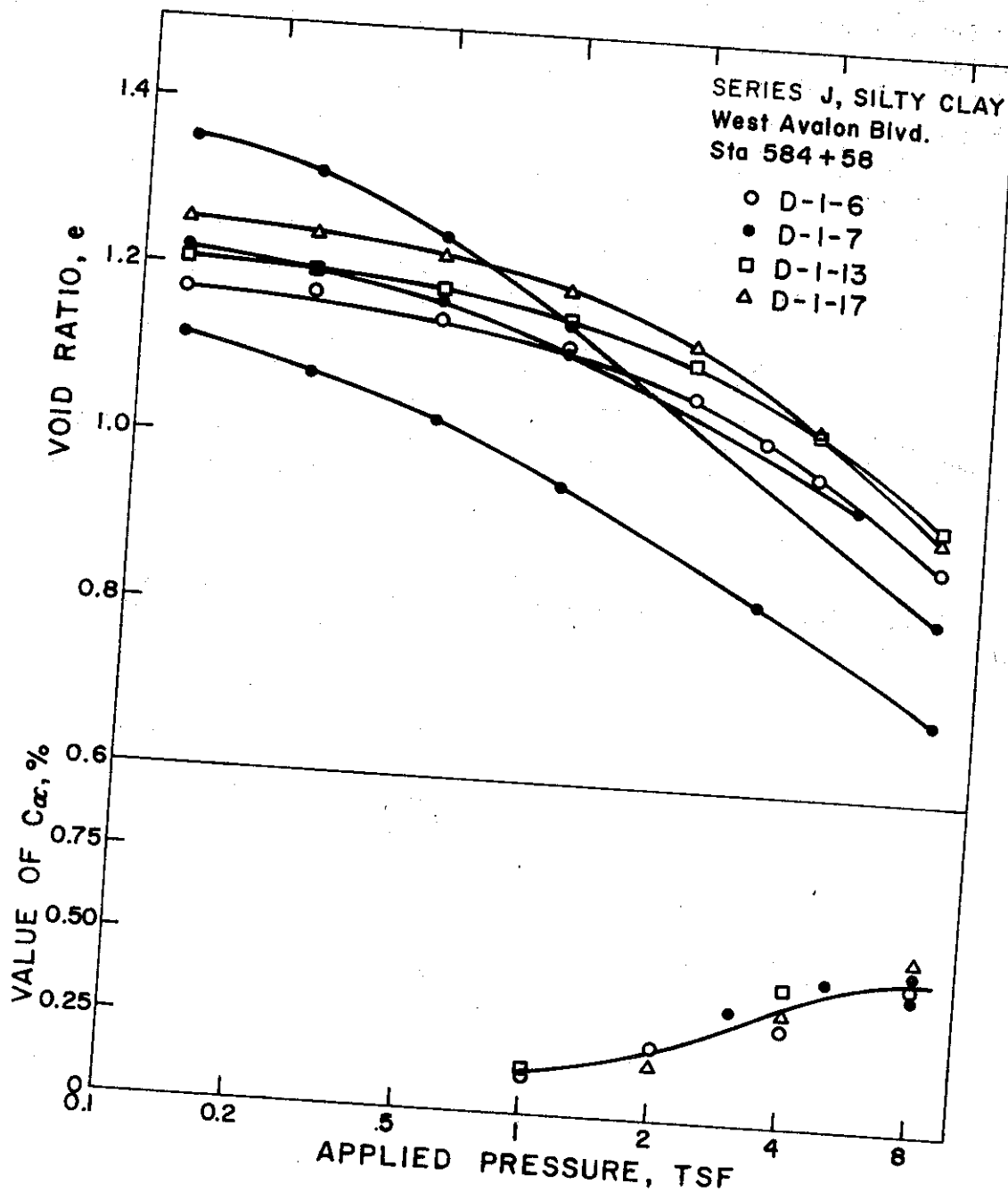


Figure 5

# COEFFICIENT OF SECONDARY COMPRESSION VS VOID RATIO

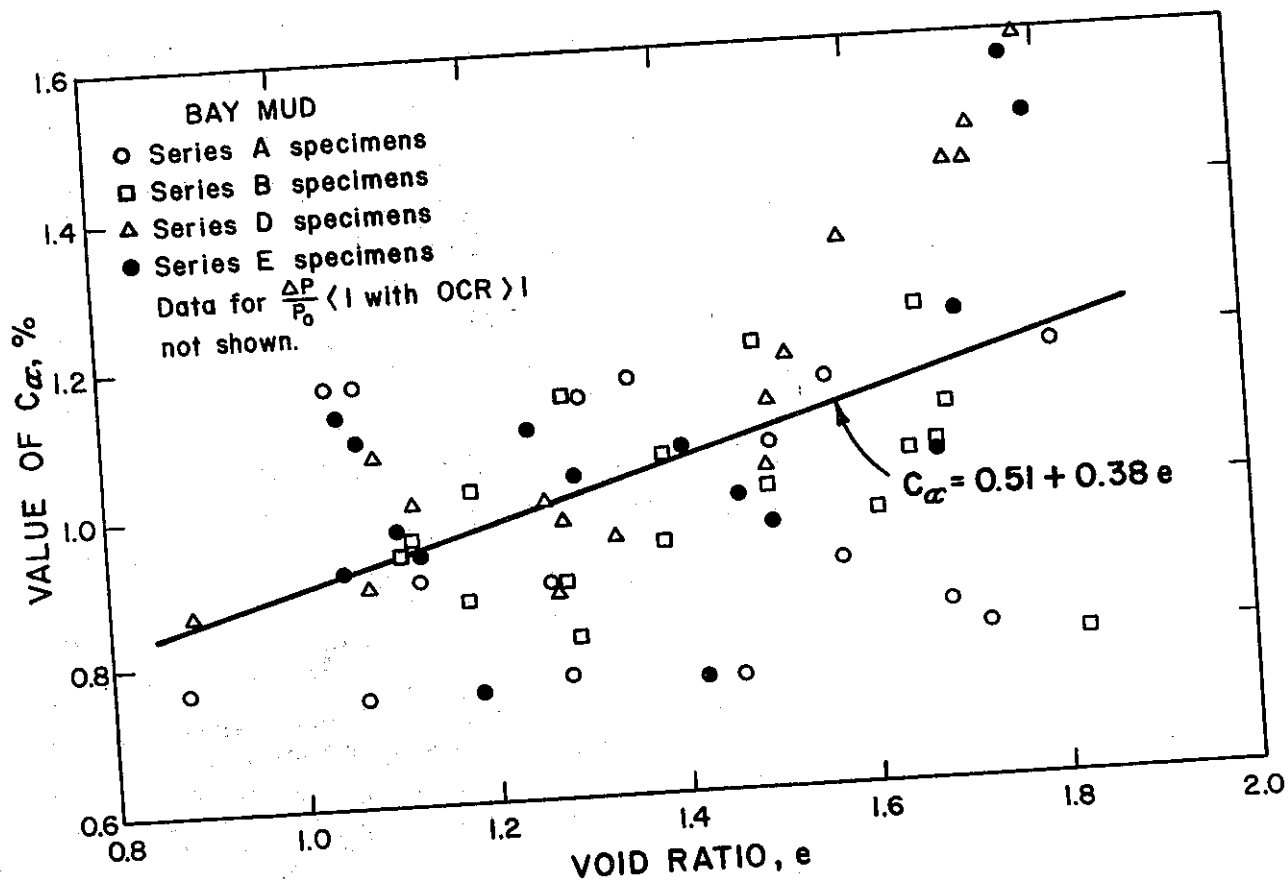


Figure 6

# RELATIONSHIP BETWEEN OVERCONSOLIDATION RATIO AND COEFFICIENT OF SECONDARY COMPRESSION

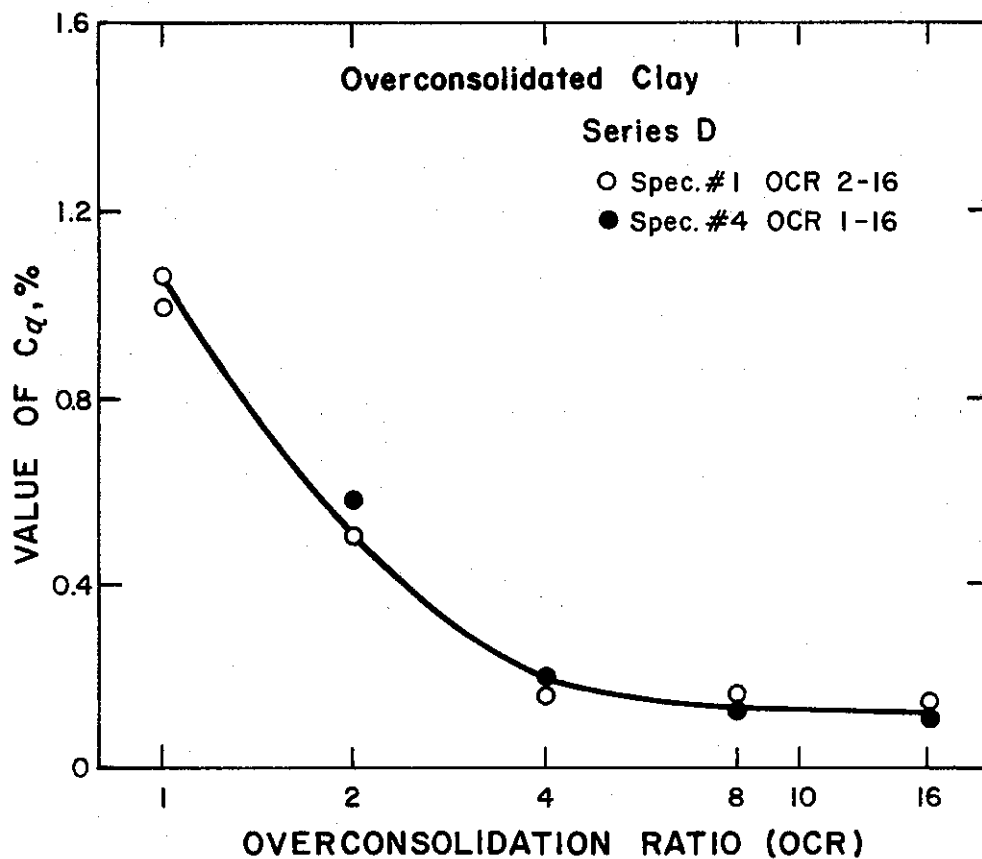
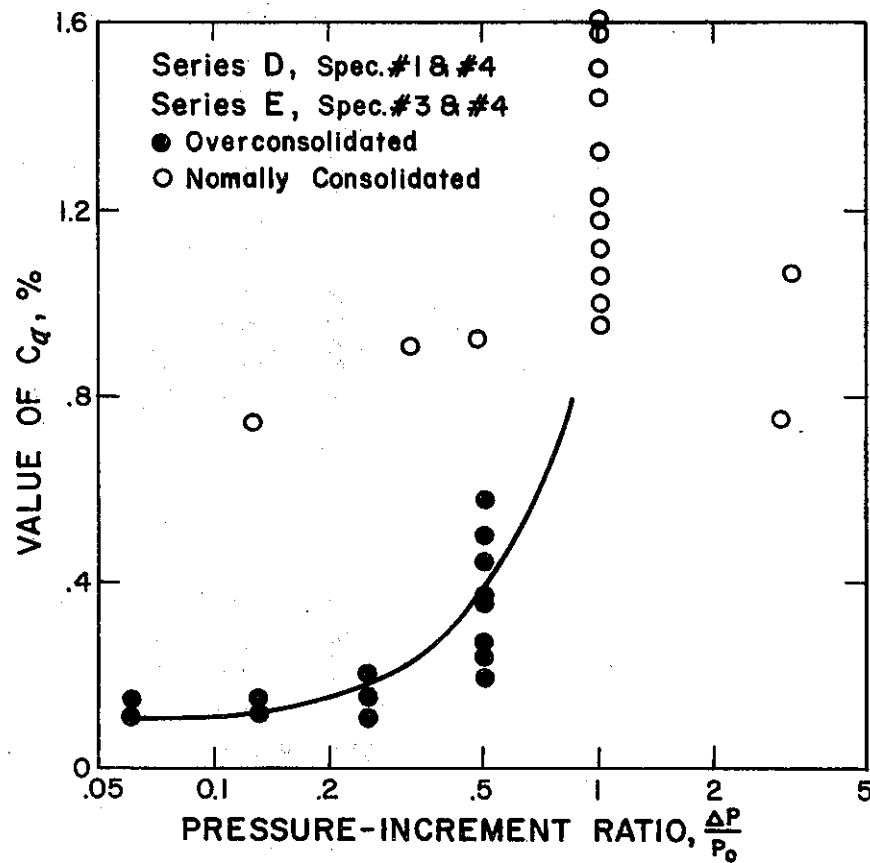


Figure 7

# RELATIONSHIP BETWEEN PRESSURE-INCREMENT RATIO AND COEFFICIENT OF SECONDARY COMPRESSION



RELATIONSHIP BETWEEN PRESSURE-INCREMENT RATIO AND THE RATIO OF SECONDARY TO PRIMARY COMPRESSION

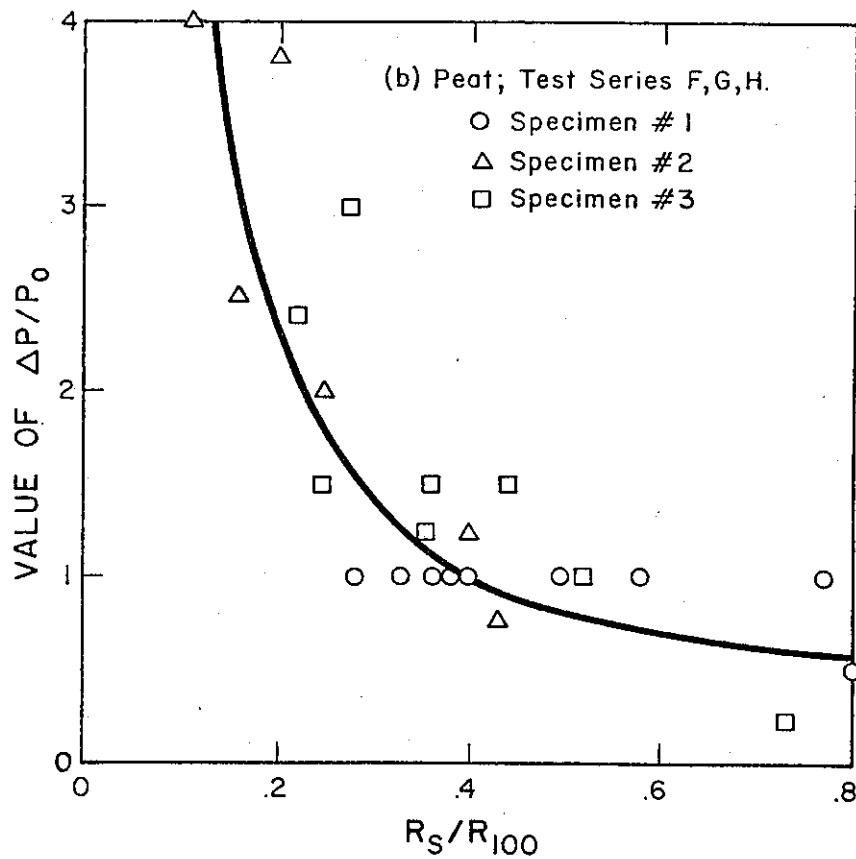
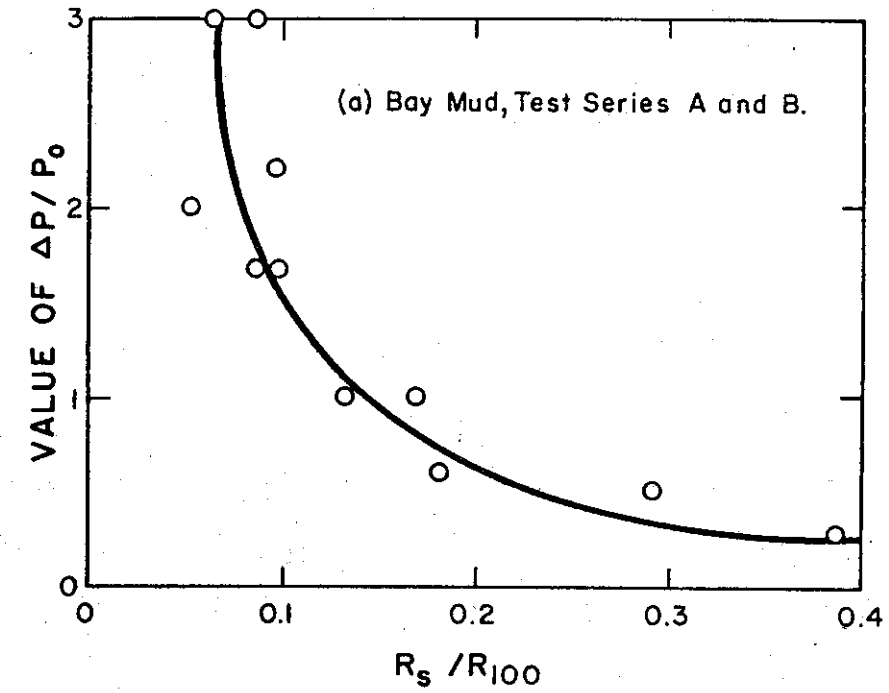


Figure 9

## CALCULATED COEFFICIENT OF CONSOLIDATION VERSUS VOID RATIO

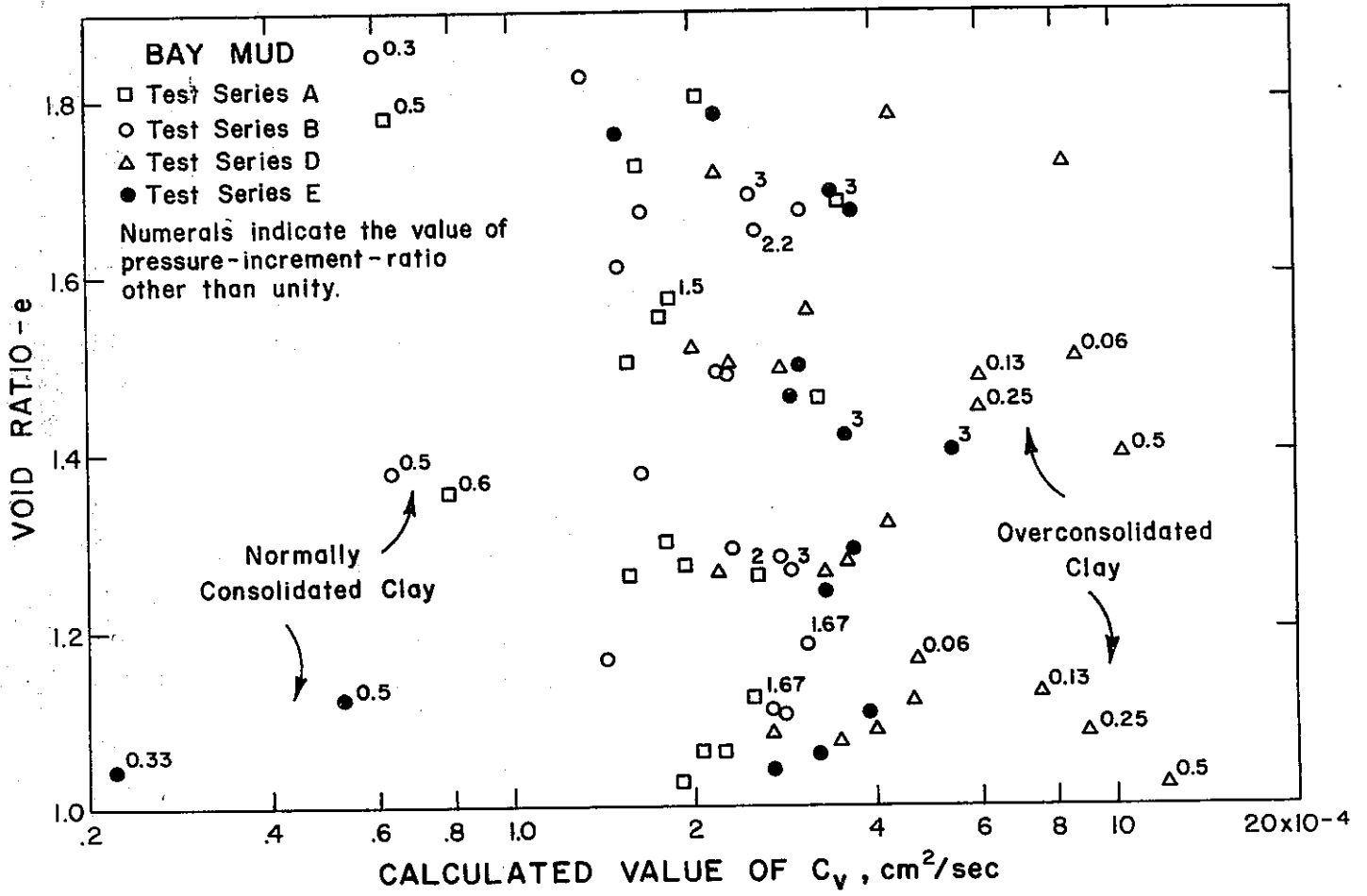


Figure 10

RELATIONSHIP BETWEEN VOID RATIO AND CALCULATED PERMEABILITY  
 FROM CONSOLIDATION TEST DATA  
 (BAY MUD)

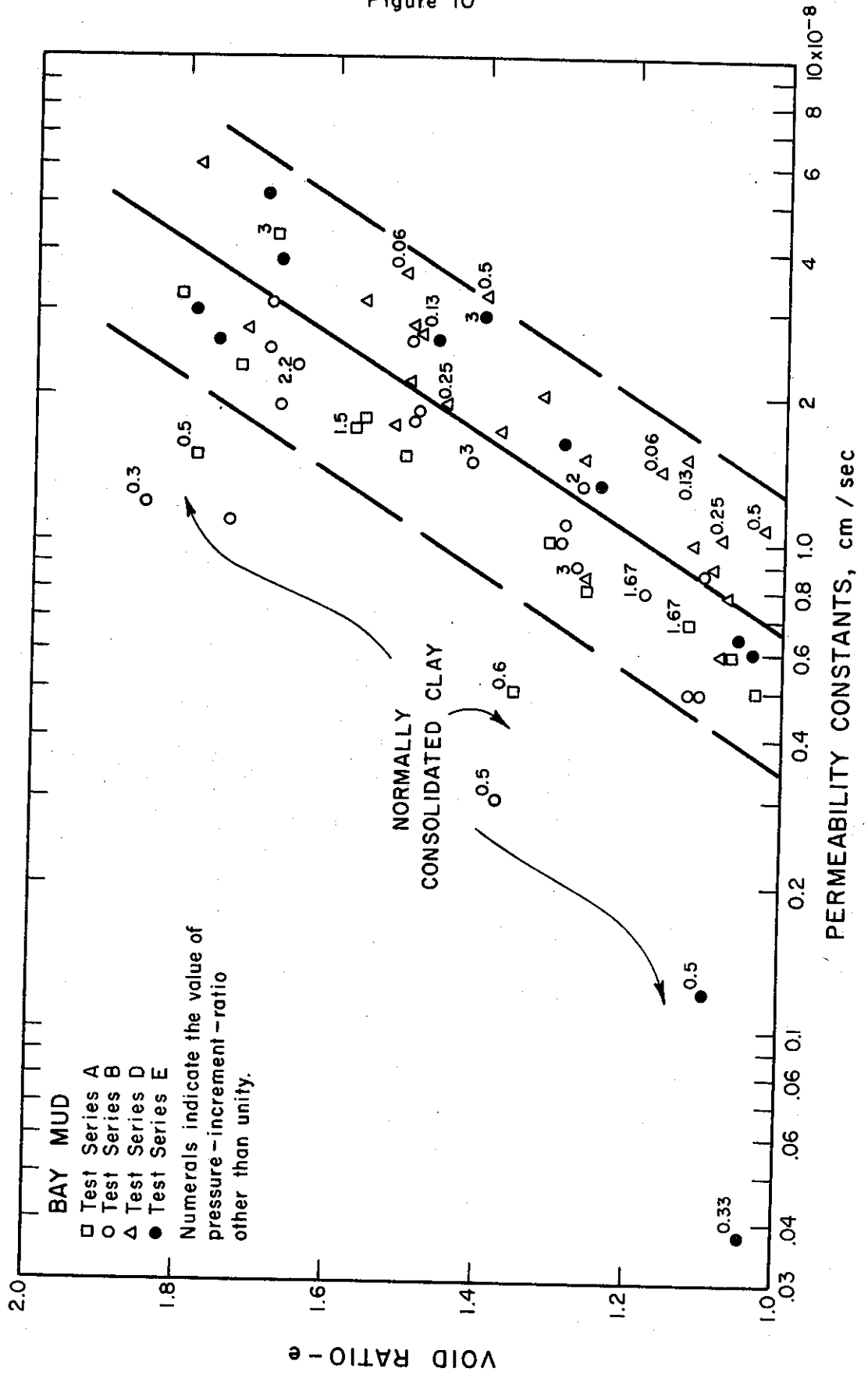
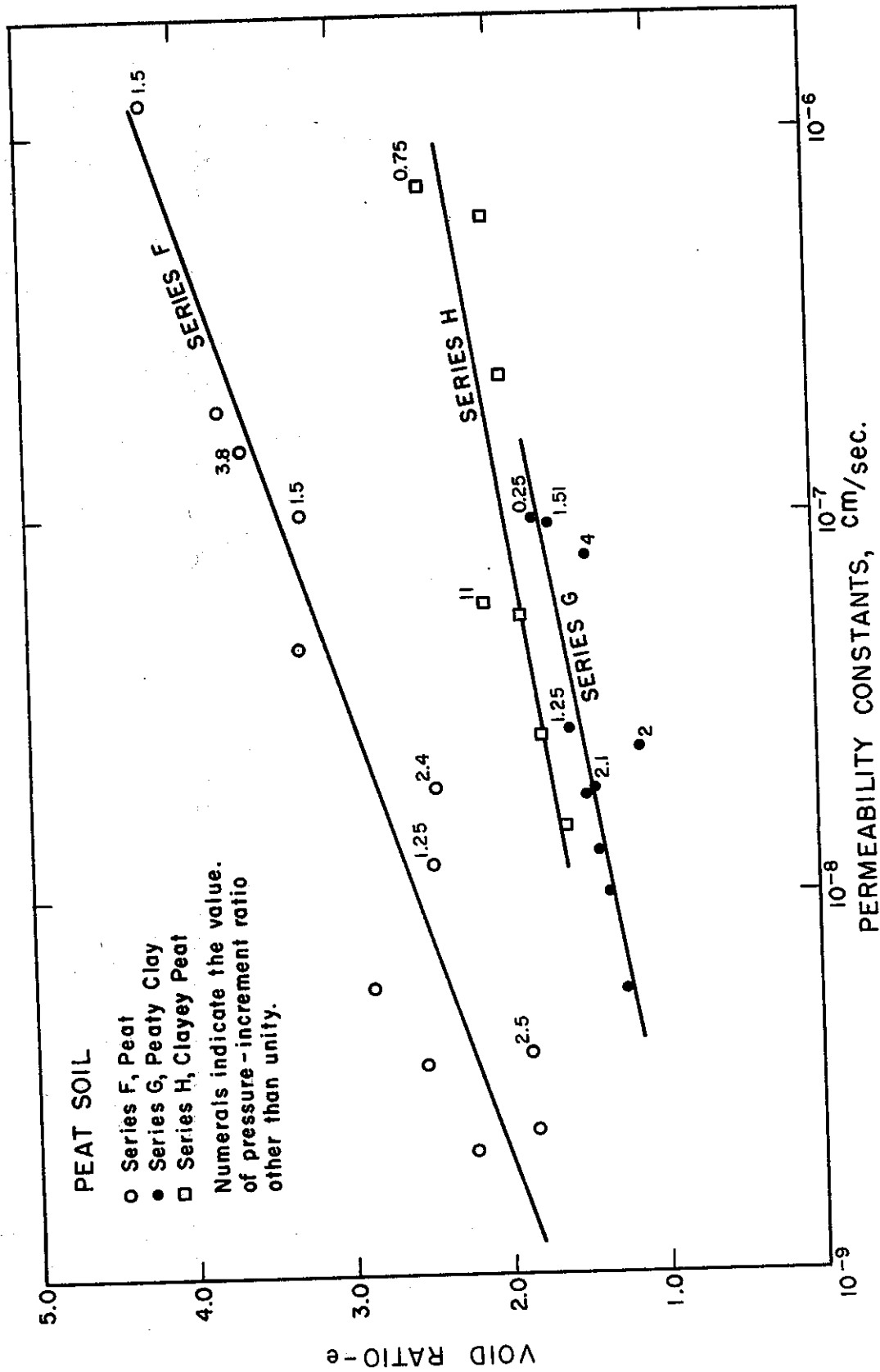


Figure 11

RELATIONSHIP BETWEEN VOID RATIO AND CALCULATED PERMEABILITY  
 FROM CONSOLIDATION TEST DATA  
 (PEAT SOIL)



VOID RATIO VS LOG PRESSURE CURVE  
AS RELATED TO LENGTH OF LOAD INCREMENT

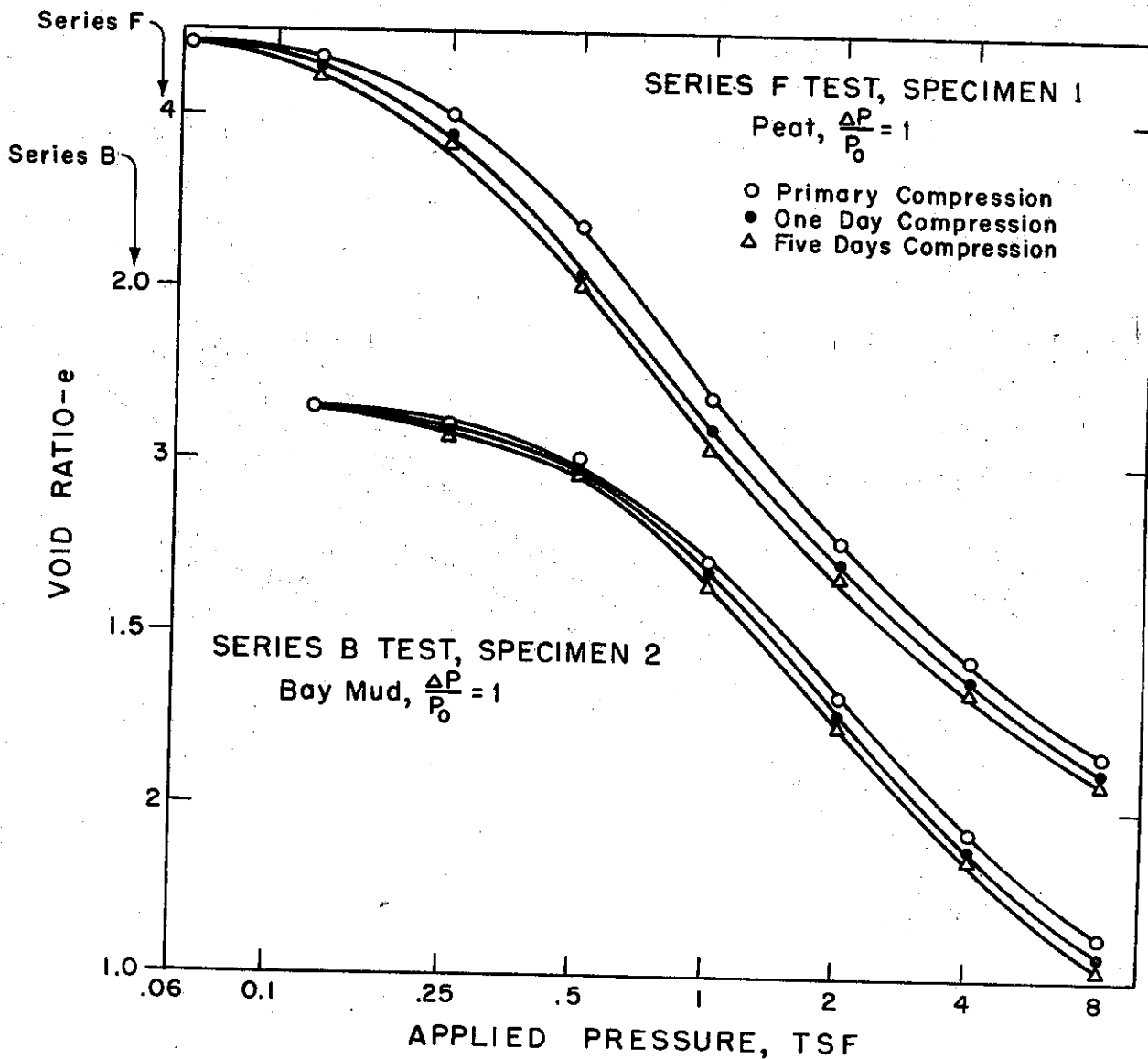


Figure 13

TERZAGHI'S METHOD OF CALCULATING TIME - COMPRESSION RELATIONSHIP

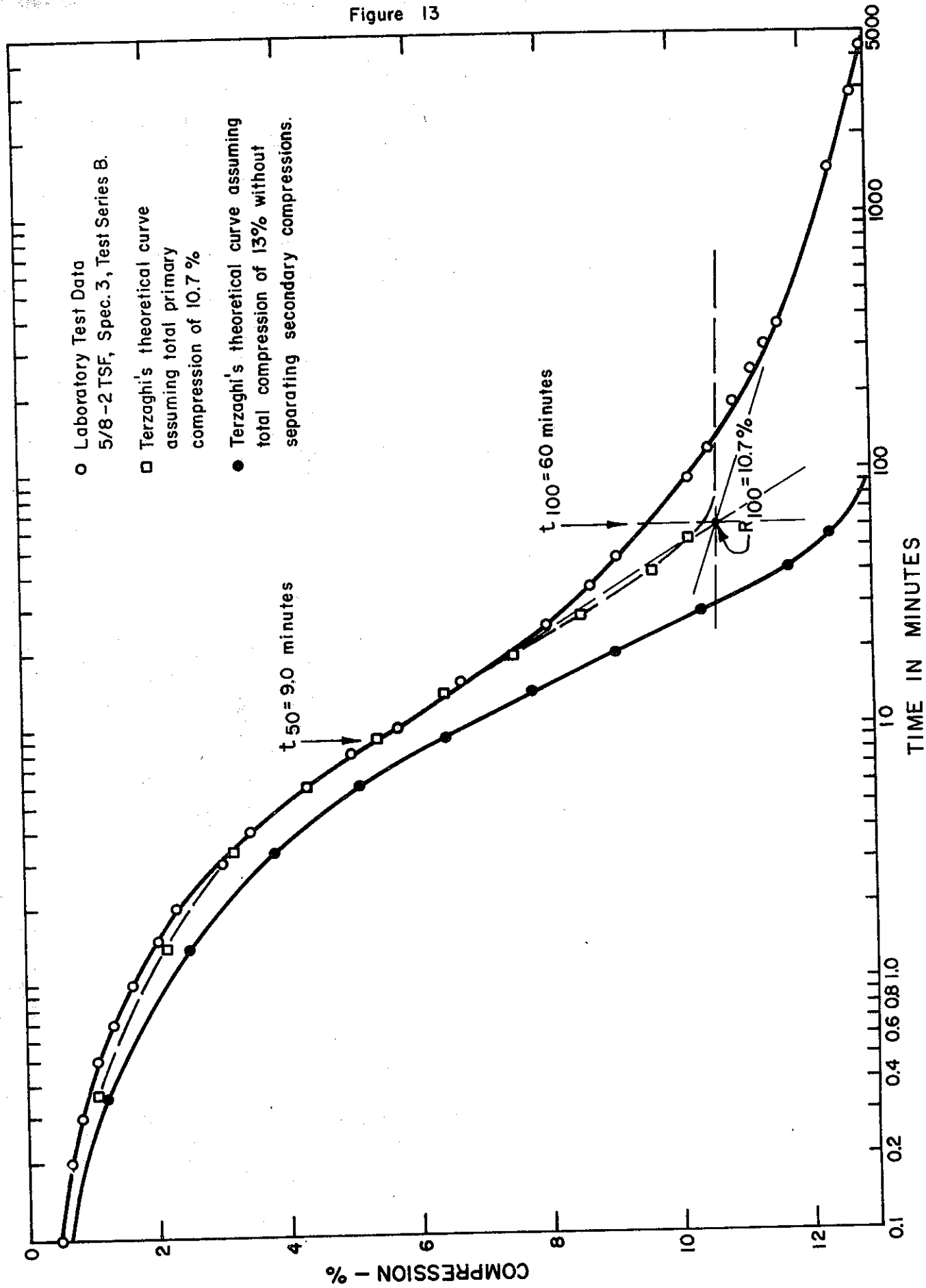


Figure 14

SAMPLE SETTLEMENT ANALYSIS - WAHLS' METHOD

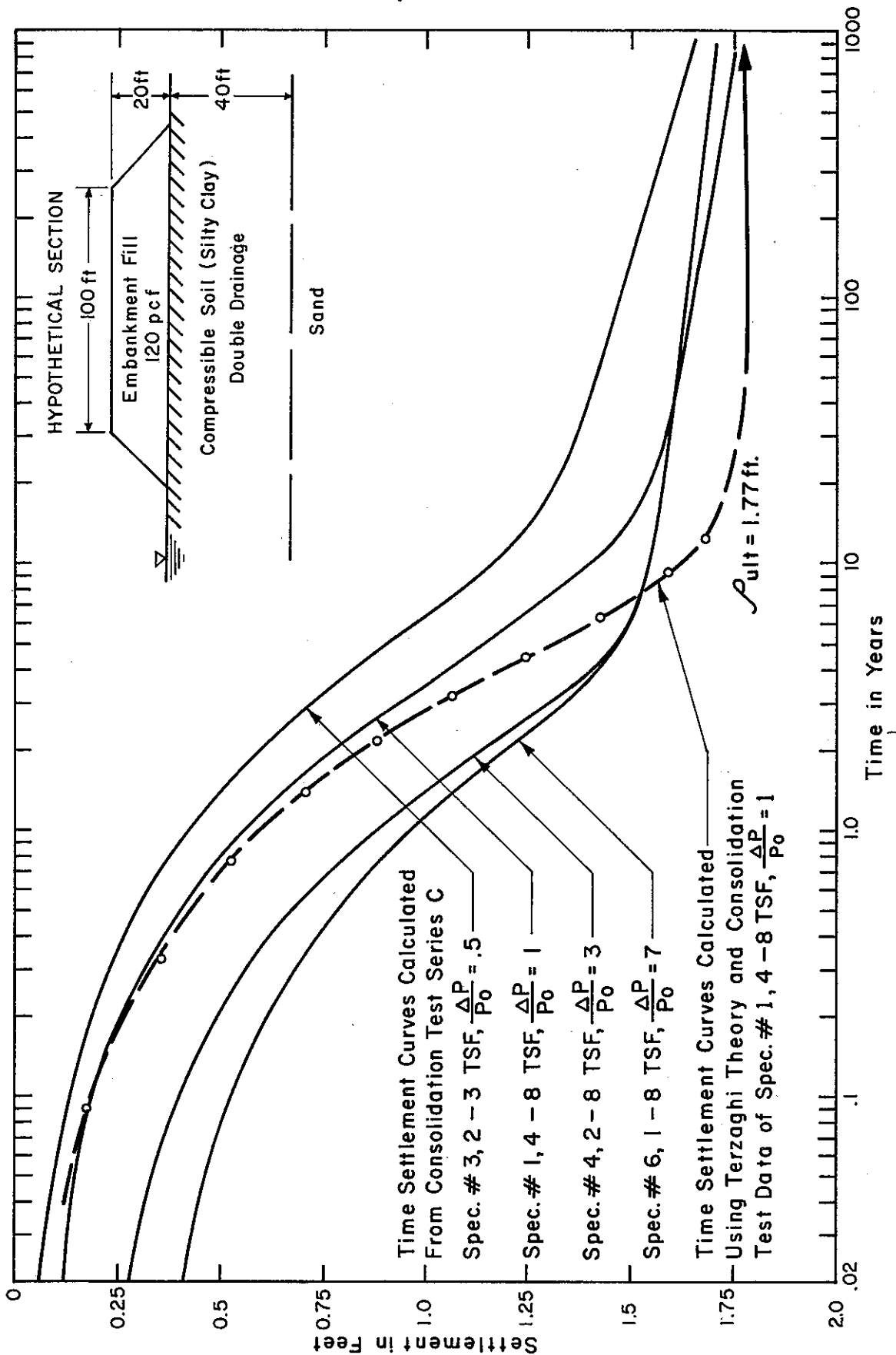
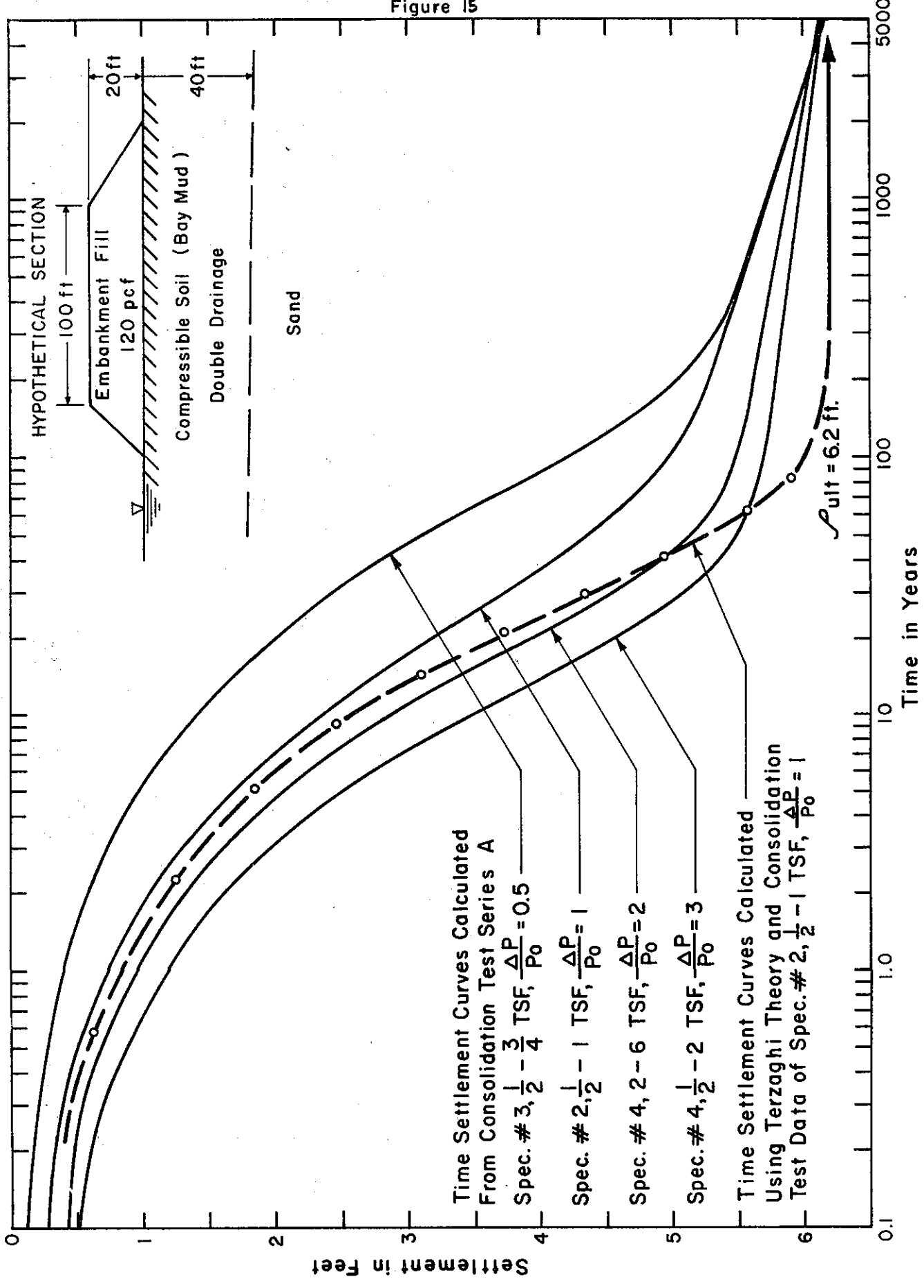


Figure 15

SAMPLE SETTLEMENT ANALYSIS - WAHLS' METHOD



COMPARISON OF METHODS OF CALCULATING TIME-COMPRESSION RELATIONSHIP

Figure 16

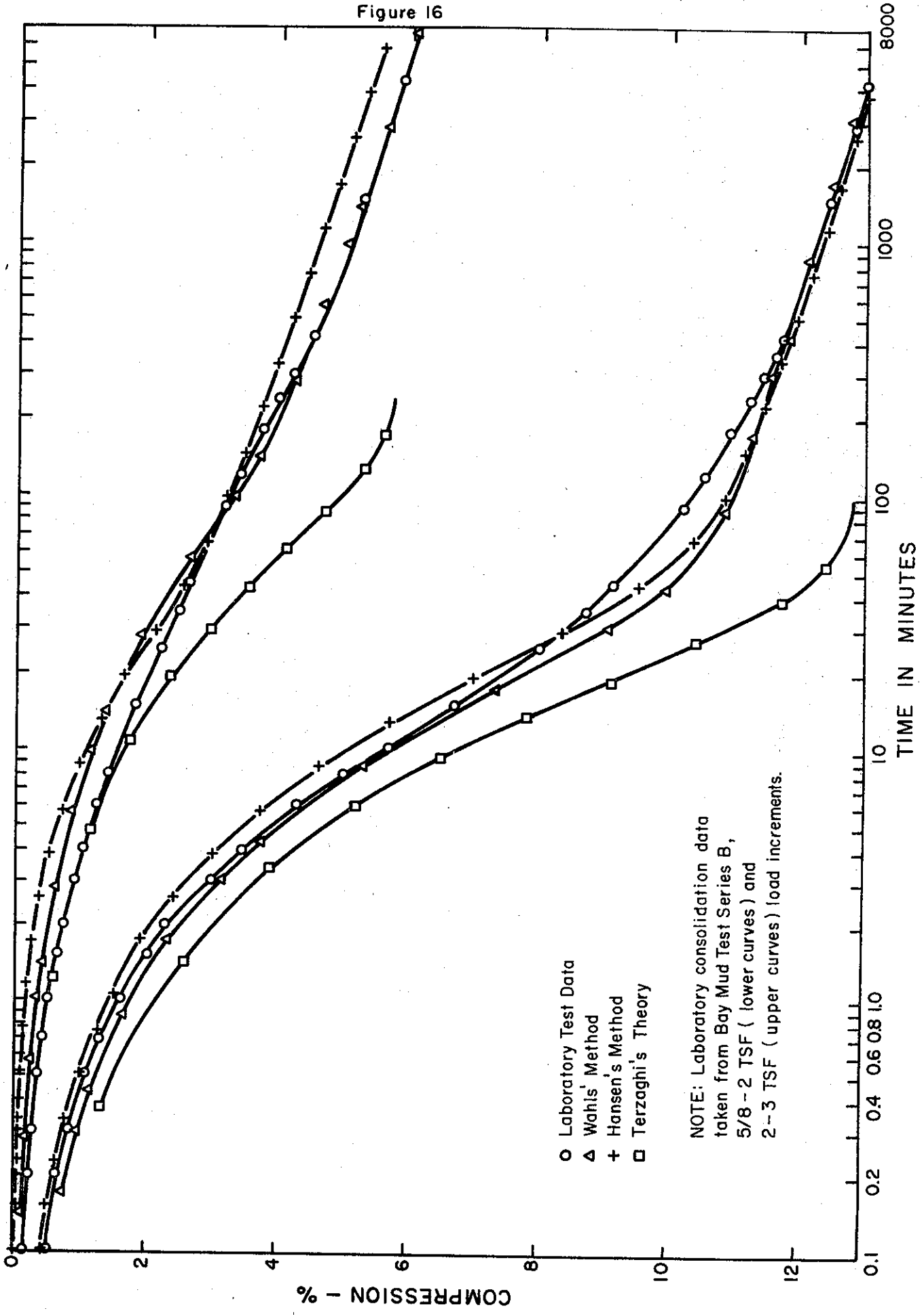


Figure 17 a

SETTLEMENTS AT SAN DIEQUITO RIVER BASIN, STA. "SD" 1278 + 50

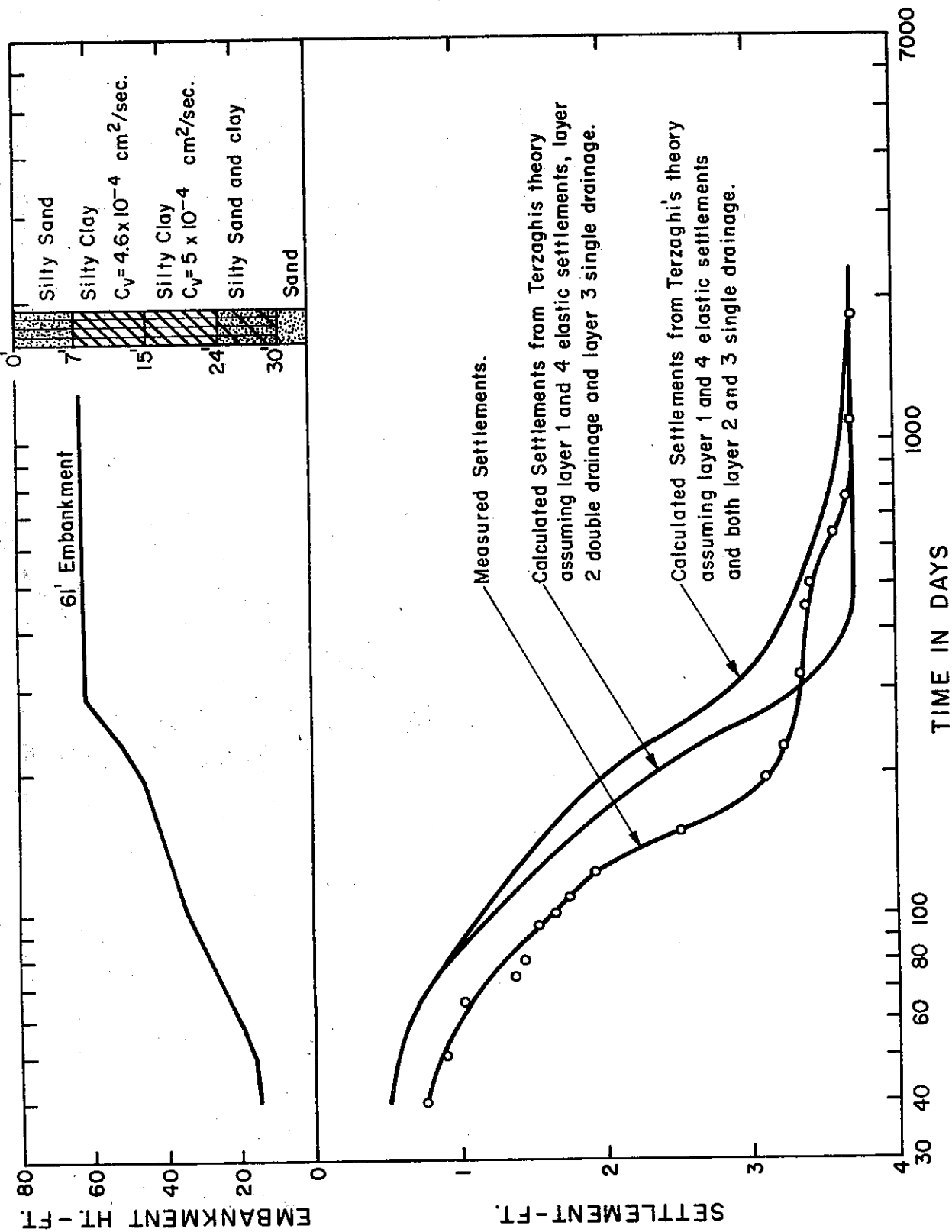


Figure 17 b

SETTLEMENTS AT LOS PENASQUITOS LAGOON, STA. "SD" 1095

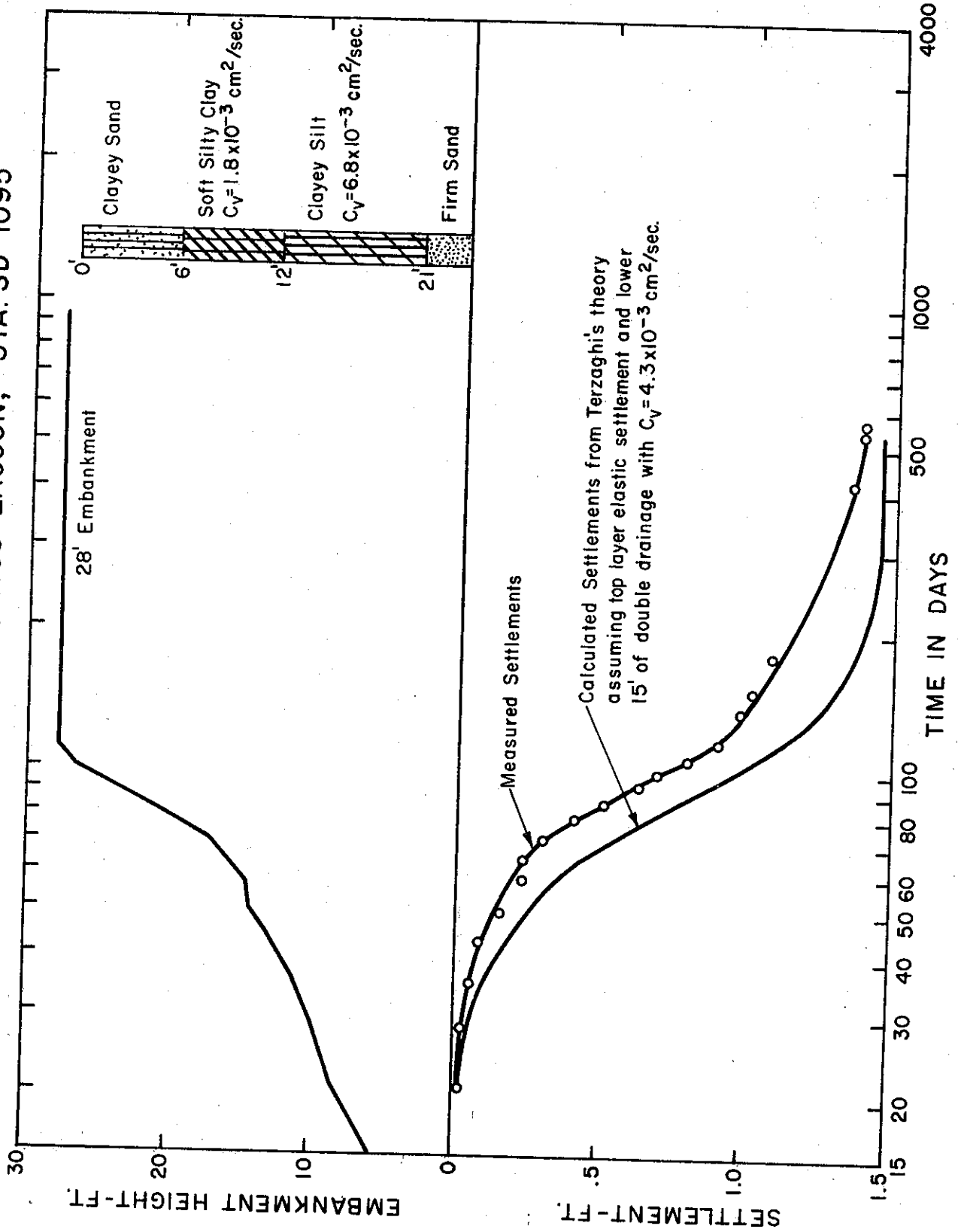


Figure 17c

SETTLEMENTS AT ARCATA-4TH ST. INTERCHANGE, STA. 88+50

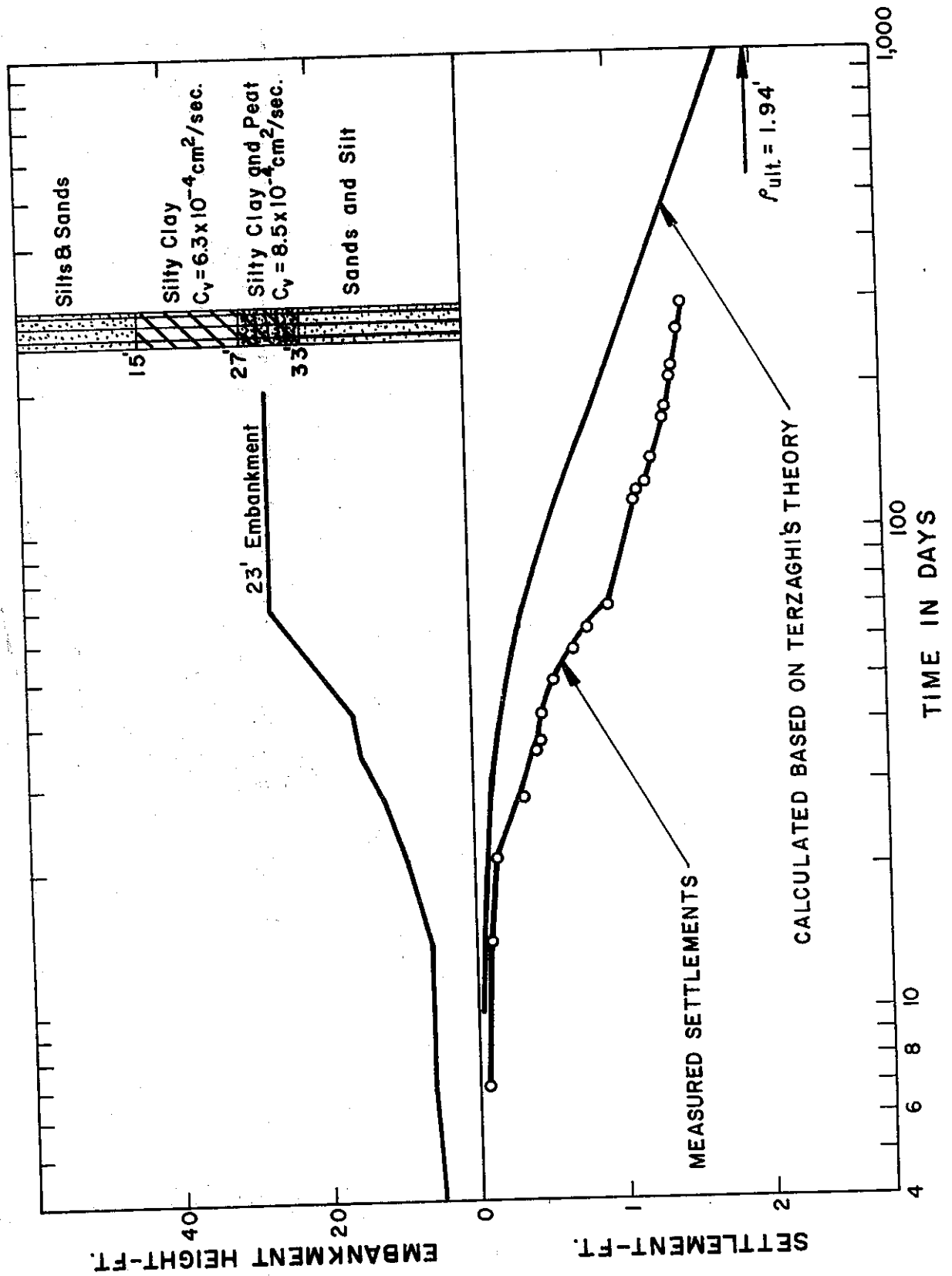


Figure 17d

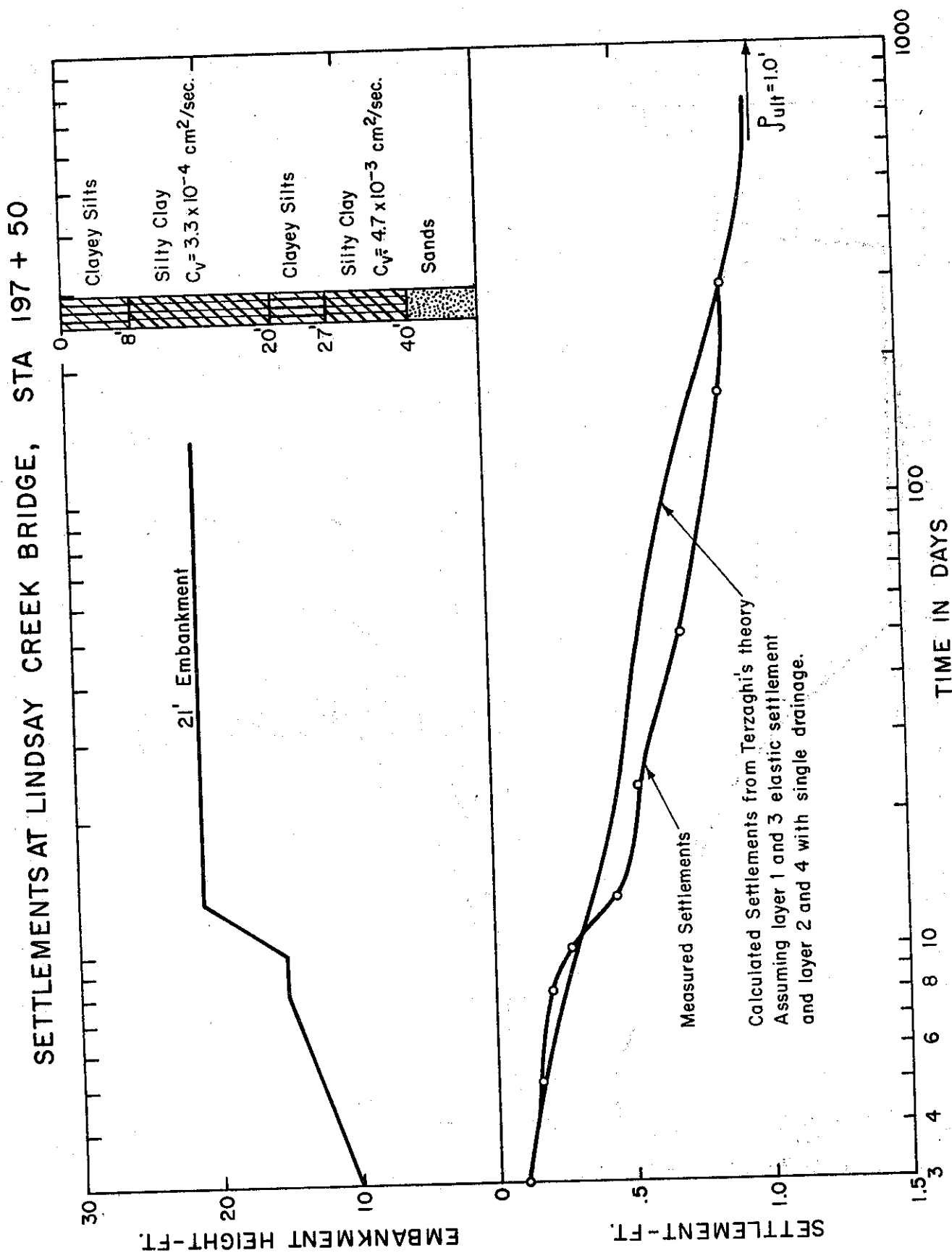


Figure 17e

SETTLEMENTS AT SAN RAMON ROAD OVERCROSSING, ABUTMENT NO. 1

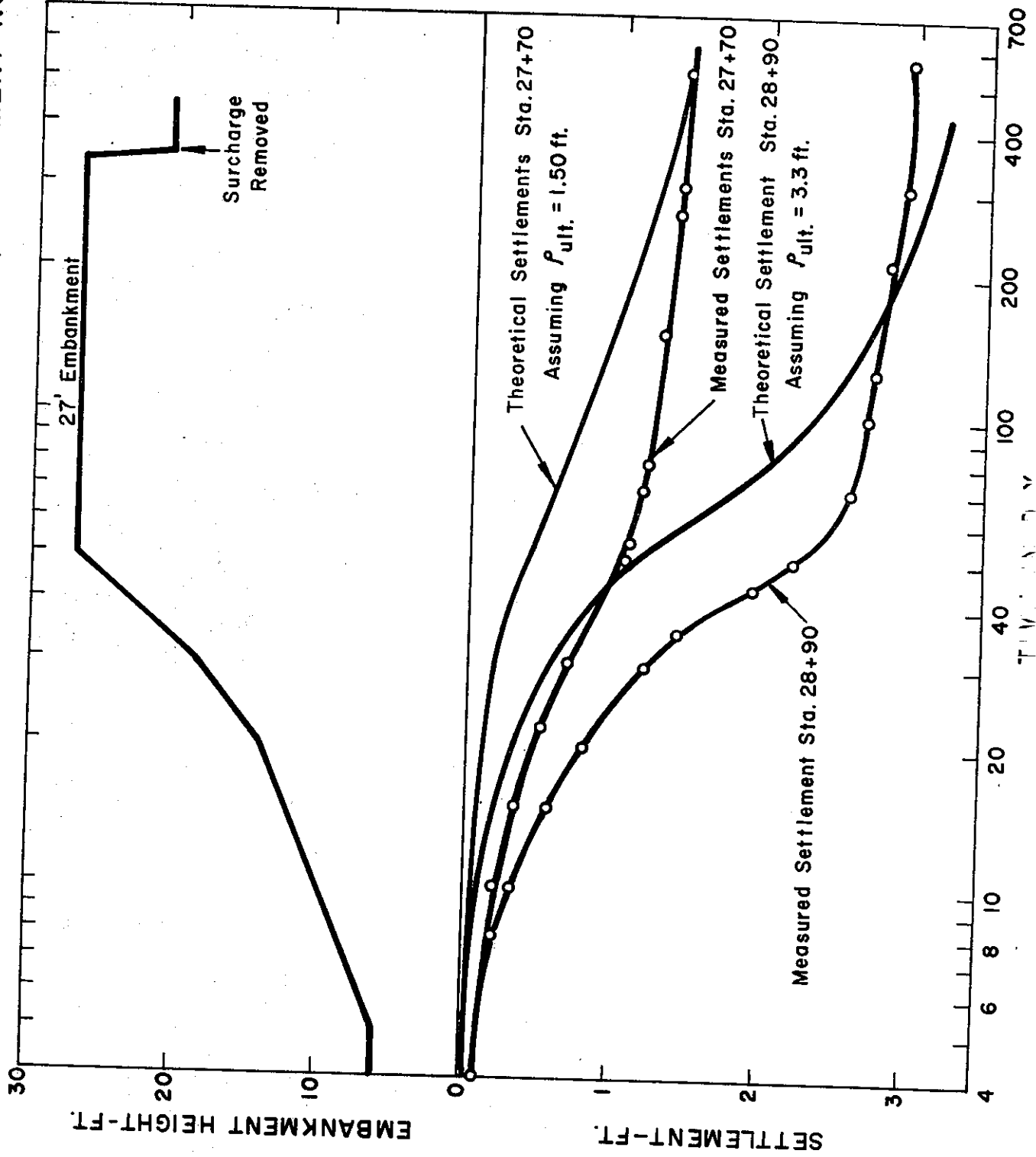
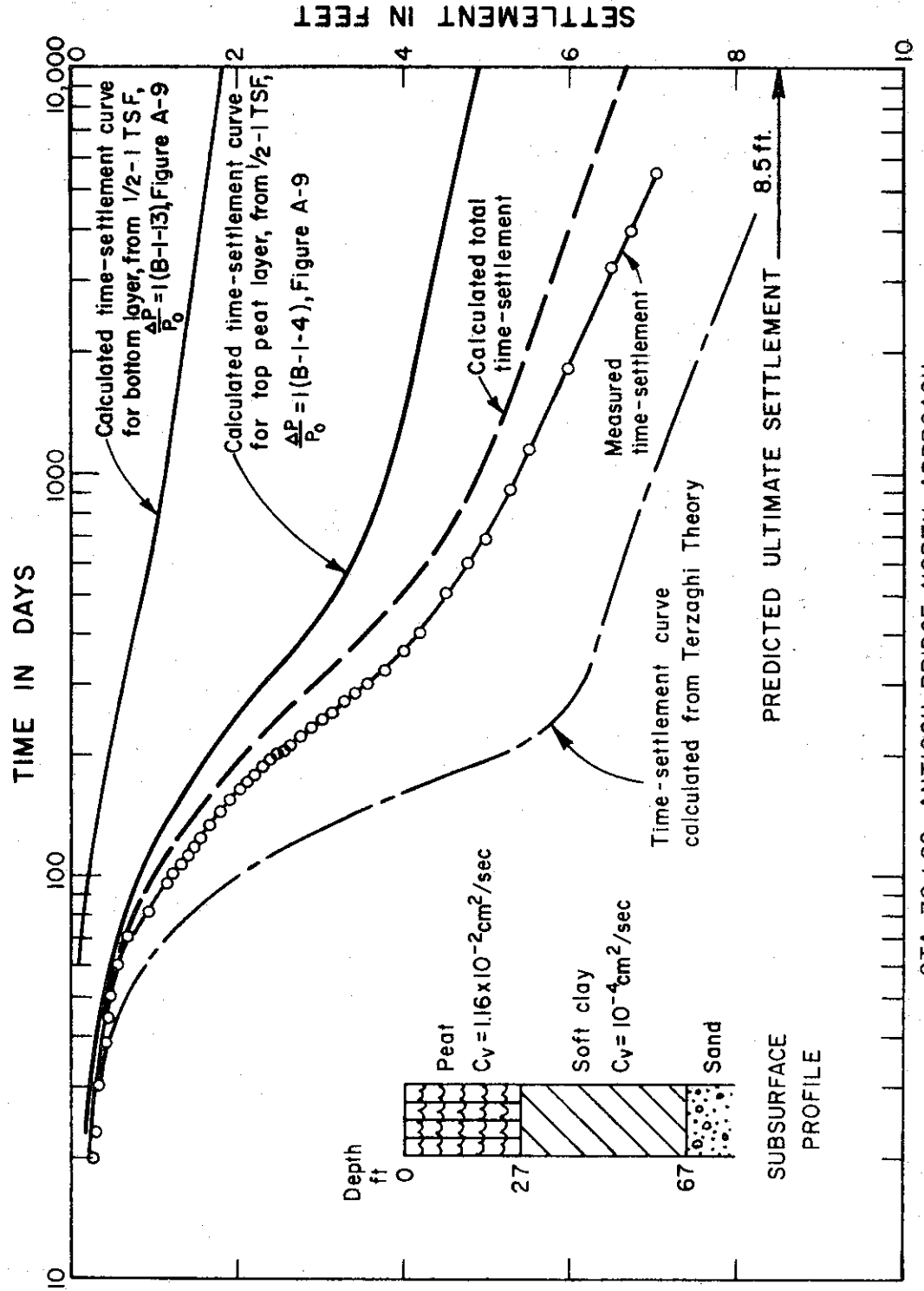


Figure 18a

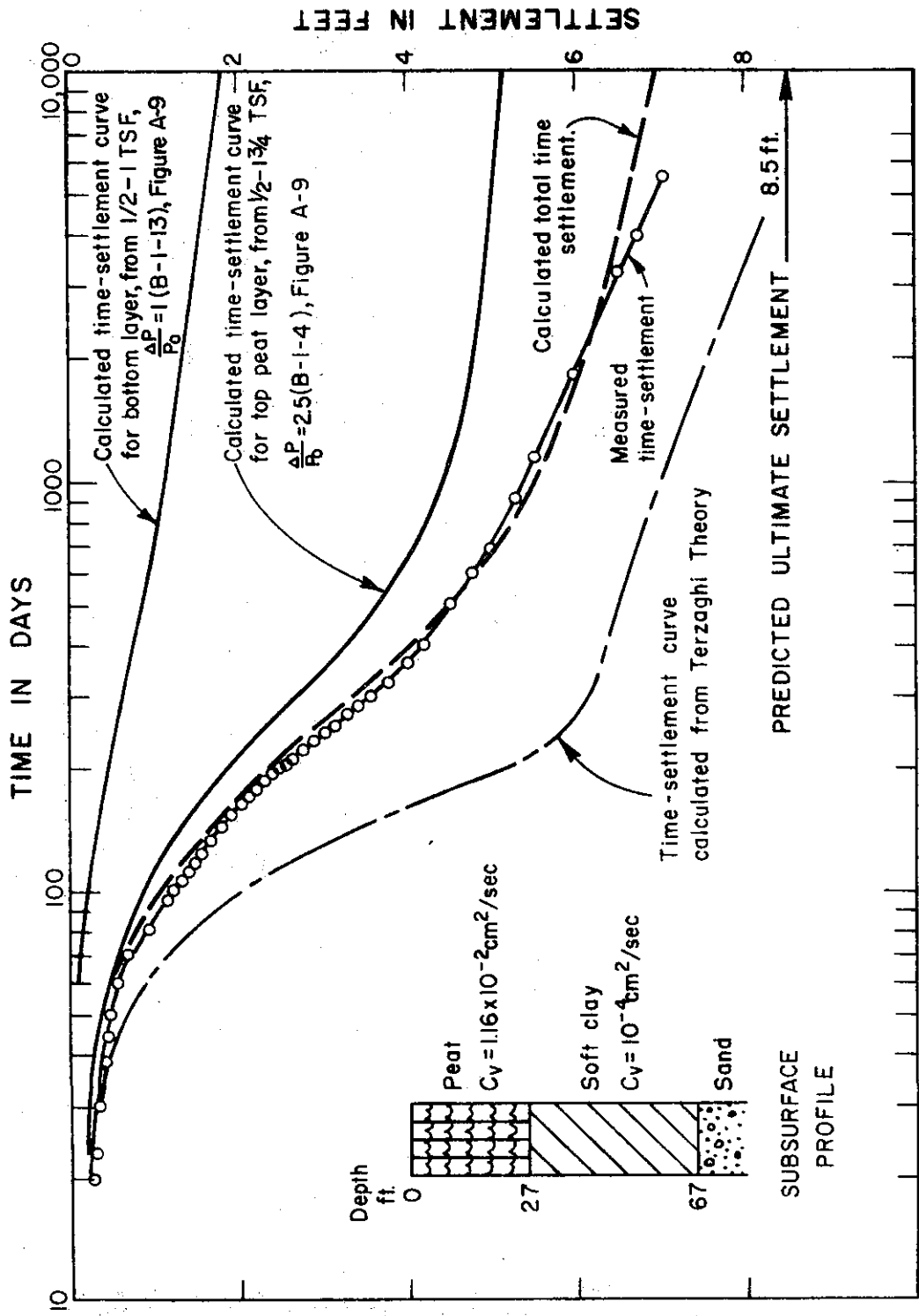
COMPARISON OF MEASURED AND CALCULATED RATE OF SETTLEMENT  
IN PEATY SOIL, USING WAHL'S METHOD



STA. 70+82, ANTIOCH BRIDGE NORTH APPROACH  
NON-SAND DRAIN AREA. TOTAL HEIGHT OF FILL, 87 FT.

Figure 18b

COMPARISON OF MEASURED AND CALCULATED RATE OF SETTLEMENT  
IN PEATY SOIL, USING WAHL'S METHOD



STA 70+82, ANTIOCH BRIDGE NORTH APPROACH  
NON-SAND DRAIN AREA. TOTAL HEIGHT OF FILL, 8.7 FT.

Figure 19

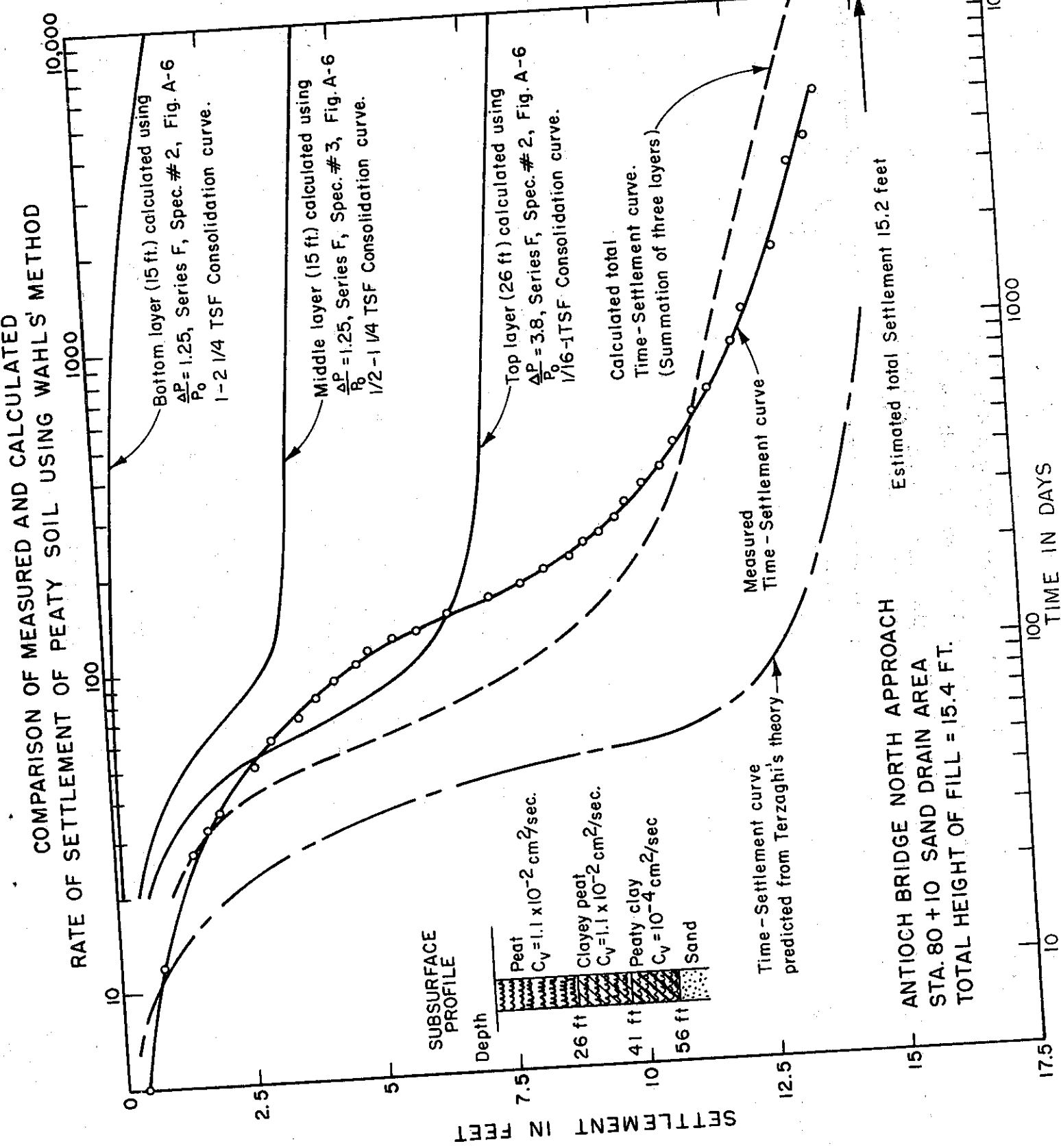


Figure 20a

COMPARISON OF CALCULATED AND MEASURED RATE OF SETTLEMENT  
 IN SILTY CLAY, USING WAHL'S METHOD ( $\Delta P/P_0 = 1$ )  
 WEST AVALON BLVD., STA. 584+58

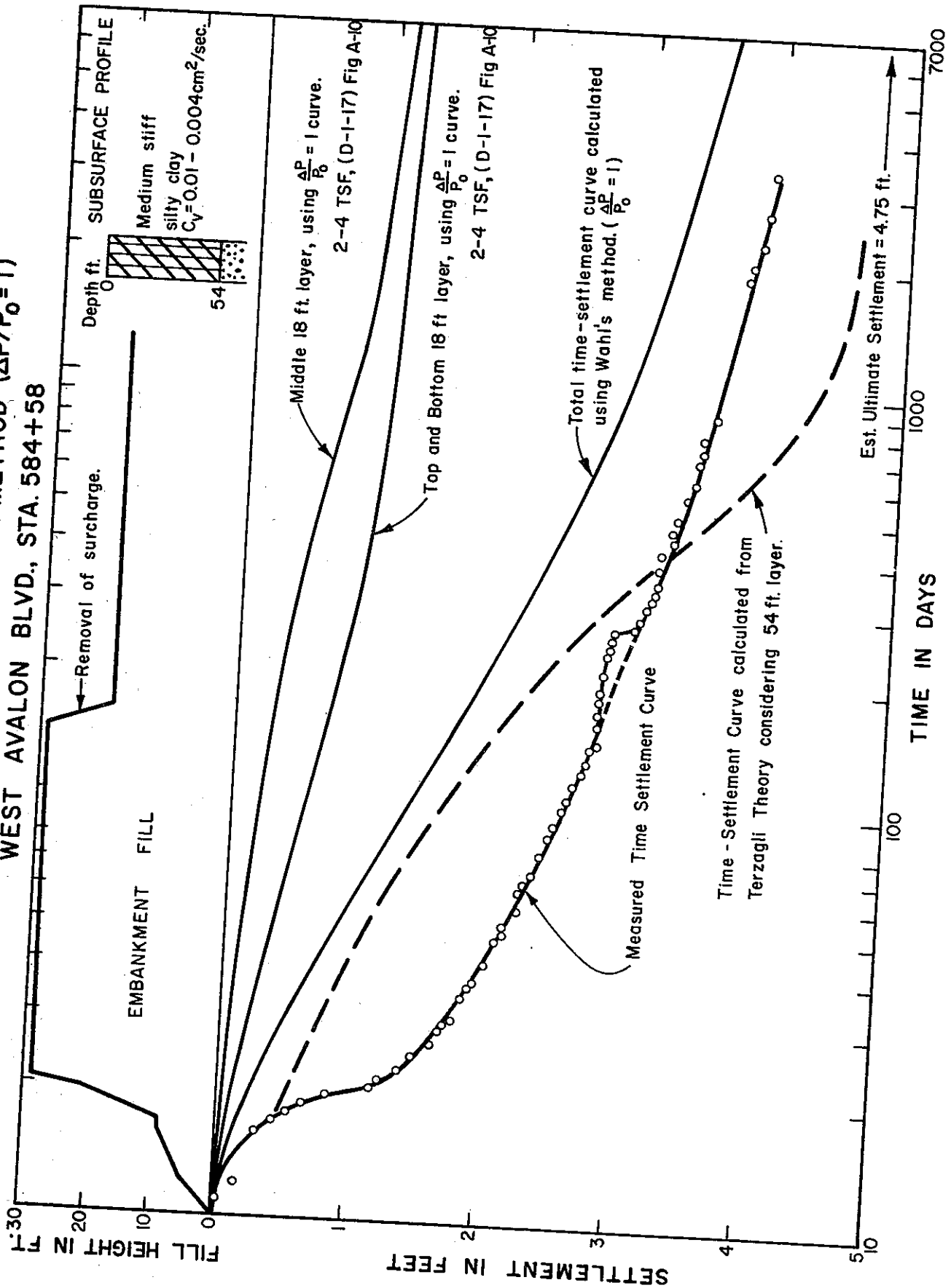


Figure 20 b

COMPARISON OF CALCULATED AND MEASURED RATE OF SETTLEMENT  
 IN SILTY CLAY, USING WAHL'S METHOD ( $\Delta P/P_0$  VARIABLE)  
 WEST AVALON BLVD., STA. 584+58

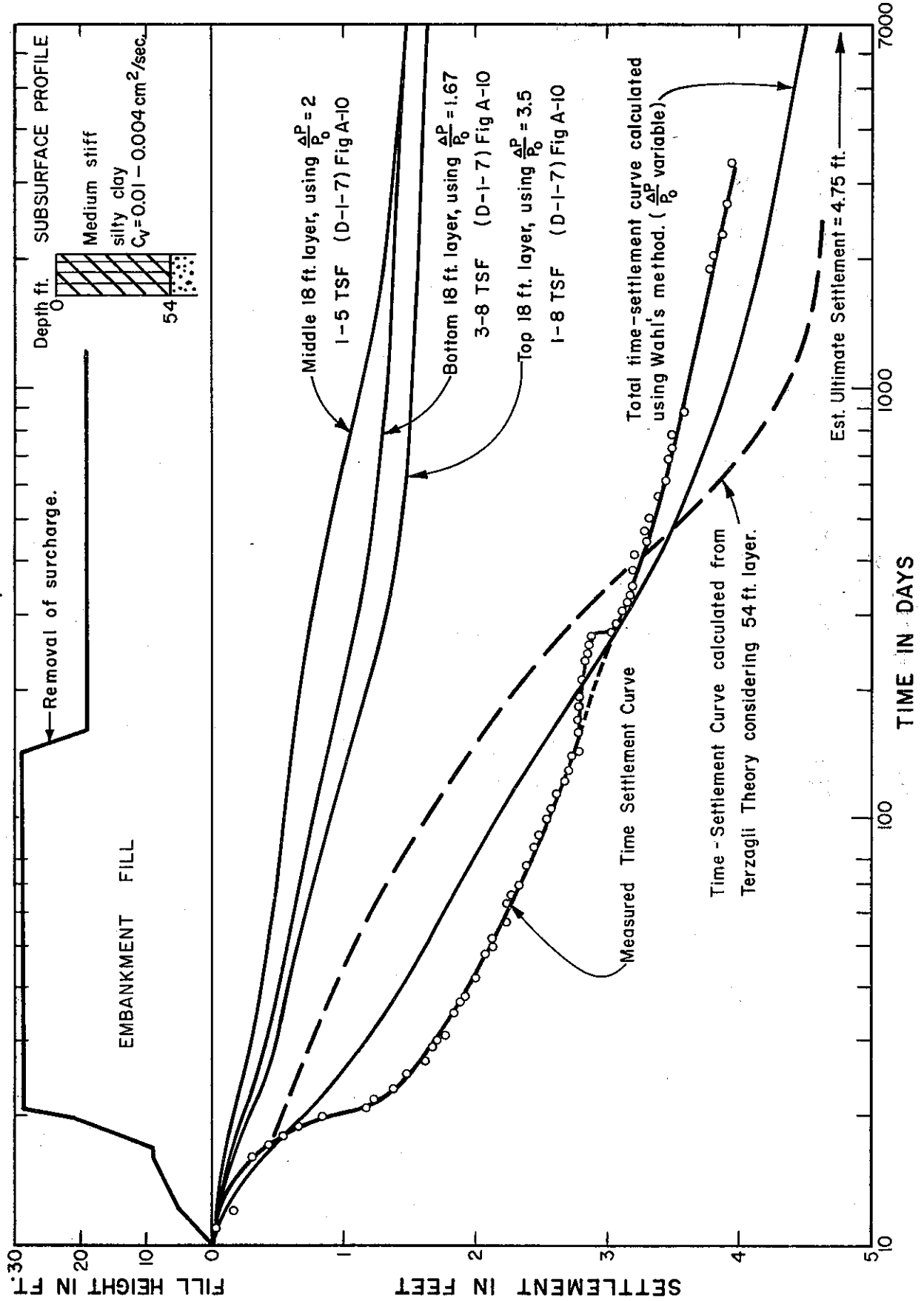


Figure 21a

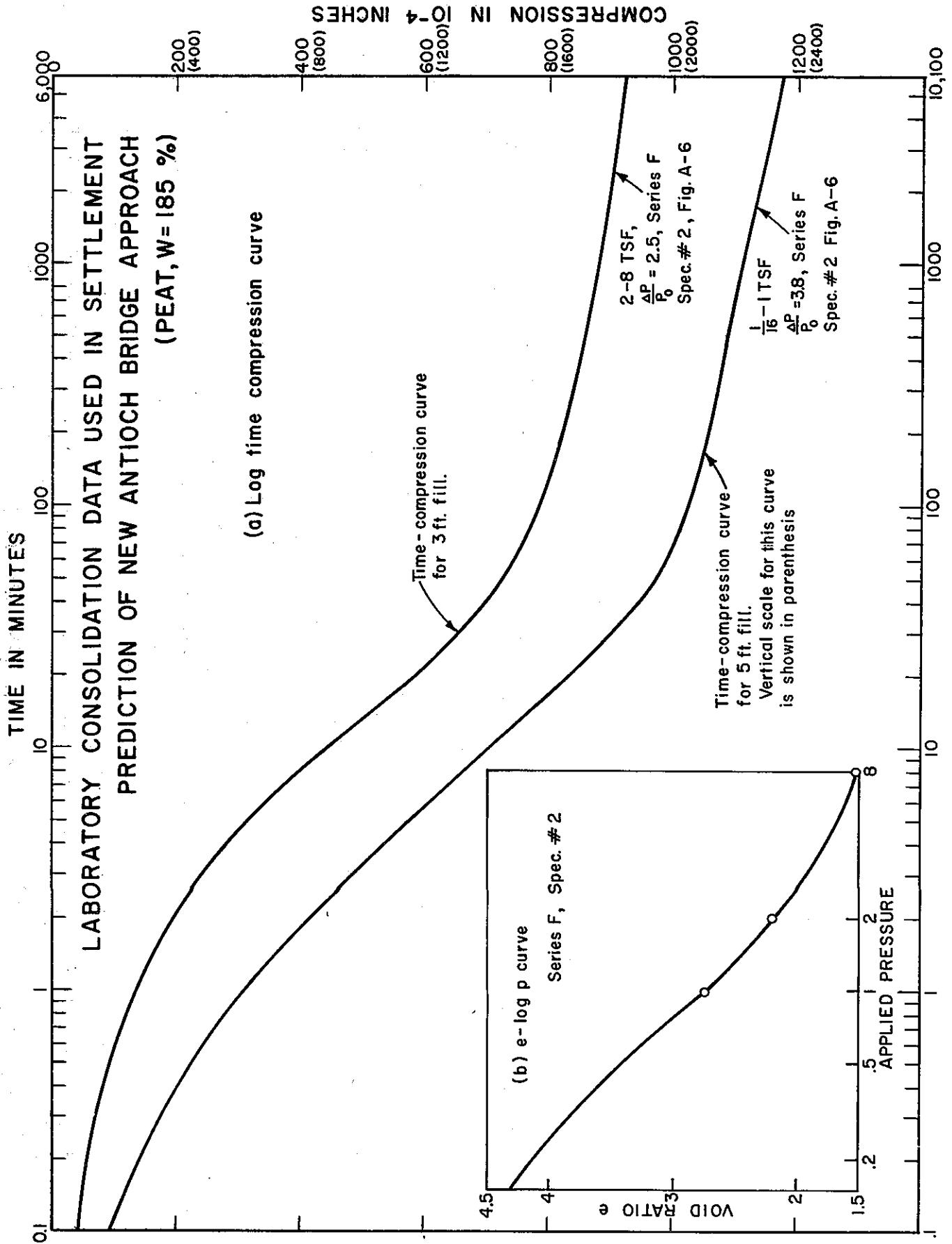


Figure 21 b

PREDICTED TIME-SETTLEMENT RELATIONSHIP  
NEW ANTIOCH BRIDGE APPROACH  
(peat, W = 185 %)

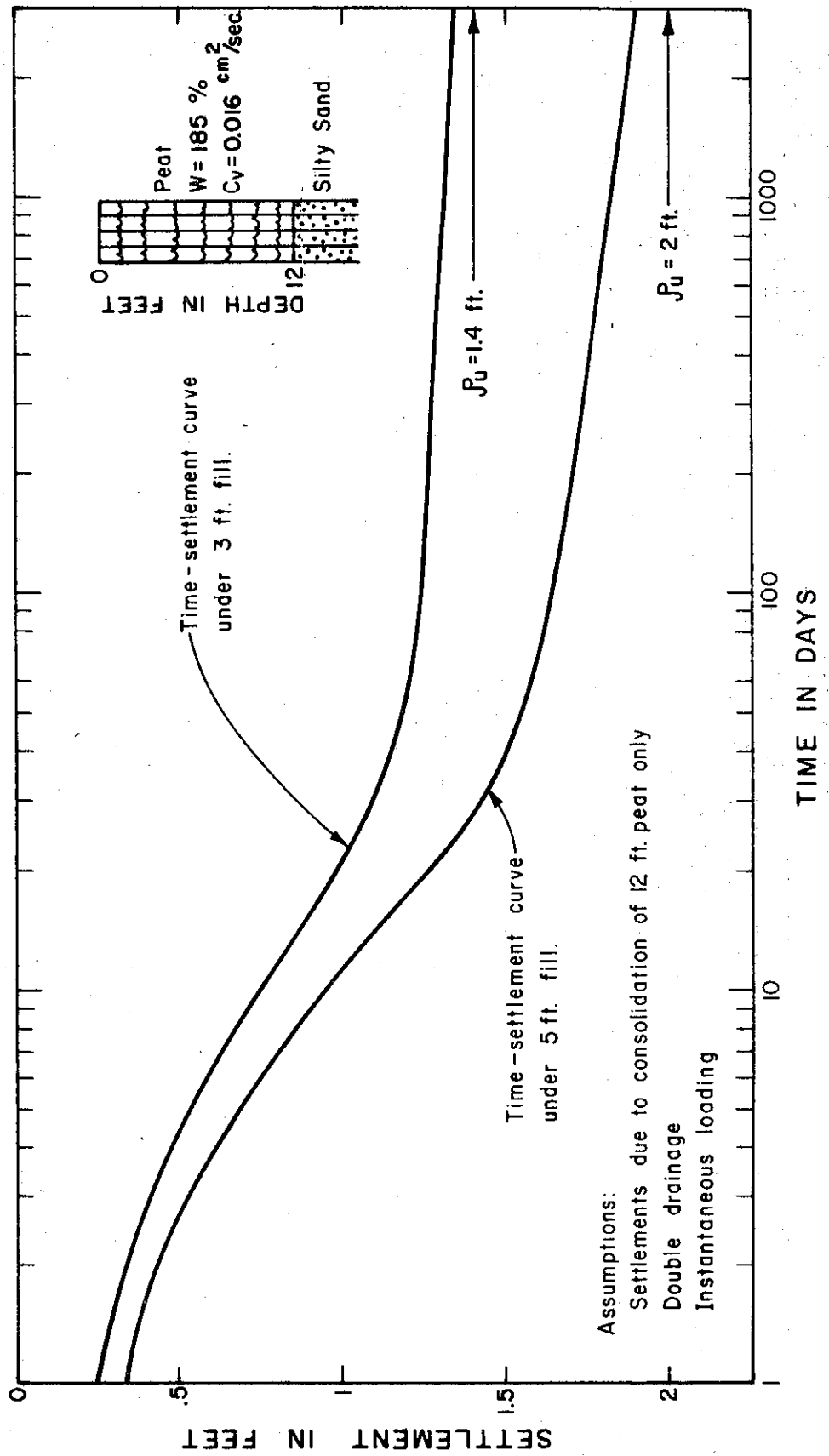


Figure 22 a

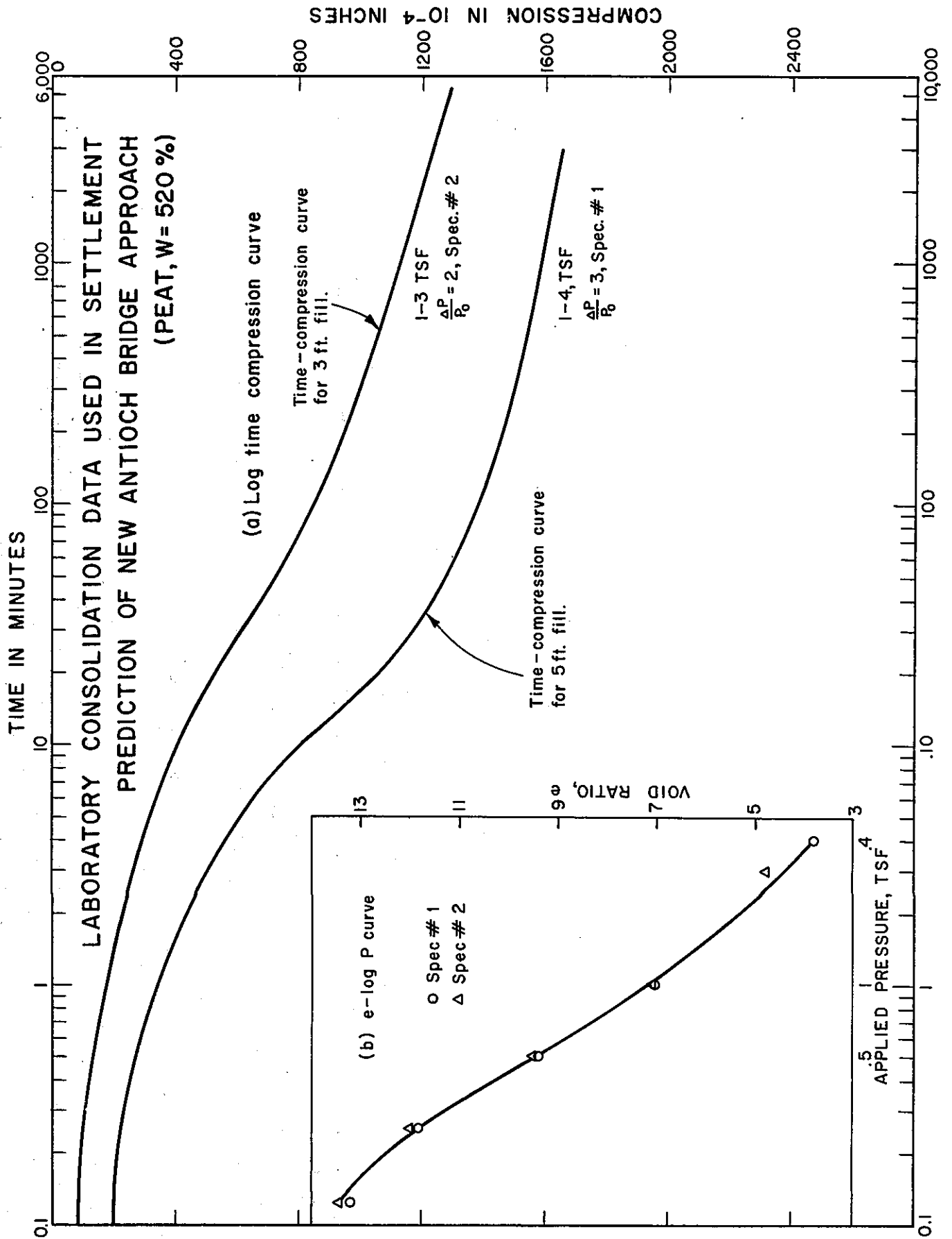
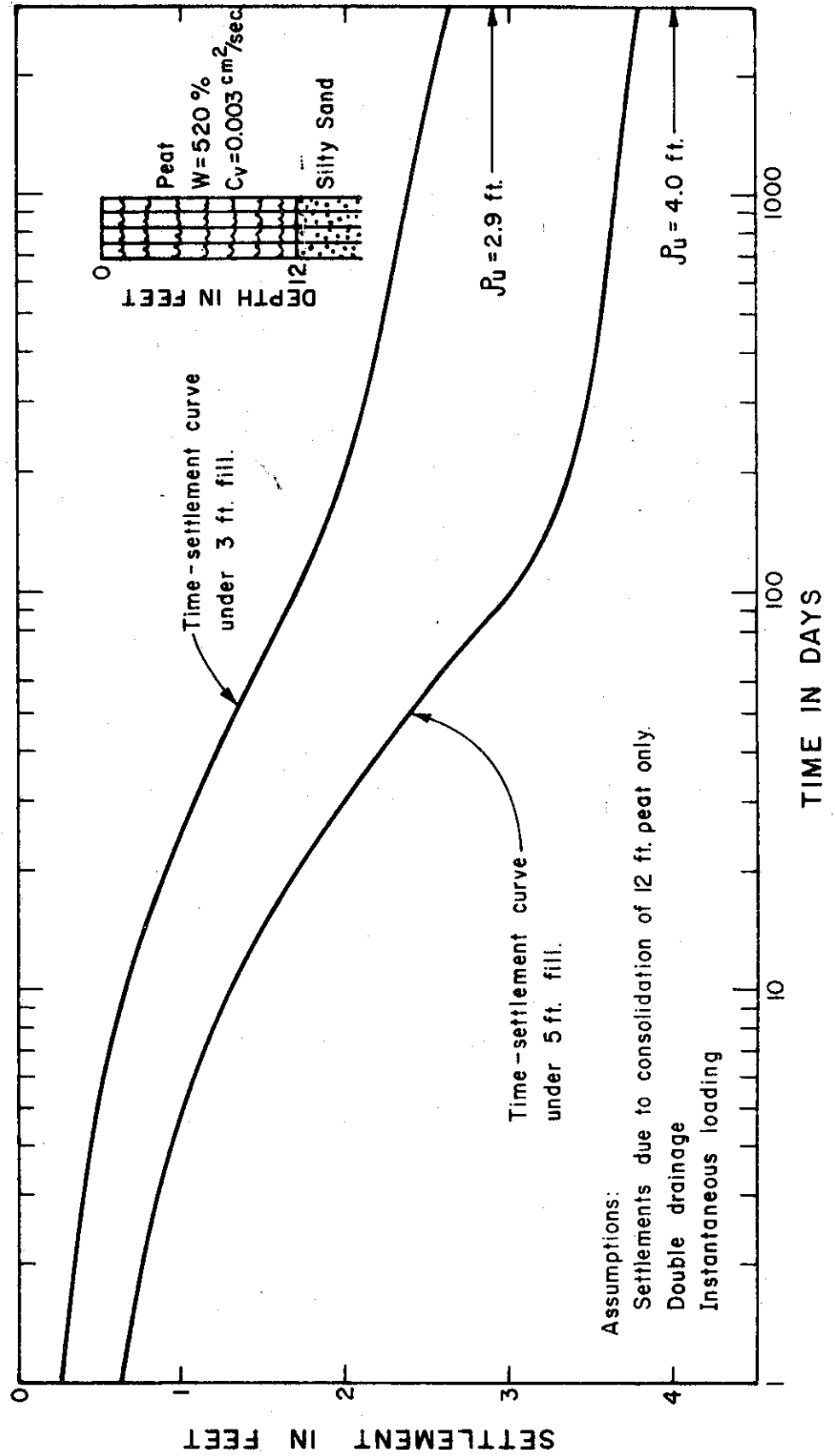
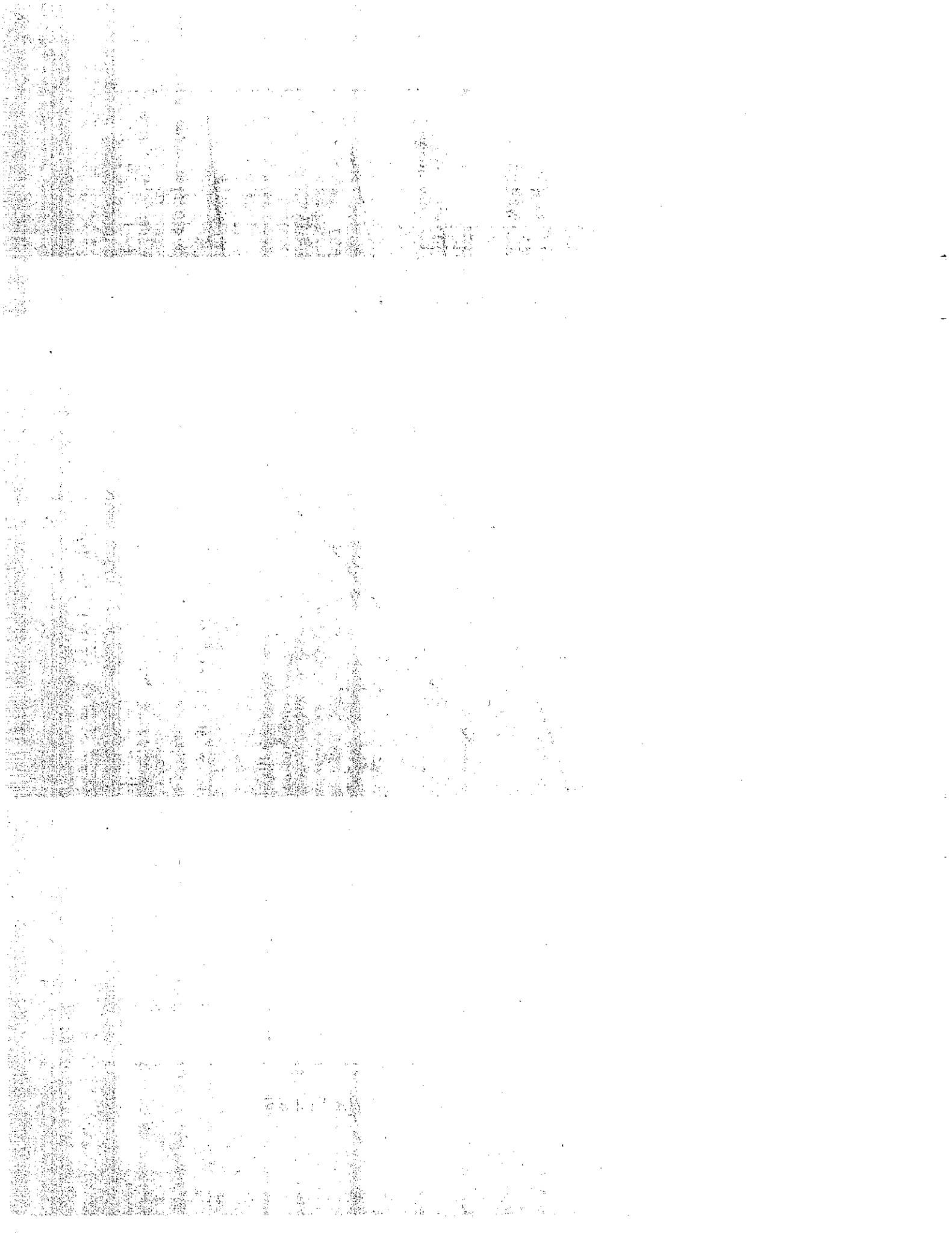
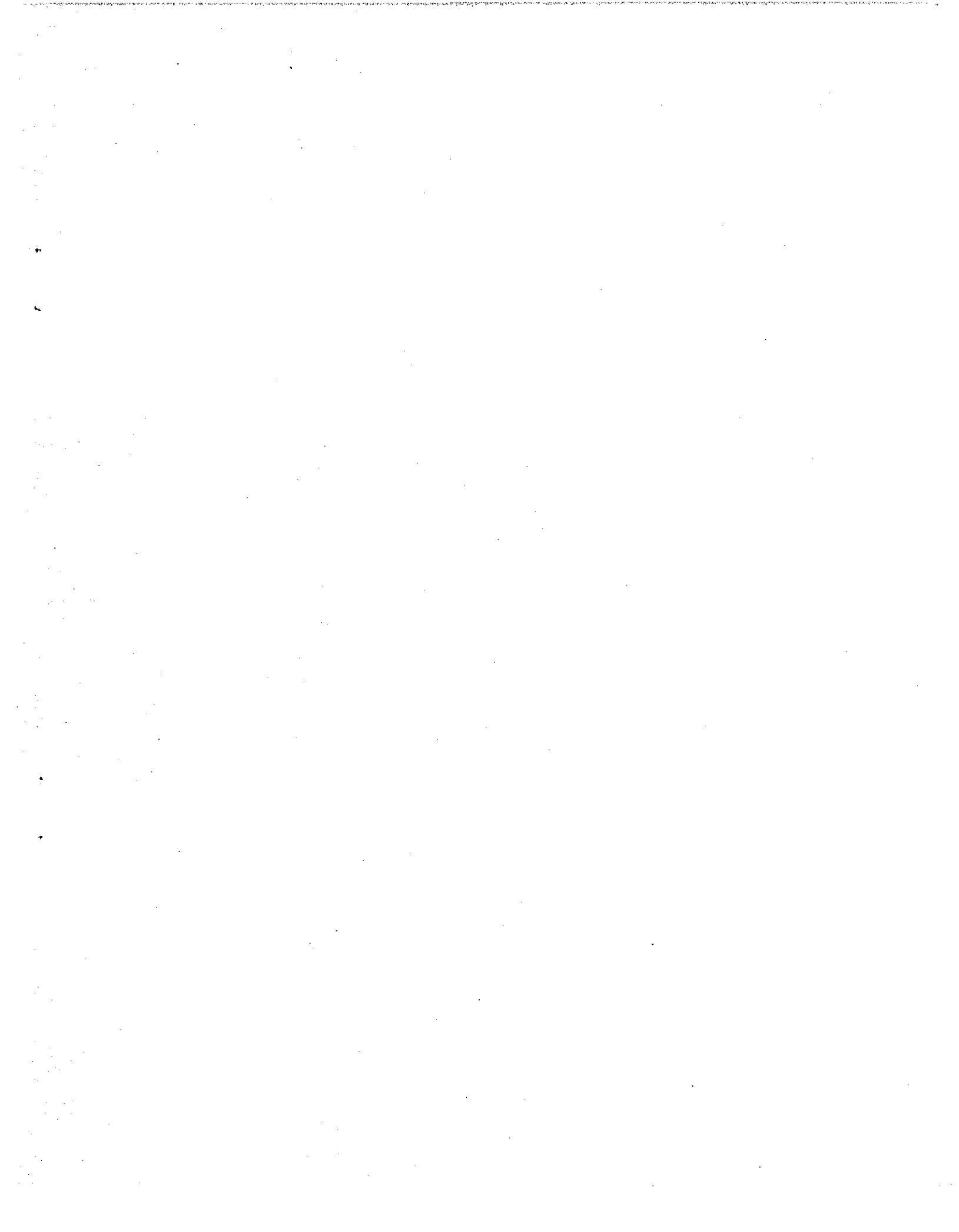


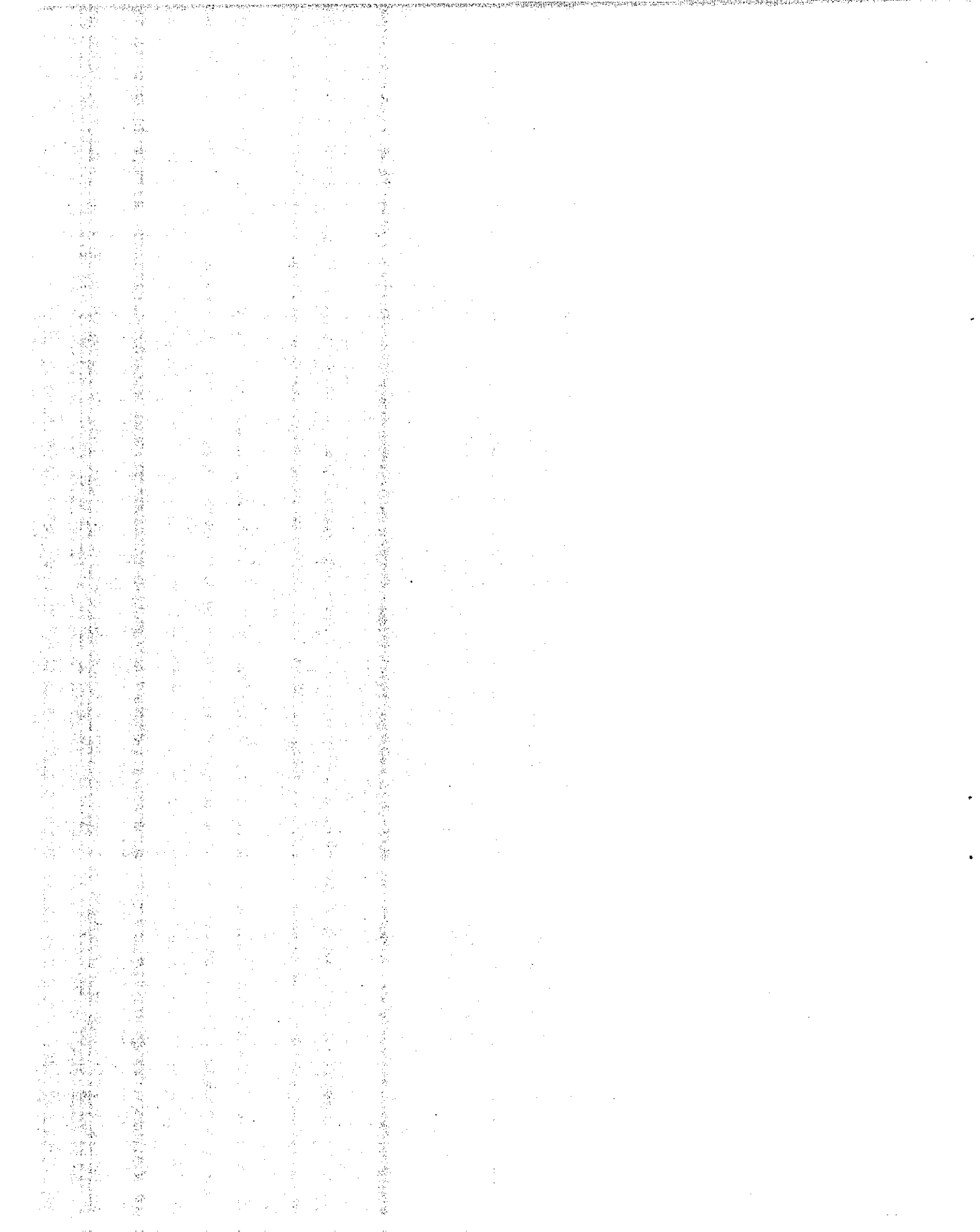
Figure 22 b

PREDICTED TIME-SETTLEMENT RELATIONSHIP  
NEW ANTIOCH BRIDGE APPROACH  
(peat,  $W=520\%$ )

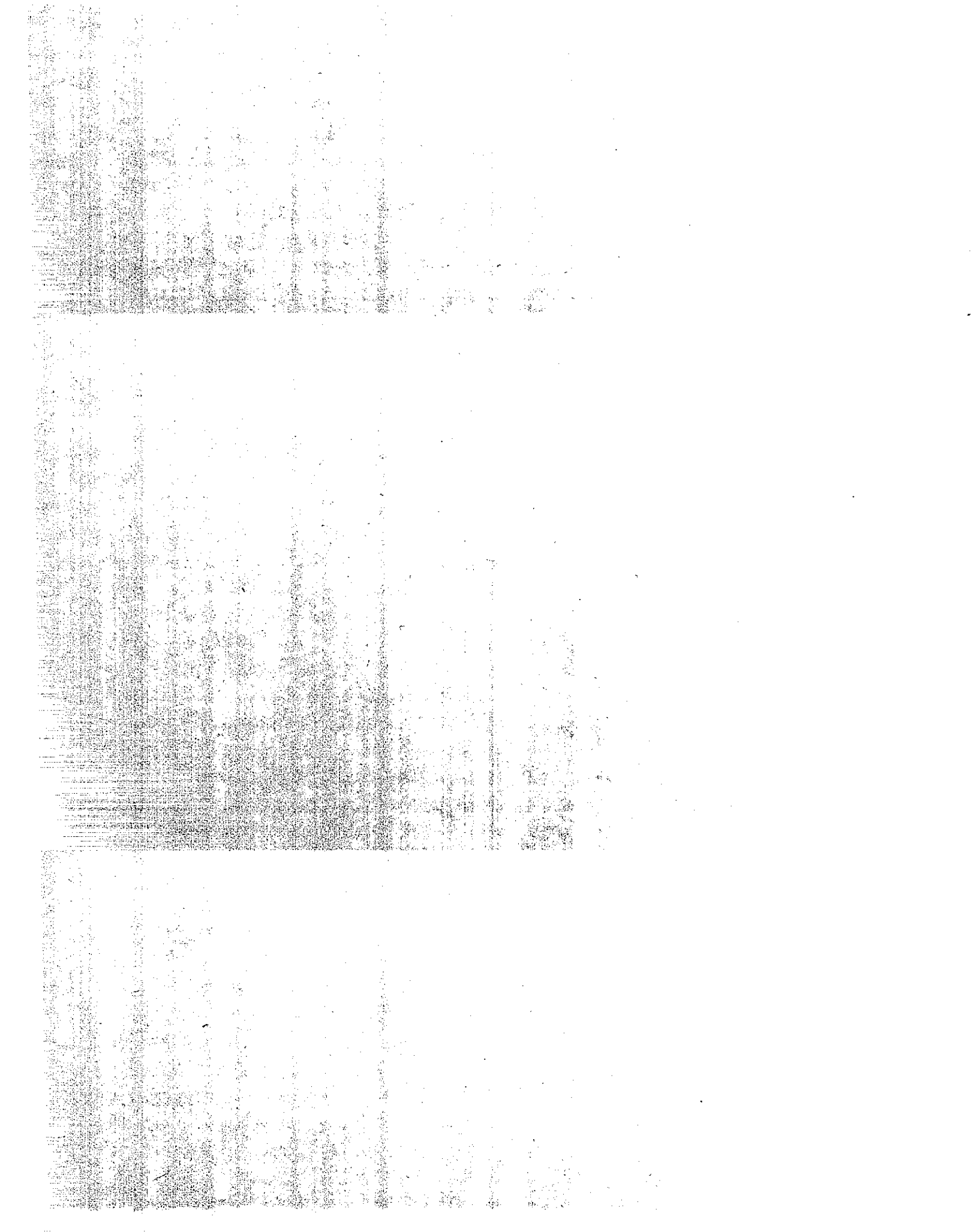






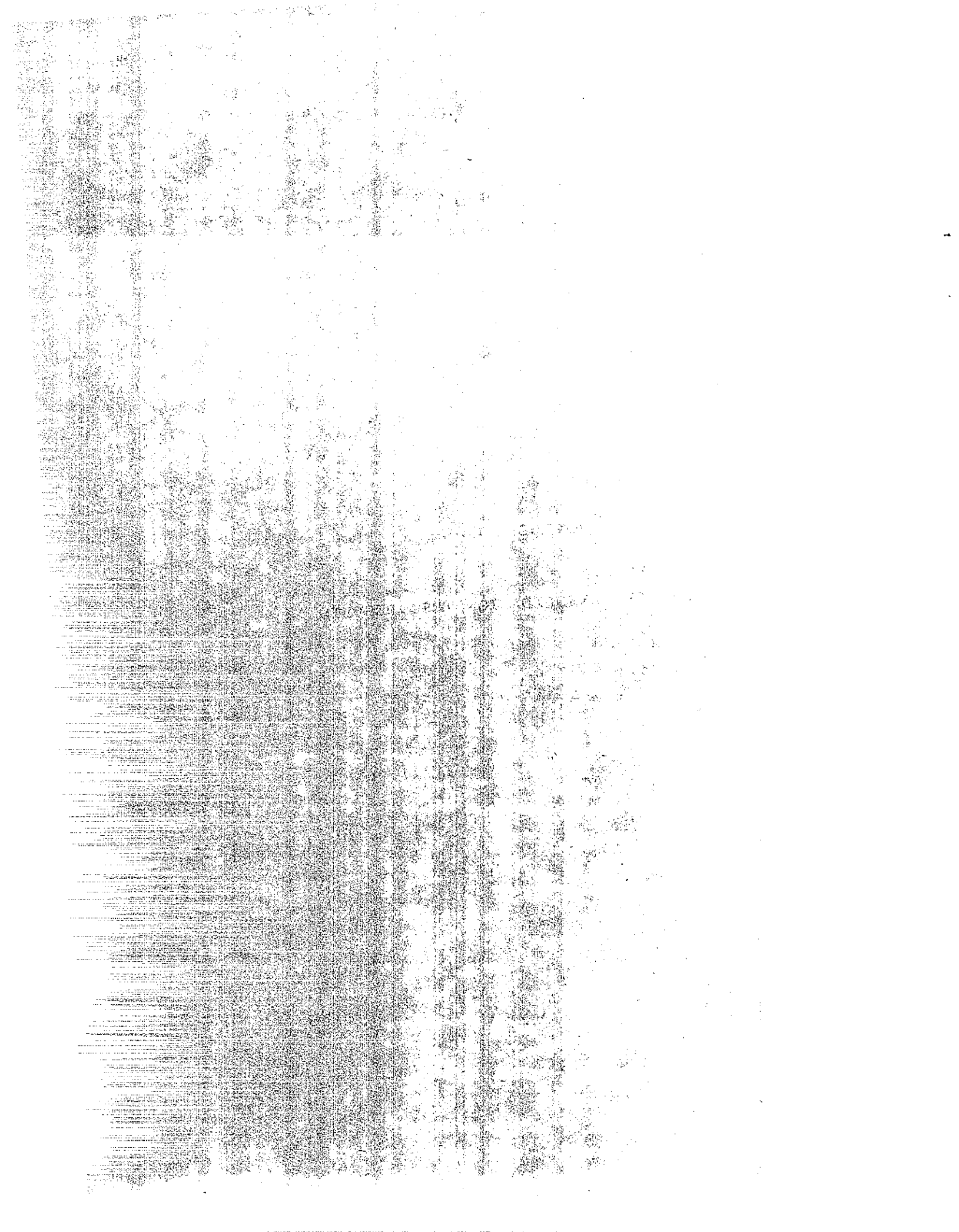


APPENDICES



APPENDIX A

SUMMARY OF CONSOLIDATION TEST RESULTS



APPENDIX A

SUMMARY OF CONSOLIDATION TEST RESULTS

Table A-1

Test Series A, Bay Mud

| Specimen Number | Load (TSF) | $\frac{\Delta P}{P_0}$ | $e_{ave.}$ | $A_{v2}$ (Cm <sup>2</sup> /Kg) | $t_{50}$ (Min) | $C_{v2}$ (Cm <sup>2</sup> /Sec)<br>x10 <sup>-4</sup> | $K$ (Cm/Sec)<br>x10 <sup>-8</sup> | $C_{\alpha}$ (%) |
|-----------------|------------|------------------------|------------|--------------------------------|----------------|------------------------------------------------------|-----------------------------------|------------------|
| 1*              | 1/2-1      | 1.0                    | 1.461      | 0.326                          | 7.2            | 3.25                                                 | 4.3                               | 0.75**           |
|                 | 1-2        | 1.0                    | 1.273      | 0.213                          | 10.4           | 1.91                                                 | 1.8                               | 0.76             |
|                 | 2-4        | 1.0                    | 1.066      | 0.100                          | 8.3            | 2.05                                                 | 1.0                               | 0.73             |
|                 | 4-8        | 1.0                    | 0.872      | 0.047                          | 5.6            | 2.50                                                 | 0.6                               | 0.75             |
| 2**             | 1/2-1      | 1.0                    | 1.724      | 0.394                          | 15.0           | 1.62                                                 | 2.3                               | 0.81             |
|                 | 1-2        | 1.0                    | 1.502      | 0.247                          | 13.0           | 1.56                                                 | 1.5                               | 1.07             |
|                 | 2-4        | 1.0                    | 1.260      | 0.118                          | 10.7           | 1.55                                                 | 0.8                               | 0.89             |
|                 | 4-8        | 1.0                    | 1.033      | 0.055                          | 7.2            | 1.92                                                 | 0.5                               | 1.16             |
| 3**             | 1/2-3/4    | .5                     | 1.779      | 0.638                          | 36.5           | 0.67                                                 | 1.5                               | -                |
|                 | 3/4-1, 7/8 | 1.5                    | 1.568      | 0.236                          | 11.5           | 1.83                                                 | 1.7                               | 0.90             |
|                 | 1, 7/8-3   | .6                     | 1.354      | 0.144                          | 22.0           | 0.79                                                 | 0.5                               | 1.16             |
|                 | 3-8        | 1.67                   | 1.123      | 0.062                          | 5.7            | 2.50                                                 | 0.7                               | 0.90             |
| 4**             | 1/2-2      | 3.0                    | 1.681      | 0.325                          | 6.5            | 3.50                                                 | 4.3                               | 0.84             |
|                 | 2-6        | 2.0                    | 1.263      | 0.116                          | 6.3            | 2.55                                                 | 1.3                               | 0.54             |
| 5*              | 1/2-1      | 1.0                    | 1.798      | 0.435                          | 12.5           | 2.05                                                 | 3.2                               | 1.18             |
|                 | 1-2        | 1.0                    | 1.557      | 0.264                          | 11.5           | 1.77                                                 | 1.8                               | 1.15             |
|                 | 2-4        | 1.0                    | 1.302      | 0.123                          | 9.0            | 1.80                                                 | 1.0                               | 1.14             |
|                 | 4-8        | 1.0                    | 1.063      | 0.058                          | 5.8            | 2.25                                                 | 0.6                               | 1.16             |
| Average         |            |                        |            |                                | 11.4           | 2.0x10 <sup>-4</sup>                                 | 1.6x10 <sup>-8</sup>              | 0.93             |

\*Standard one-day increment tests.

\*\*Load increment duration of 4-days.

\*\*\*Estimated  $C_{\alpha}$  value due to insufficient time allowed for secondary compression.

# CONSOLIDATION TEST RESULTS, BAY MUD, TEST SERIES A

Figure A-1

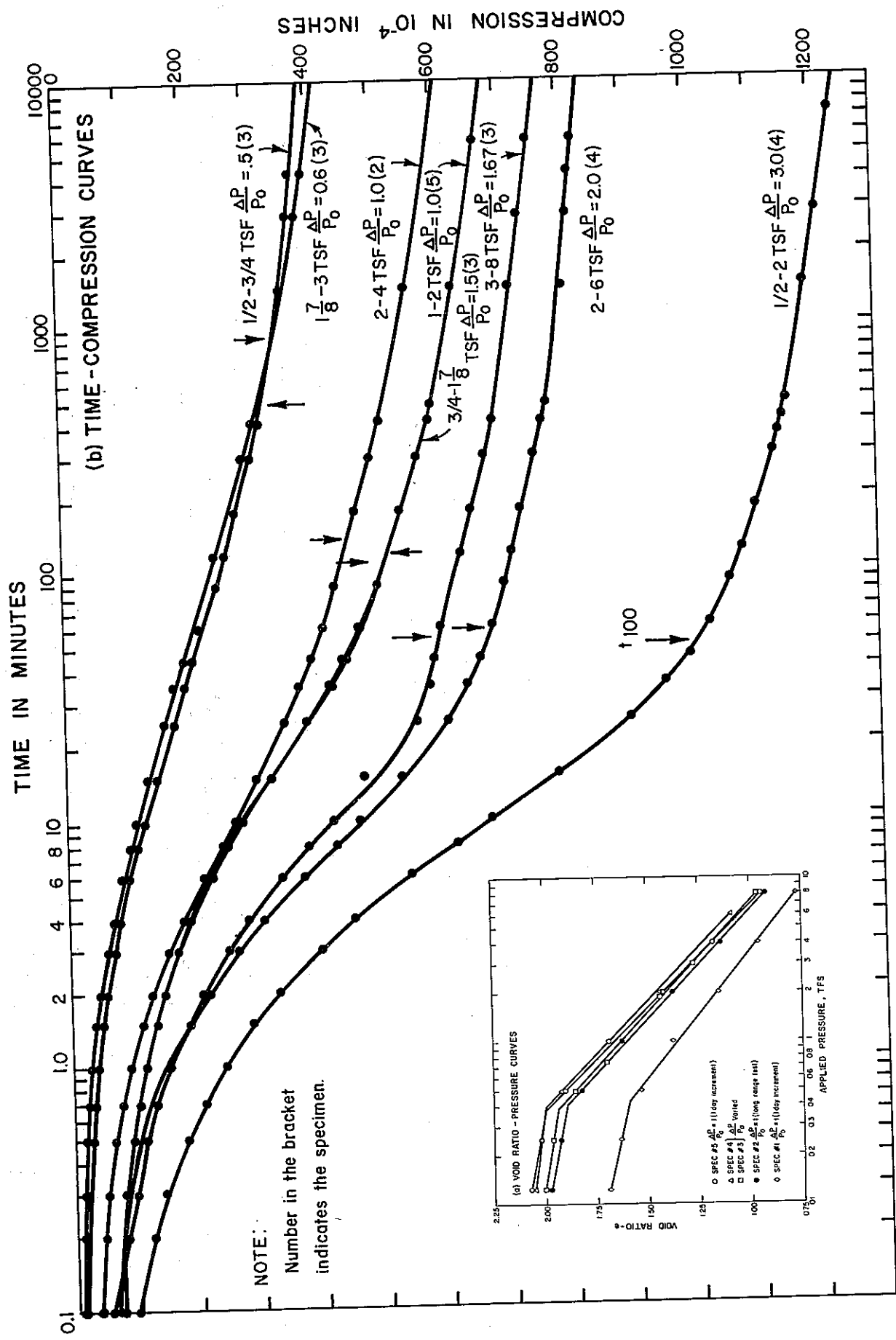


Table A-2

Test Series B, Bay Mud

| Specimen Number | Load (TSF) | $\frac{\Delta P}{P_0}$ | e ave. | $A_v$<br>( $\text{Cm}^2/\text{Fg}$ ) | $t_{50}$<br>(Min) | $C_v$<br>( $\text{Cm}^2/\text{Sec}$ ) | K<br>( $\text{Cm}/\text{Sec}$ ) | $C_\alpha$<br>(%) |
|-----------------|------------|------------------------|--------|--------------------------------------|-------------------|---------------------------------------|---------------------------------|-------------------|
|                 |            |                        |        |                                      |                   | $\times 10^{-4}$                      | $\times 10^{-8}$                |                   |
| 1*              | 1/2-1      | 1.0                    | 1.663  | 0.284                                | 8.7               | 3.00                                  | 3.2                             | 1.24              |
|                 | 1-2        | 1.0                    | 1.486  | 0.212                                | 10.0              | 2.25                                  | 1.9                             | 1.20              |
|                 | 2-4        | 1.0                    | 1.286  | 0.095                                | 7.0               | 2.75                                  | 1.1                             | 1.14              |
|                 | 4-8        | 1.0                    | 1.109  | 0.041                                | 5.8               | 2.80                                  | 0.5                             | 0.93              |
| 2**             | 1/2-1      | 1.0                    | 1.669  | 0.300                                | 15.5              | 1.65                                  | 1.9                             | 1.06              |
|                 | 1-2        | 1.0                    | 1.491  | 0.206                                | 10.1              | 2.23                                  | 1.8                             | 1.01              |
|                 | 2-4        | 1.0                    | 1.293  | 0.095                                | 8.2               | 2.32                                  | 1.0                             | 0.86              |
|                 | 4-8        | 1.0                    | 1.116  | 0.041                                | 5.8               | 2.78                                  | 0.5                             | 0.95              |
| 3**             | 1/2-5/8    | 0.3                    | 1.850  | 0.568                                | 45.0              | 0.59                                  | 1.2                             | 0.70              |
|                 | 5/8-2      | 2.2                    | 1.646  | 0.238                                | 9.0               | 2.55                                  | 2.3                             | 1.05              |
|                 | 2-3        | 0.5                    | 1.377  | 0.121                                | 31.0              | 0.63                                  | 0.3                             | 1.06              |
|                 | 3-8        | 1.67                   | 1.179  | 0.055                                | 5.3               | 3.06                                  | 0.8                             | 1.02              |
| 4**             | 1/2-2      | 3.0                    | 1.685  | 0.271                                | 9.5               | 2.47                                  | 2.5                             | 1.11              |
|                 | 2-8        | 3.0                    | 1.272  | 0.071                                | 5.7               | 2.92                                  | 0.9                             | 0.88              |
| 5*              | 1/2-1      | 1.0                    | 1.825  | 0.374                                | 19.4              | 1.31                                  | 1.7                             | 0.79              |
|                 | 1-2        | 1.0                    | 1.607  | 0.239                                | 14.5              | 1.50                                  | 1.4                             | 0.97              |
|                 | 2-4        | 1.0                    | 1.377  | 0.110                                | 11.0              | 1.64                                  | 0.7                             | 0.93              |
|                 | 4-8        | 1.0                    | 1.167  | 0.050                                | 10.5              | 1.43                                  | 0.3                             | 0.87              |
| Average         |            |                        |        |                                      | 12.9              | $2.1 \times 10^{-4}$                  | $1.1 \times 10^8$               | 1.00              |

\* Standard one-day increment tests.

\*\* Long term consolidation test.

# CONSOLIDATION TEST RESULTS, BAY MUD, TEST SERIES B

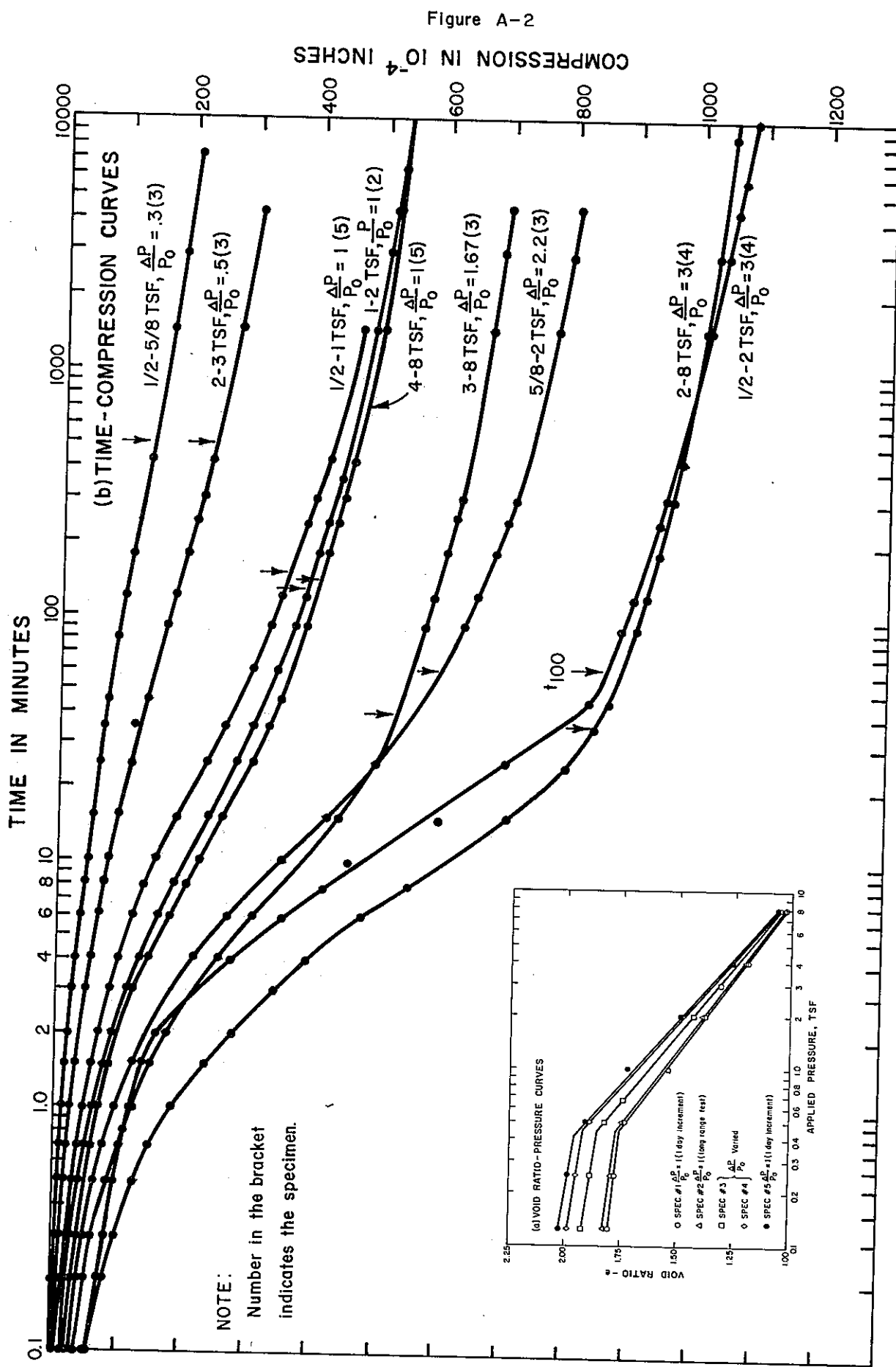


Figure A-2

Table A-3

Test Series C, Silty Clay

| Specimen Number | Load (TSF) | $\frac{\Delta P}{P_0}$ | e ave. | $A_v$ (Cm <sup>2</sup> /Kg) | $t_{50}$ (Min) | $C_v$ (Cm <sup>2</sup> /Sec) | K (Cm/Sec)           | $C_a$ (%) |
|-----------------|------------|------------------------|--------|-----------------------------|----------------|------------------------------|----------------------|-----------|
|                 |            |                        |        |                             |                | $\times 10^{-3}$             | $\times 10^{-8}$     |           |
| 1*              | 1/2-1      | 1.0                    | 1.148  | 0.064                       | 1.0            | 2.84                         | 8.4                  | .19**     |
|                 | 1-2        | 1.0                    | 1.106  | 0.052                       | 1.7            | 1.61                         | 4.0                  | .30       |
|                 | 2-4        | 1.0                    | 1.035  | 0.046                       | 2.2            | 1.17                         | 2.6                  | .34       |
|                 | 4-8        | 1.0                    | 0.931  | 0.029                       | 2.3            | 1.06                         | 1.6                  | .51       |
| 2               | 1/2-1      | 1.0                    | 1.152  | 0.056                       | ---            | ---                          | ---                  | .11**     |
|                 | 1-2        | 1.0                    | 1.111  | 0.054                       | 1.7            | 1.62                         | 4.1                  | .26       |
|                 | 2-4        | 1.0                    | 1.038  | 0.046                       | 2.45           | 1.04                         | 2.4                  | .34       |
|                 | 4-8        | 1.0                    | 0.933  | 0.030                       | 2.1            | 1.10                         | 1.7                  | .45       |
| 3               | 3/4-2      | 1.67                   | 1.128  | 0.068                       | 1.2            | 2.32                         | 7.4                  | 0.35      |
|                 | 2-3        | 0.5                    | 1.062  | 0.049                       | 2.6            | 0.92                         | 2.2                  | 0.34      |
|                 | 3-8        | 1.67                   | .948   | 0.019                       | 1.5            | 1.53                         | 1.5                  | 0.45      |
| 4               | 1/2-2      | 3.0                    | 1.198  | 0.073                       | .81            | 3.40                         | 11.3                 | .27       |
|                 | 2-8        | 3.0                    | 1.007  | 0.044                       | 1.0            | 2.34                         | 5.1                  | .42       |
| 5               | 1/2-4      | 7.0                    | 1.057  | 0.075                       | .7             | 3.65                         | 13.3                 | .57       |
|                 | 4-8        | 1.0                    | 0.864  | 0.031                       | 1.55           | 1.33                         | 2.2                  | .59       |
| 6               | 1/2-3/4    | 0.50                   | 1.269  | 0.096                       | ---            | ---                          | ---                  | .19**     |
|                 | 3/4-1      | 0.33                   | 1.249  | 0.076                       | ---            | ---                          | ---                  | .23       |
|                 | 1-8        | 7.0                    | 1.080  | 0.045                       | .90            | 2.70                         | 5.8                  | 0.60      |
| Average         |            |                        |        |                             | 1.6            | $1.9 \times 10^{-3}$         | $4.9 \times 10^{-8}$ | 0.40      |

\* Standard one-day increment tests.

\*\* Value of  $C_a$  not included in calculation of the average value. The applied pressure for this increment is below the precompression pressure.

CONSOLIDATION TEST RESULTS, SILTY CLAY, TEST SERIES C

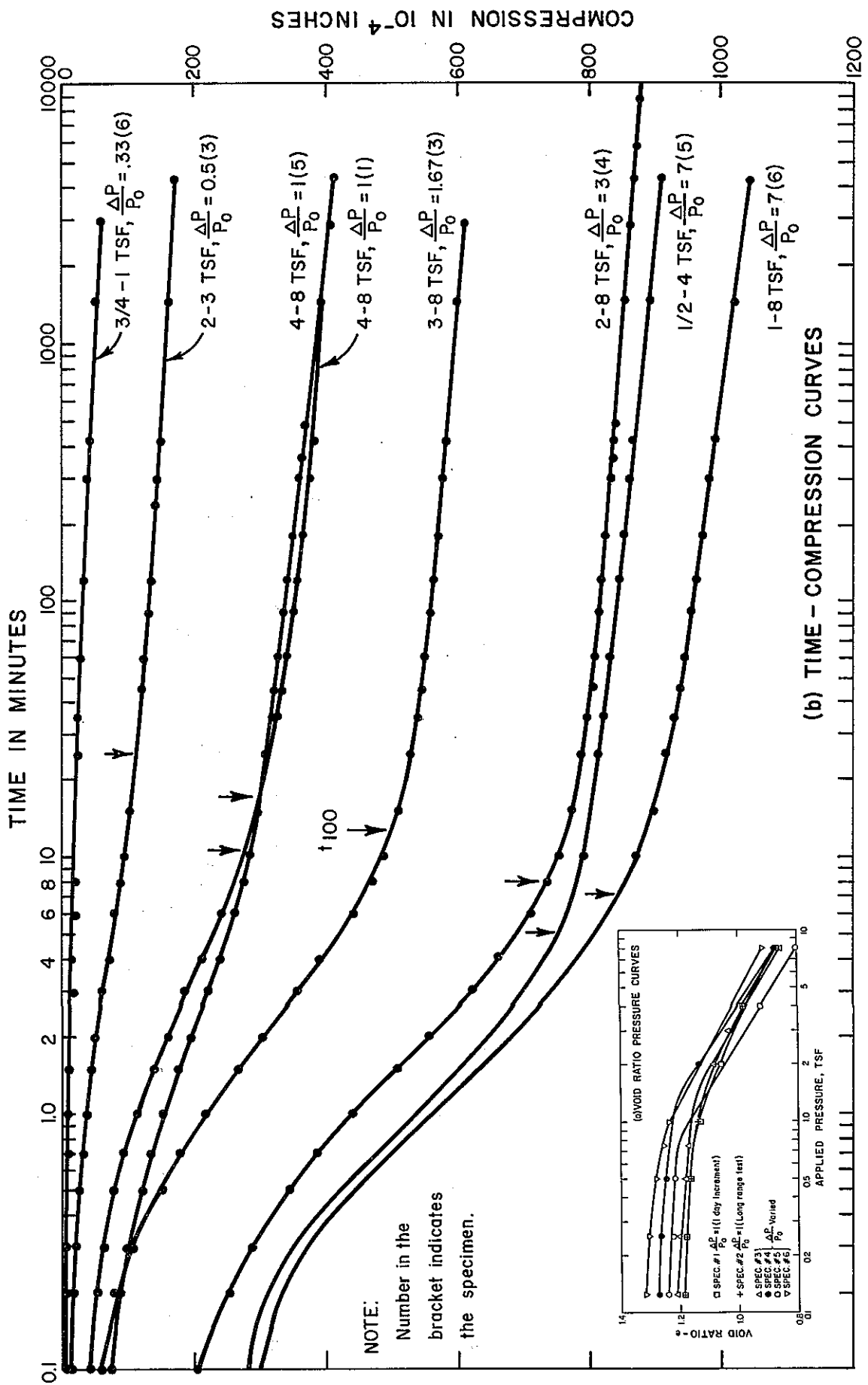


Table A-4

Test Series D, Bay Mud

| Specimen Number | Load (TSF) | $\frac{\Delta P}{P_0}$ | e ave. | $A_v$ (Cm <sup>2</sup> /Kg) | $t_{50}$ (Min) | $C_v$ (Cm <sup>2</sup> /Sec) | K (Cm/Sec)           | $C_c$ (%) |
|-----------------|------------|------------------------|--------|-----------------------------|----------------|------------------------------|----------------------|-----------|
|                 |            |                        |        |                             |                | $\times 10^{-4}$             | $\times 10^{-8}$     |           |
| 1               | 1/8-1/4    | .25                    | 1.943  | ---                         | ---            | ---                          | ---                  | 0.11      |
|                 | 1/4-1/2    | .50                    | 1.906  | ---                         | ---            | ---                          | ---                  | 0.45      |
|                 | 1/2-1      | 1                      | 1.783  | 0.386                       | 6.0            | 4.3                          | 6.0                  | 1.61      |
|                 | 1-2        | 1                      | 1.560  | 0.252                       | 7.0            | 3.1                          | 3.1                  | 1.33      |
|                 | 2-4        | 1                      | 1.326  | 0.108                       | 5.0            | 4.2                          | 2.0                  | 0.95      |
|                 | 4-8        | 1                      | 1.124  | 0.047                       | 3.9            | 4.6                          | 1.0                  | 1.00      |
|                 | 1*         | 1/2-1                  | 0.06   | 1.165                       | 0.066          | 3.3                          | 4.7                  | 1.4       |
| 1-2             |            | 0.13                   | 1.130  | 0.042                       | 2.0            | 7.5                          | 1.5                  | 0.15      |
| 2-4             |            | 0.25                   | 1.085  | 0.024                       | 1.6            | 9.0                          | 1.0                  | 0.15      |
| 4-8             |            | 0.50                   | 1.026  | 0.018                       | 1.1            | 12.2                         | 1.1                  | 0.50      |
| 2               | 1/4-1/2    | 0.5                    | 1.857  | ---                         | ---            | ---                          | ---                  | 0.35      |
|                 | 1/2-1      | 1                      | 1.725  | 0.408                       | 3.1            | 8.3                          | 1.3                  | 1.48      |
|                 | 1-2        | 1                      | 1.494  | 0.257                       | 7.8            | 2.8                          | 2.8                  | 1.03      |
|                 | 2-4        | 1                      | 1.265  | 0.101                       | 5.4            | 3.3                          | 1.5                  | 0.88      |
|                 | 4-8        | 1                      | 1.072  | 0.046                       | 4.3            | 3.5                          | 0.8                  | 0.88      |
| 3               | 1/4-1/2    | 0.5                    | 1.817  | ---                         | ---            | ---                          | ---                  | 0.24      |
|                 | 1/2-1      | 1                      | 1.707  | ---                         | ---            | ---                          | ---                  | 1.44      |
|                 | 1-2        | 1                      | 1.502  | 0.235                       | 9.4            | 2.3                          | 2.2                  | 1.12      |
|                 | 2-4        | 1                      | 1.278  | 0.106                       | 5.2            | 3.6                          | 1.7                  | 0.97      |
|                 | 4-8        | 1                      | 1.088  | 0.047                       | 3.9            | 4.0                          | 0.9                  | 0.85      |
| 4               | 1/4-1/2    | 0.5                    | 1.833  | ---                         | ---            | ---                          | ---                  | 0.37      |
|                 | 1/2-1      | 1                      | 1.718  | 0.340                       | 11.5           | 2.2                          | 2.8                  | 1.44      |
|                 | 1-2        | 1                      | 1.520  | 0.217                       | 11.0           | 2.0                          | 1.8                  | 1.18      |
| 4*              | 1/8-1/4    | 0.06                   | 1.506  | 0.104                       | 2.5            | 8.7                          | 3.6                  | 0.11      |
|                 | 1/4-1/2    | 0.13                   | 1.485  | 0.112                       | 3.6            | 6.0                          | 2.7                  | 0.12      |
|                 | 1/2-1      | 0.25                   | 1.451  | 0.078                       | 3.5            | 6.0                          | 1.9                  | 0.20      |
|                 | 1-2        | 0.5                    | 1.395  | 0.075                       | 1.9            | 10.5                         | 3.3                  | 0.58      |
|                 | 2-4        | 1                      | 1.264  | 0.088                       | 8.0            | 2.2                          | 0.9                  | 1.00      |
|                 | 4-8        | 1                      | 1.082  | 0.045                       | 5.6            | 2.7                          | 0.6                  | 1.06      |
| Average**       |            |                        |        |                             | 5.1            | $5.1 \times 10^{-4}$         | $2.0 \times 10^{-8}$ | 1.14      |

\*Second cycle consolidation after unloading to 1/8 TSF.

\*\*The average value of C is calculated only for those increments where  $P/P_0 = 1$ .

Figure A-4

CONSOLIDATION TEST RESULTS, BAY MUD, TEST SERIES D

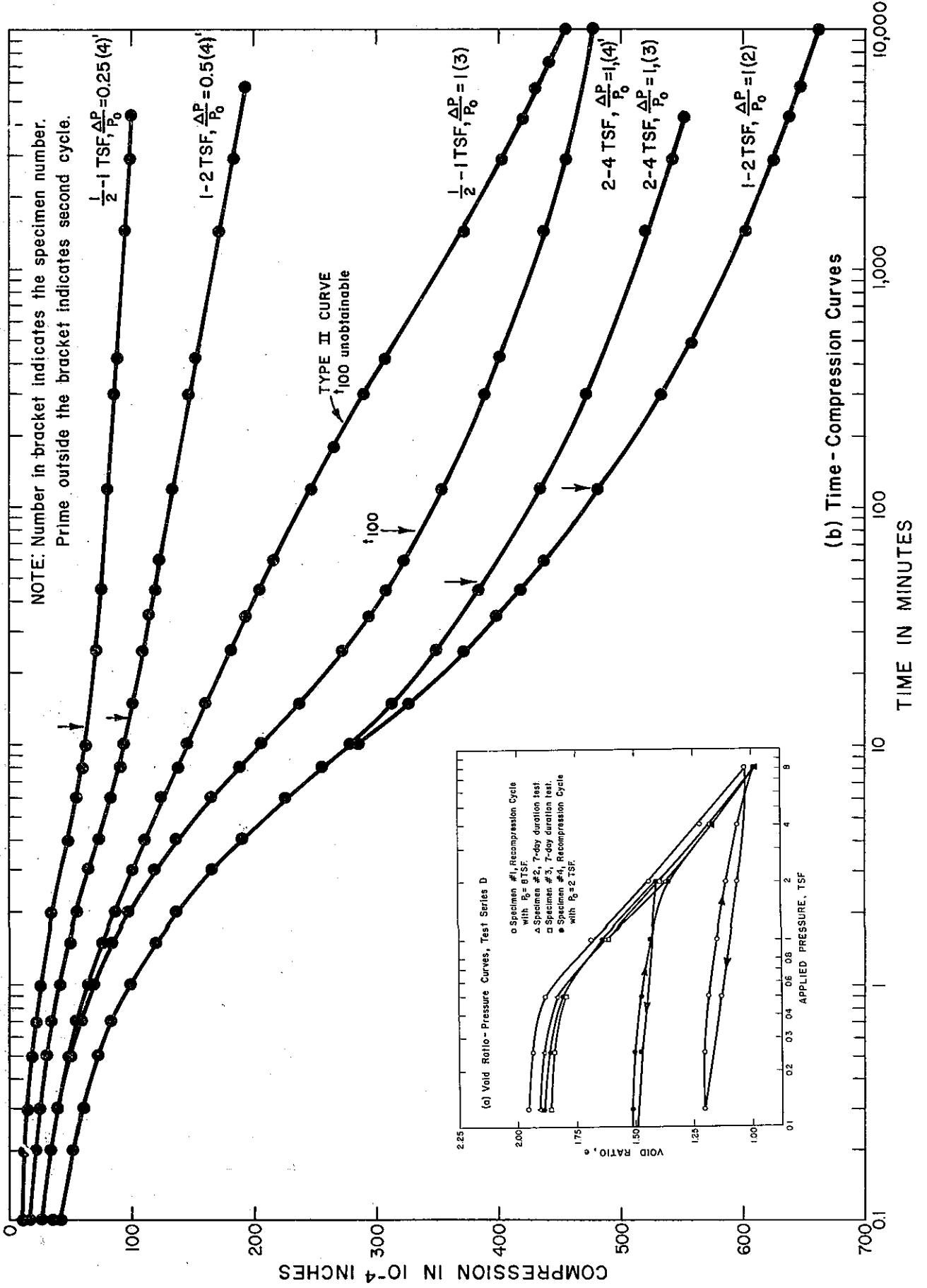


Table A-5

Test Series E, Bay Mud

| Specimen Number | Load (TSF)    | $\frac{\Delta P}{P_0}$ | e ave. | $A_v$ (Cm <sup>2</sup> /Kg) | $t_{50}$ (Min) | $C_v$ (Cm <sup>2</sup> /Sec) | K (Cm/Sec)           | $C_{av}$ (%) |
|-----------------|---------------|------------------------|--------|-----------------------------|----------------|------------------------------|----------------------|--------------|
|                 |               |                        |        |                             |                | $\times 10^{-4}$             | $\times 10^{-8}$     |              |
| 1               | 1/4-1/2       | 0.5                    | 1.756  | ---                         | ---            | ---                          | ---                  | 0.19         |
|                 | 1/2-1         | 1                      | 1.673  | 0.276                       | 7.2            | 3.7                          | 3.8                  | 1.05         |
|                 | 1-2           | 1                      | 1.497  | 0.214                       | 7.8            | 3.0                          | 2.6                  | 0.96         |
|                 | 2-4           | 1                      | 1.292  | 0.098                       | 5.2            | 3.7                          | 1.6                  | 1.03         |
|                 | 4-8           | 1                      | 1.103  | 0.045                       | 4.0            | 3.9                          | 0.86                 | 0.97         |
| 2               | 1/4-1/2       | 0.5                    | 1.815  | ---                         | ---            | ---                          | ---                  | 0.27         |
|                 | 1/2-1         | 1                      | 1.694  | 0.408                       | 7.6            | 3.4                          | 5.2                  | 1.23         |
|                 | 1-2, 1/8      | 1.125                  | 1.462  | 0.224                       | 6.6            | 2.9                          | 2.6                  | 1.00         |
|                 | 2-4, 25       | 1.06                   | 1.242  | 0.088                       | 5.5            | 3.3                          | 1.3                  | 1.10         |
|                 | 4-8           | 1                      | 1.059  | 0.041                       | 4.8            | 3.2                          | 0.63                 | 1.08         |
| 3               | 1/4-1/2       | 0.5                    | 1.893  | ---                         | ---            | ---                          | ---                  | 0.50         |
|                 | 1/2-1         | 1                      | 1.784  | 0.384                       | 11.5           | 2.2                          | 3.0                  | 1.50         |
|                 | 1-4, 1/8      | 3.125                  | 1.399  | 0.130                       | 3.6            | 5.4                          | 2.9                  | 1.07         |
|                 | 4-8, 1/8      | 1                      | 1.039  | 0.043                       | 5.2            | 2.7                          | 5.9                  | 1.12         |
| 4               | 1/4-1/2       | 0.5                    | 1.890  | ---                         | ---            | ---                          | ---                  | 0.37         |
|                 | 1/2-1         | 1                      | 1.758  | 0.418                       | 17.0           | 1.5                          | 2.6                  | 1.58         |
|                 | 1-4           | 3                      | 1.418  | 0.118                       | 5.3            | 3.6                          | 1.7                  | 0.75         |
|                 | 4-4, 1/8      | 0.125                  | 1.178  | 0.072                       | ---            | ---                          | ---                  | 0.74         |
|                 | 4, 1/8-6, 1/8 | 0.485                  | 1.125  | 0.048                       | 28.0           | 0.52                         | 0.12                 | 0.93         |
|                 | 6, 1/8-8, 1/8 | 0.325                  | 1.042  | 0.035                       | 60.0           | 0.22                         | 0.04                 | 0.91         |
| Average**       |               |                        |        |                             | 7.1            | $3.2 \times 10^{-4}$         | $2.8 \times 10^{-8}$ | 1.07         |

\*\*The average value of  $t_{50}$ ,  $C_v$  and K are for  $\frac{\Delta P}{P_0} \geq 1$  only.

CONSOLIDATION TEST RESULTS; BAY MUD, TEST SERIES, E

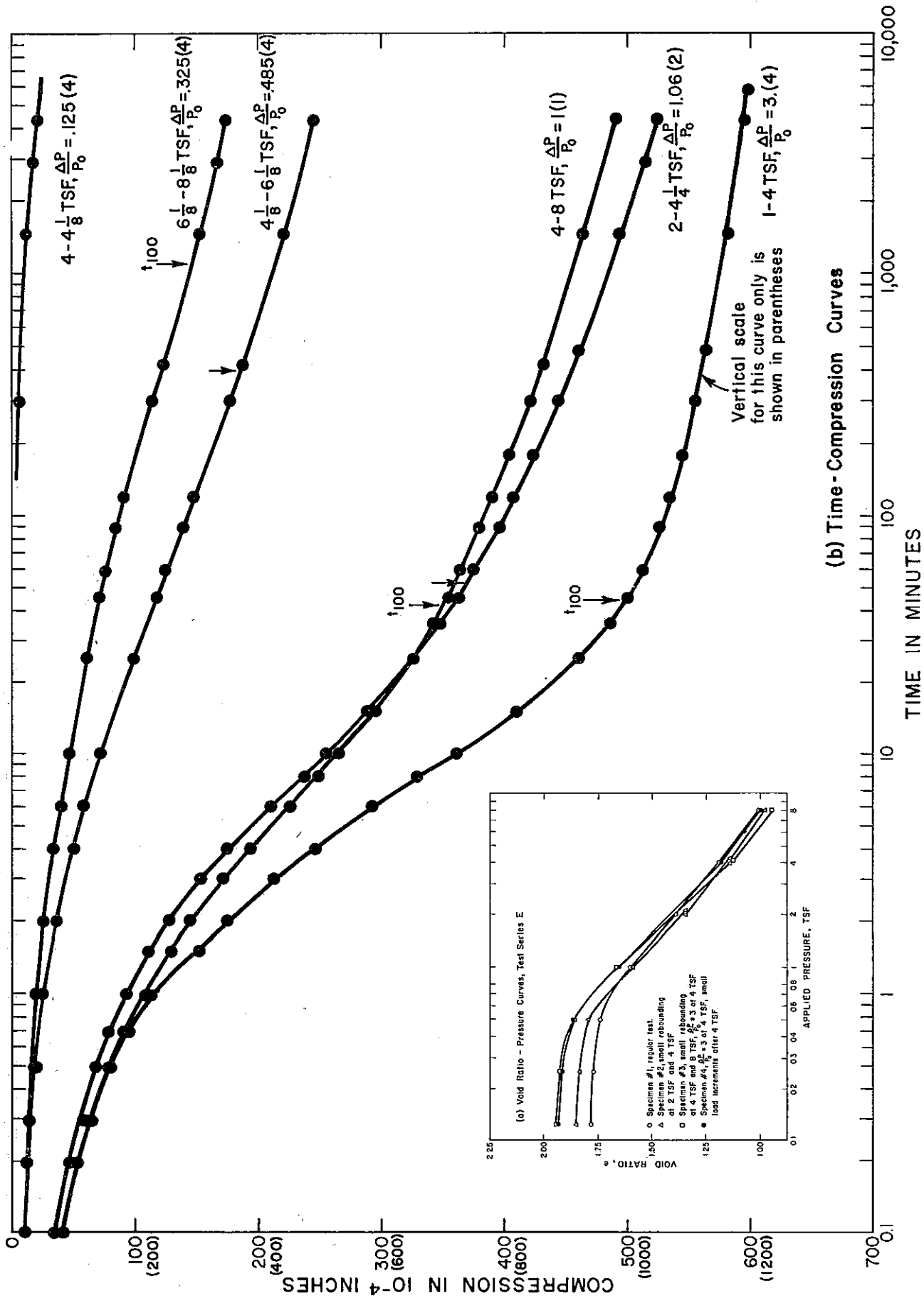


Table A-6

Test Series F, Peat

| Specimen Number | Load (TSF) | $\frac{\Delta P}{P_0}$ | e ave. | $A_v$ (Cm <sup>2</sup> /Kg) | $t_{50}$ (Min) | $C_v$ (Cm <sup>2</sup> /Sec) | K (Cm/Sec)           | $C_{av}$ (%) |
|-----------------|------------|------------------------|--------|-----------------------------|----------------|------------------------------|----------------------|--------------|
| 1               | 1/4-1/2    | 1.0                    | 3.714  | 1.68                        | 3.5            | $5.4 \times 10^{-4}$         | $1.9 \times 10^{-7}$ | 2.05         |
|                 | 1/2-1      | 1.0                    | 3.275  | 0.92                        | 7.7            | $2.1 \times 10^{-4}$         | $4.5 \times 10^{-8}$ | 2.07         |
|                 | 1-2        | 1.0                    | 2.862  | 0.37                        | 21.0           | $6 \times 10^{-5}$           | $5.7 \times 10^{-9}$ | 1.92         |
|                 | 2-4        | 1.0                    | 2.515  | 0.164                       | 18.0           | $5.5 \times 10^{-5}$         | $3.6 \times 10^{-9}$ | 1.74         |
|                 | 4-8        | 1.0                    | 2.226  | 0.063                       | 10.0           | $7.5 \times 10^{-5}$         | $2.1 \times 10^{-9}$ | 1.76         |
| 2               | 1/16-1     | 3.8                    | 3.607  | 1.75                        | 5.0            | $4.0 \times 10^{-4}$         | $1.5 \times 10^{-7}$ | 2.10         |
|                 | 1-2, 1/4   | 1.25                   | 2.465  | 0.43                        | 11.5           | $1.0 \times 10^{-4}$         | $1.2 \times 10^{-8}$ | 2.06         |
|                 | 2-8        | 2.5                    | 1.856  | 0.114                       | 8.0            | $9.5 \times 10^{-5}$         | $3.8 \times 10^{-9}$ | 1.40         |
| 3               | 1/8-1/2    | 1.5                    | 4.194  | 2.68                        | 1.1            | $2.3 \times 10^{-3}$         | $1.2 \times 10^{-6}$ | 1.96         |
|                 | 1/2-1, 1/4 | 1.25                   | 3.252  | 1.14                        | 4.0            | $3.8 \times 10^{-4}$         | $1.0 \times 10^{-7}$ | 2.05         |
|                 | 1-4        | 2.4                    | 2.407  | 0.28                        | 4.0            | $2.3 \times 10^{-4}$         | $1.9 \times 10^{-8}$ | 1.40         |
|                 | 4-8        | 1.0                    | 1.818  | 0.085                       | 8.2            | $8.0 \times 10^{-5}$         | $2.4 \times 10^{-9}$ | 1.88         |
| Average         |            |                        |        |                             | 8.5            | $3.8 \times 10^{-4}$         | -----                | 1.86         |

Figure A-6

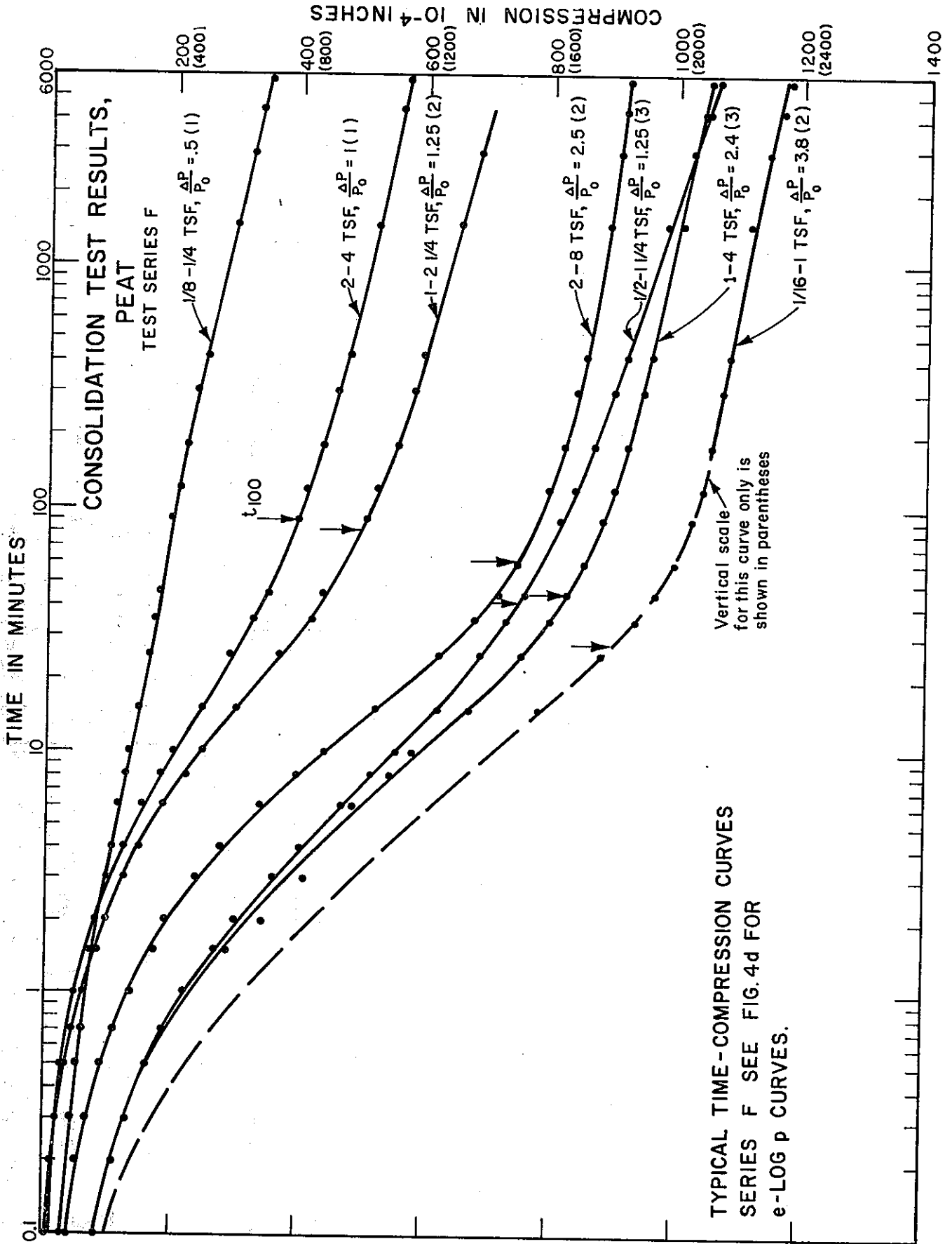


Table A-7

Test Series G, Peaty Clay

| Specimen Number | Load (TSF) | $\frac{\Delta P}{P_0}$ | e ave. | $A_{v2}$ (Cm <sup>2</sup> /Kg) | $t_{50}$ (Min) | $C_v$ (Cm <sup>2</sup> /Sec) | K (Cm/Sec)           | $C_{av}$ (%) |
|-----------------|------------|------------------------|--------|--------------------------------|----------------|------------------------------|----------------------|--------------|
| 1               | 1/2-1      | 1                      | 1.467  | 0.134                          | 6.3            | $3.3 \times 10^{-4}$         | $1.8 \times 10^{-8}$ | 0.54         |
|                 | 1-2        | 1                      | 1.397  | 0.073                          | 4.5            | $4.2 \times 10^{-4}$         | $1.3 \times 10^{-8}$ | 0.66         |
|                 | 2-4        | 1                      | 1.318  | 0.043                          | 3.2            | $5.3 \times 10^{-4}$         | $1.0 \times 10^{-9}$ | 0.77         |
|                 | 4-8        | 1                      | 1.232  | 0.021                          | 2.5            | $6.0 \times 10^{-4}$         | $5.6 \times 10^{-8}$ | 0.70         |
| 2               | 1/8-2      | 4                      | 1.430  | 0.226                          | 2.8            | $8.3 \times 10^{-4}$         | $7.7 \times 10^{-8}$ | 0.63         |
|                 | 2-6        | 2                      | 1.108  | 0.055                          | 1.9            | $9.1 \times 10^{-4}$         | $2.4 \times 10^{-8}$ | 0.74         |
|                 | 6-8        | 0.33                   | .972   | 0.027                          | —              | —                            | —                    | 0.73         |
| 3               | 1/8-1/4    | 0.25                   | 1.783  | 0.427                          | 4.0            | $6.3 \times 10^{-3}$         | $9.7 \times 10^{-8}$ | 0.53         |
|                 | 1/4-1      | 1.5                    | 1.684  | 0.198                          | 1.8            | $1.3 \times 10^{-4}$         | $9.6 \times 10^{-8}$ | 0.68         |
|                 | 1-2, 1/4   | 1.25                   | 1.560  | 0.082                          | 2.2            | $8.6 \times 10^{-4}$         | $2.7 \times 10^{-8}$ | 0.71         |
|                 | 2-8        | 2.7                    | 1.412  | 0.030                          | 1.0            | $1.5 \times 10^{-3}$         | $1.9 \times 10^{-8}$ | 0.69         |
| Average         |            |                        |        |                                | 3.0            | $7.9 \times 10^{-4}$         | $3.9 \times 10^{-8}$ | 0.67         |

Figure A-7

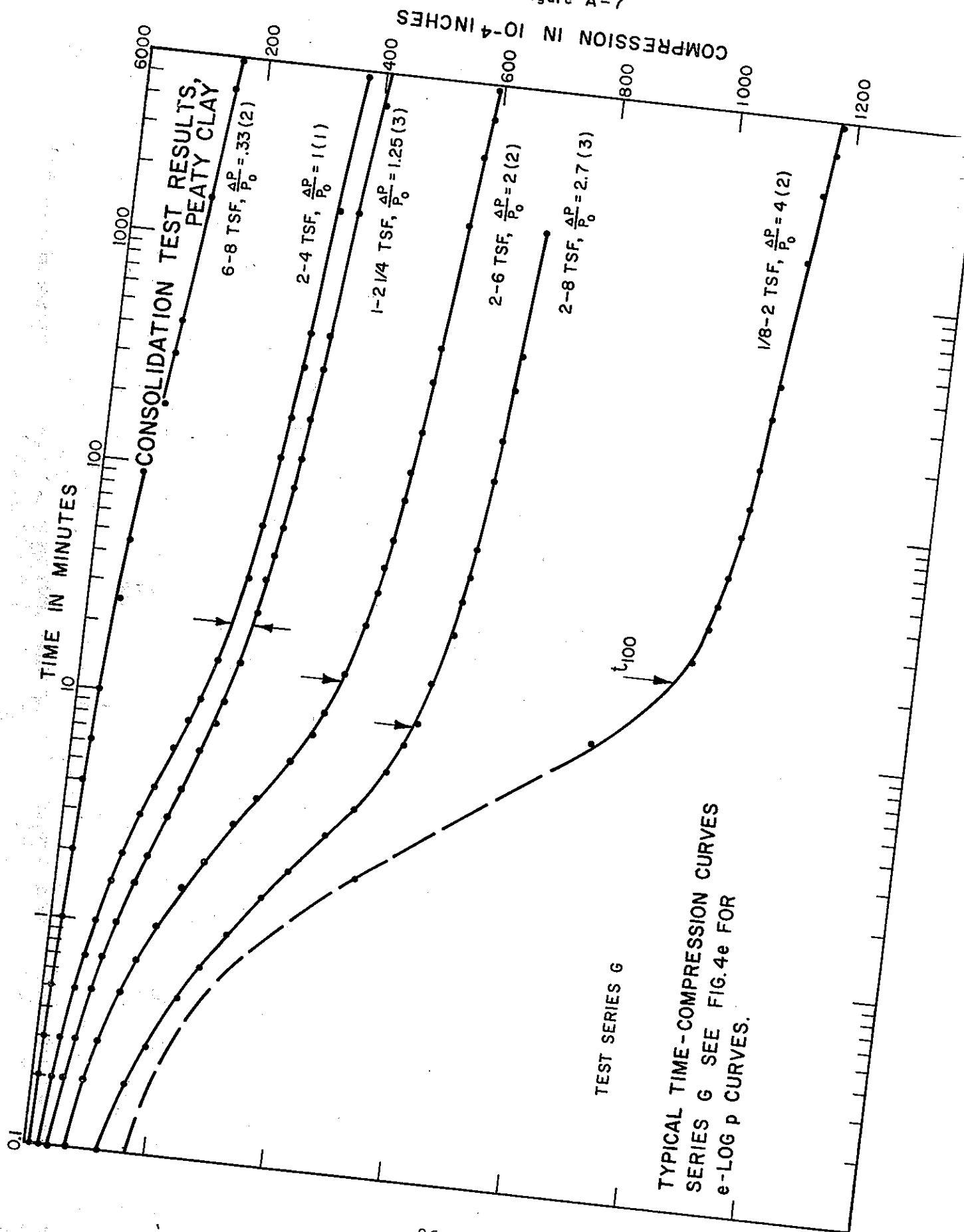


Table A-8

Test Series H, Clayey Peat

| Specimen Number | Load (TSF) | $\frac{\Delta P}{P_0}$ | e ave. | $A_v$ (Cm <sup>2</sup> /Kg) | $t_{50}$ (Min) | $C_v$ Cm <sup>2</sup> /Sec | K (Cm/Sec)           | $C_u$ (%)    |
|-----------------|------------|------------------------|--------|-----------------------------|----------------|----------------------------|----------------------|--------------|
| 1               | 1/4-1/2    | .5                     | 2.044  | 0.220                       | .33            | $8.3 \times 10^{-3}$       | $6.0 \times 10^{-7}$ |              |
|                 | 1/2-1      | 1                      | 1.973  | 0.172                       | .64            | $4.0 \times 10^{-3}$       | $2.3 \times 10^{-7}$ | 0.35         |
|                 | 1-2        | 1                      | 1.870  | 0.120                       | 1.75           | $1.3 \times 10^{-3}$       | $5.4 \times 10^{-8}$ | 0.59         |
|                 | 2-4        | 1                      | 1.740  | 0.071                       | 2.0            | $1.0 \times 10^{-3}$       | $2.6 \times 10^{-8}$ | 0.69         |
|                 | 4-8        | 1                      | 1.600  | .035                        | 1.60           | $1.1 \times 10^{-3}$       | $1.5 \times 10^{-8}$ | 0.75<br>0.76 |
| 2               | 1/8-1/2    | .75                    | 2.465  | 0.272                       | 0.30           | $9.3 \times 10^{-3}$       | $7.2 \times 10^{-7}$ | 0.38         |
|                 | 1/2-6      | 11                     | 2.104  | 0.113                       | 1.25           | $1.6 \times 10^{-3}$       | $5.8 \times 10^{-8}$ | 0.84         |
|                 | 6-8, 1/4   | .38                    | 1.756  | 0.034                       | ---            | ---                        | ---                  | 1.08         |
| Average         |            |                        |        |                             | 1.1            | $3.8 \times 10^{-2}$       | $2.5 \times 10^{-7}$ | 0.68         |

Figure A-8

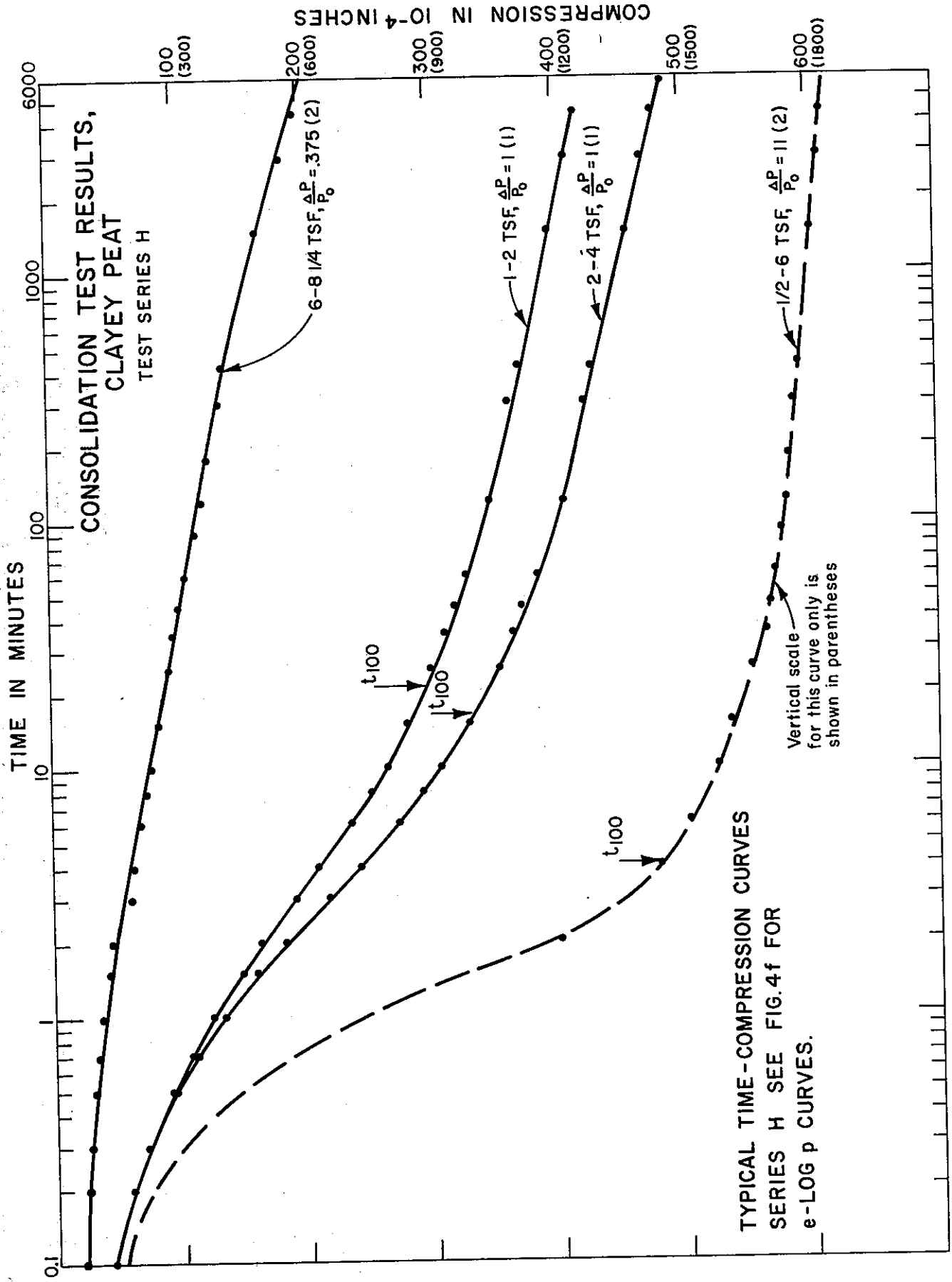


Table A-9

Test Series I, Peat and Peaty Clay

| Specimen Number                 | Load (TSF) | $\frac{\Delta P}{P_0}$ | e ave. | $A_v$ (Cm <sup>2</sup> /Kg) | t <sub>50</sub> (Min) | $C_v$ (Cm <sup>2</sup> /Sec) | K (Cm/Sec)           | $C_d$ (%) |
|---------------------------------|------------|------------------------|--------|-----------------------------|-----------------------|------------------------------|----------------------|-----------|
| B-1-4                           | 1/8-1/4    | *                      | 9.555  | 6.45                        | ---                   | ---                          | ---                  | 2.1       |
| (Peat,<br>W/c=420%)             | 1/4-1/2    | *                      | 8.473  | 5.40                        | ---                   | ---                          | ---                  | 3.0       |
|                                 | 1/2-1      | 1.0                    | 7.022  | 3.10                        | 2.6                   | $5.1 \times 10^{-4}$         | $2.0 \times 10^{-7}$ | 3.5       |
|                                 | 1-2        | 1.0                    | 5.589  | 1.32                        | 5.0                   | $1.8 \times 10^{-4}$         | $3.6 \times 10^{-8}$ | 3.5       |
|                                 | 2-4        | 1.0                    | 4.410  | 0.52                        | 5.6                   | $1.0 \times 10^{-4}$         | $9.6 \times 10^{-9}$ | 3.9       |
|                                 | 4-8        | 1.0                    | 3.478  | 0.21                        | 9.4                   | $4.6 \times 10^{-5}$         | $2.2 \times 10^{-9}$ | 3.3       |
|                                 | 1/2-1.75   | 2.5                    | 3.444  | 0.93                        | 1.35                  | $1.2 \times 10^{-3}$         | $2.5 \times 10^{-7}$ | 2.0       |
| B-1-8                           | 1/4-1/2    | *                      | 5.937  | 2.64                        | ---                   | ---                          | ---                  | 2.1       |
| (Peat,<br>W/c=260%)             | 1/2-1      | 1.0                    | 5.030  | 2.30                        | 6.0                   | $3.2 \times 10^{-4}$         | $1.5 \times 10^{-7}$ | 3.1       |
|                                 | 1-2        | 1.0                    | 3.973  | .96                         | 7.0                   | $1.8 \times 10^{-4}$         | $3.5 \times 10^{-8}$ | 3.5       |
|                                 | 2-4        | 1.0                    | 3.115  | .38                         | 8.5                   | $1.0 \times 10^{-4}$         | $9.2 \times 10^{-9}$ | 3.0       |
|                                 | 4-8        | 1.0                    | 2.402  | .17                         | 9.4                   | $6.4 \times 10^{-5}$         | $3.2 \times 10^{-9}$ | 2.45      |
| B-1-13                          | 1/8-1/4    | *                      | 2.935  | .43                         | ---                   | ---                          | ---                  | 0.3       |
| (Peaty Clay<br>W/c=120%)        | 1/4-1/2    | *                      | 2.851  | .46                         | 2.0                   | $1.3 \times 10^{-3}$         | $1.6 \times 10^{-7}$ | 0.5       |
|                                 | 1/2-1      | 1.0                    | 2.663  | 0.52                        | 4.0                   | $6.1 \times 10^{-4}$         | $8.6 \times 10^{-8}$ | 1.3       |
|                                 | 1-2        | 1.0                    | 2.348  | 0.37                        | 5.8                   | $3.4 \times 10^{-4}$         | $5.4 \times 10^{-8}$ | 1.4       |
|                                 | 2-4        | 1.0                    | 1.986  | 0.18                        | 4.8                   | $2.8 \times 10^{-4}$         | $1.7 \times 10^{-8}$ | 1.5       |
|                                 | 4-8        | 1.0                    | 1.650  | .08                         | 4.2                   | $3.1 \times 10^{-4}$         | $9.4 \times 10^{-9}$ | 1.5       |
|                                 | 1/2-1.75   | 2.5                    | 2.831  | .66                         | 5.2                   | $4.1 \times 10^{-4}$         | $9.6 \times 10^{-8}$ | 1.5       |
| Average for Peat (B-1-4,8)      |            |                        |        |                             | ---                   | ---                          | $7.8 \times 10^{-8}$ | 3.3       |
| Average for Peaty Clay (B-1-13) |            |                        |        |                             | ---                   | ---                          | $7.2 \times 10^{-8}$ | 1.4       |

\*Time-compression curves are of Type II and not included in calculation of average  $C_d$ .

Figure A-9

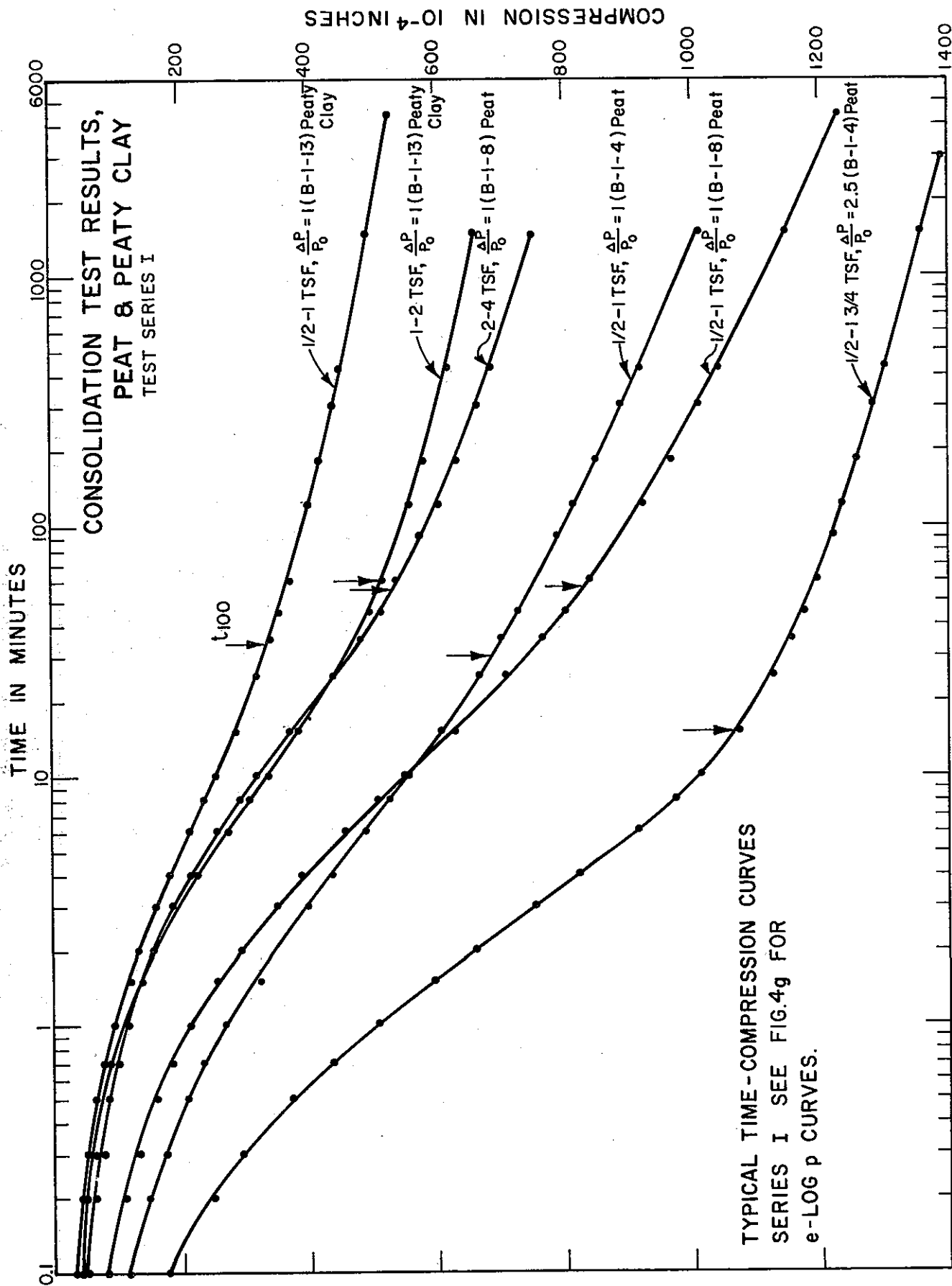
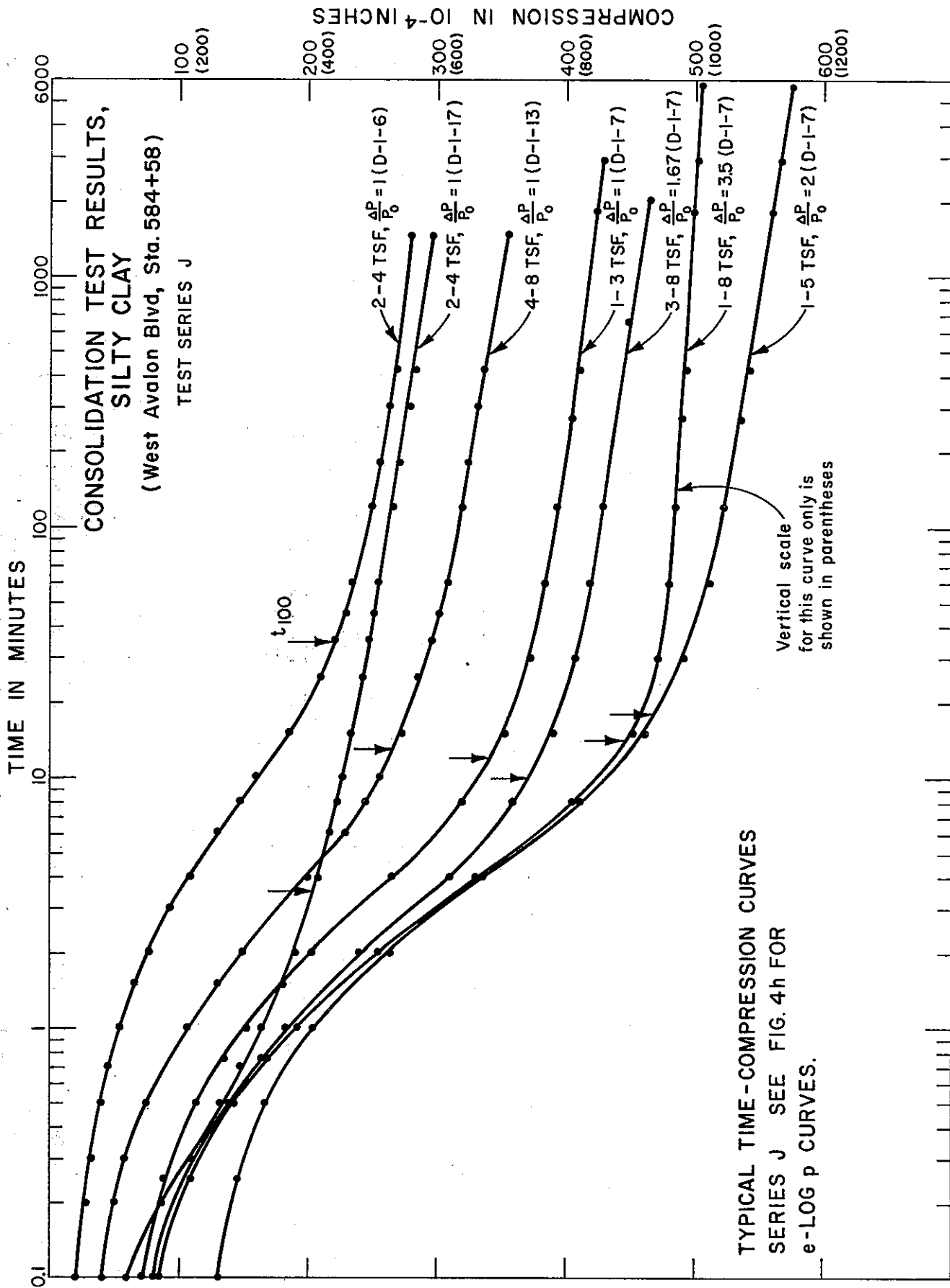
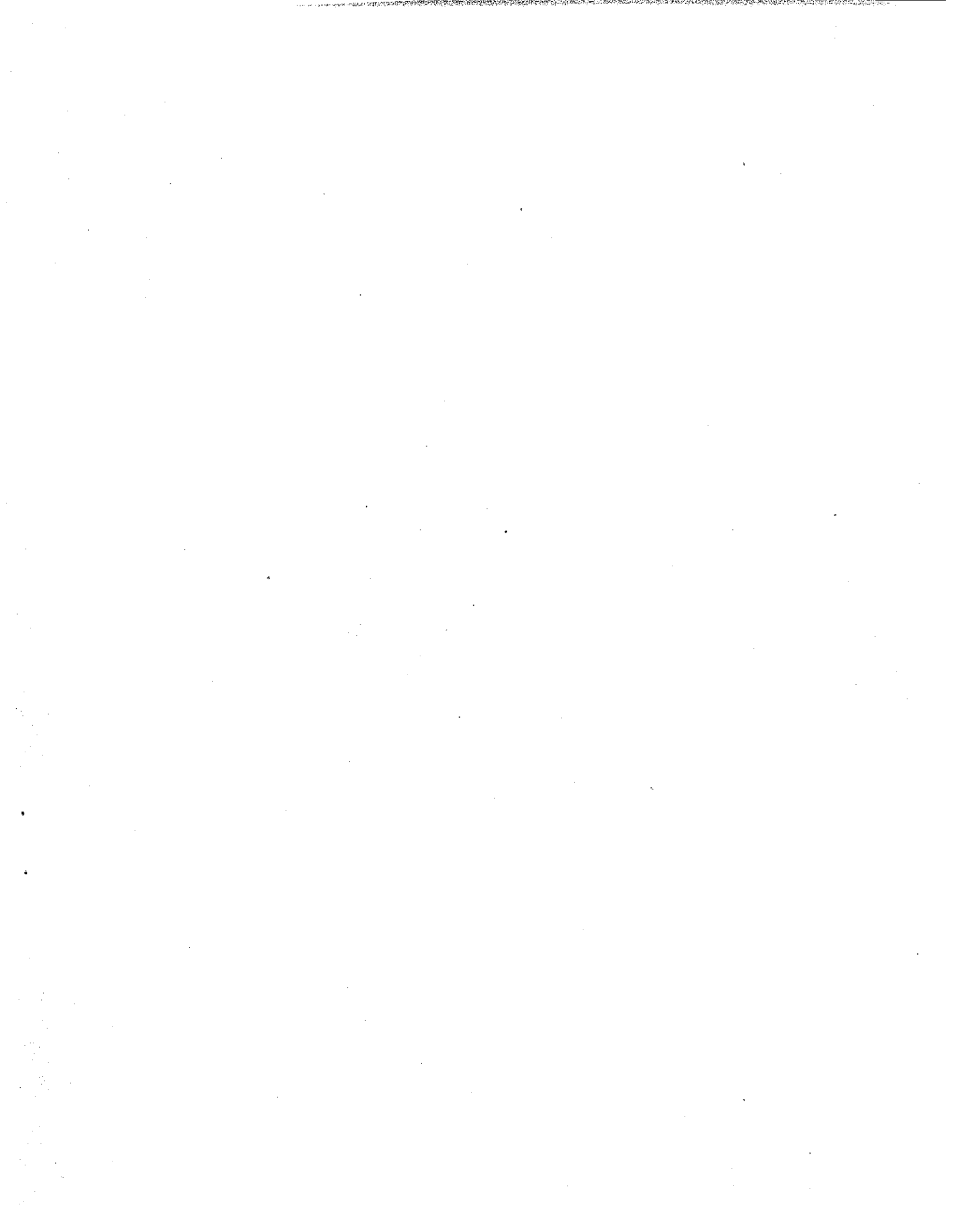


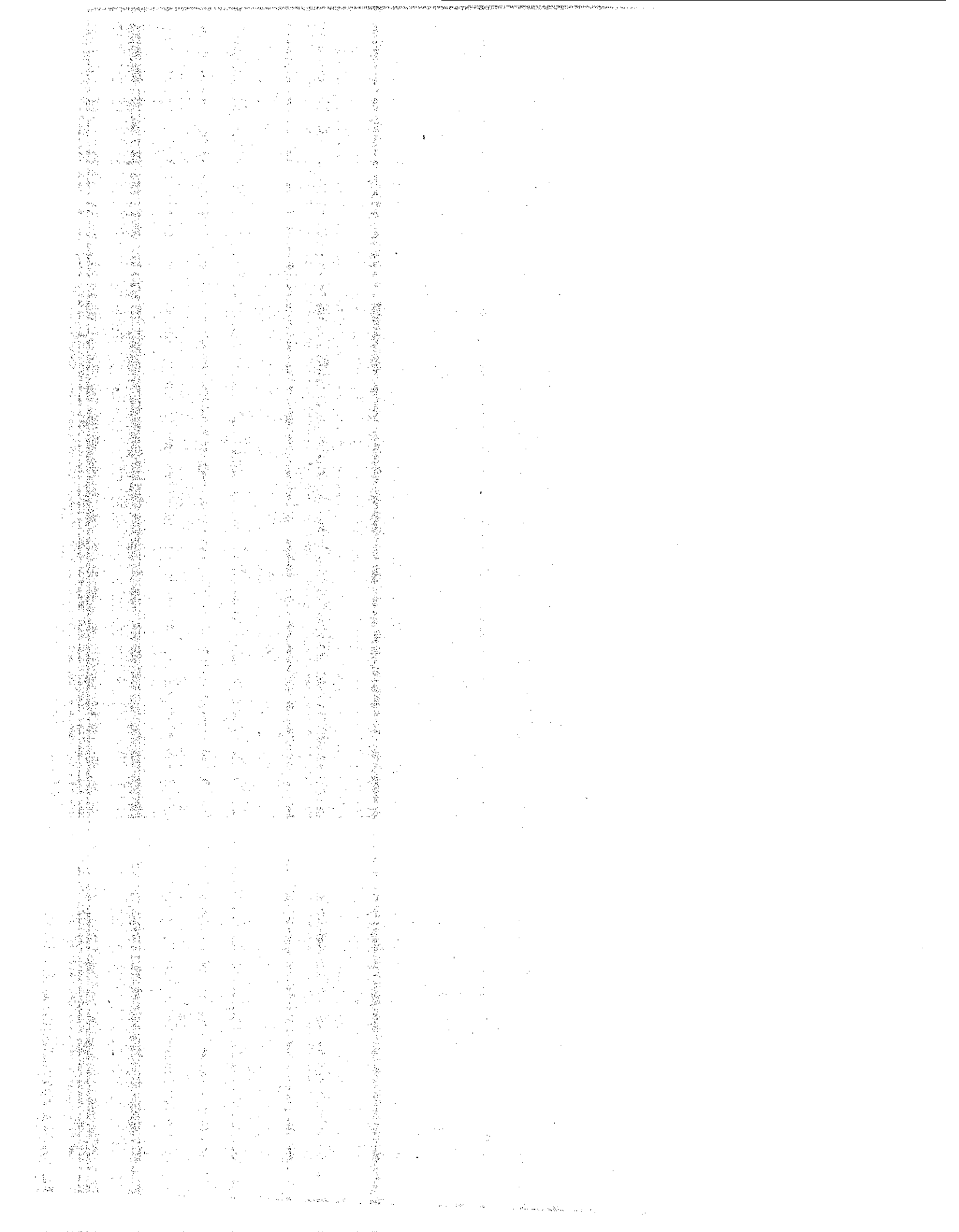
Table A-10

Test Series J, Silty Clay,  
West Avalon Blvd., Sta. 584 + 58

| Specimen Number | Load (TSF) | $\frac{\Delta P}{P_0}$ | e ave. | $A_{v2}$ (Cm <sup>2</sup> /Kg) | t <sub>50</sub> (Min) | $C_v$ (Cm <sup>2</sup> /Sec) | K (Cm/Sec)           | $C_a$ (%) |
|-----------------|------------|------------------------|--------|--------------------------------|-----------------------|------------------------------|----------------------|-----------|
| D-1-6           | 1-2        | 0.5                    | 1.092  | 0.052                          | 3.6                   | $7.9 \times 10^{-4}$         | $2.0 \times 10^{-8}$ | 0.22      |
|                 | 2-4        | 1.0                    | 1.026  | 0.041                          | 4.7                   | $5.7 \times 10^{-4}$         | $1.2 \times 10^{-8}$ | 0.30      |
|                 | 4-8        | 1.0                    | 0.933  | 0.026                          | 4.8                   | $5.3 \times 10^{-4}$         | $7.2 \times 10^{-9}$ | 0.44      |
| D-1-7           | 3-8        | 1.67                   | 0.763  | 0.027                          | 1.20                  | $1.6 \times 10^{-3}$         | $2.4 \times 10^{-8}$ | 0.41      |
|                 | 1-3        | 1.0                    | 0.894  | 0.0635                         | 1.65                  | $1.3 \times 10^{-3}$         | $4.4 \times 10^{-8}$ | 0.34      |
|                 | 1-5        | 2.0                    | 1.035  | 0.0425                         | 2.50                  | $1. \times 10^{-3}$          | $2.1 \times 10^{-8}$ | 0.45      |
|                 | 1-8        | 3.5                    | 0.985  | 0.0470                         | 1.80                  | $1.1 \times 10^{-3}$         | $2.6 \times 10^{-8}$ | 0.48      |
| D-1-13          | 1-2        | 0.5                    | 1.128  | 0.055                          | 1.70                  | $1.6 \times 10^{-3}$         | $4.1 \times 10^{-8}$ | 0.16      |
|                 | 2-4        | 1.0                    | 1.069  | 0.032                          | 1.7                   | $1.5 \times 10^{-3}$         | $2.3 \times 10^{-8}$ | 0.42      |
|                 | 4-8        | 1.0                    | 0.985  | 0.026                          | 1.6                   | $1.5 \times 10^{-3}$         | $2.0 \times 10^{-8}$ | 0.50      |
| D-1-17          | 2-4        | 1.0                    | 1.086  | 0.046                          | 0.30                  | $8.6 \times 10^{-3}$         | $1.9 \times 10^{-7}$ | 0.35      |
|                 | 4-8        | 1.0                    | 0.978  | 0.032                          | 0.44                  | $5.3 \times 10^{-3}$         | $8.6 \times 10^{-8}$ | 0.51      |
| Average         |            |                        |        |                                |                       | $2.1 \times 10^{-3}$         | $4.3 \times 10^{-8}$ | 0.42      |







APPENDIX B

COMPARISON OF LABORATORY DATA WITH FIELD  
SETTLEMENT MEASUREMENTS



APPENDIX B

COMPARISON OF LABORATORY DATA WITH FIELD  
SETTLEMENT MEASUREMENTS

TABLE B-1 San Dieguito River Basin Sta. "SD" 1278 + 50

| Depth<br>(ft) | Soil Type              | From Laboratory Data                  |                                 |              | Field<br>Settlement<br>Data<br>$C_a$<br>(%) |
|---------------|------------------------|---------------------------------------|---------------------------------|--------------|---------------------------------------------|
|               |                        | $C_v$<br>( $\text{cm}^2/\text{Sec}$ ) | K<br>( $\text{cm}/\text{Sec}$ ) | $C_a$<br>(%) |                                             |
| 0 - 7         | Silty Sand             | -                                     | $2.5 \times 10^{-5}$            | -            |                                             |
| 7 -15         | Silty Clay             | $4.6 \times 10^{-4}$                  | $6.1 \times 10^{-8}$            | 0.84         |                                             |
| 15 -24        | Silty Clay             | $5.0 \times 10^{-4}$                  | $4.3 \times 10^{-7}$            | 0.48         |                                             |
| 24 -30        | Silty Sand<br>and Clay | $2.4 \times 10^{-4}$                  | $2.4 \times 10^{-7}$            | 0.37         |                                             |
| AVERAGE       |                        | -                                     | -                               | 0.56         | 0.52                                        |

TABLE B-2 Los Penasquitos Lagoon, Sta. "SD" 1095

| Depth<br>(ft) | Soil Type          | From Laboratory Data                  |                                 |              | Field<br>Settlement<br>Data<br>$C_a$<br>(%) |
|---------------|--------------------|---------------------------------------|---------------------------------|--------------|---------------------------------------------|
|               |                    | $C_v$<br>( $\text{cm}^2/\text{Sec}$ ) | K<br>( $\text{cm}/\text{Sec}$ ) | $C_a$<br>(%) |                                             |
| 0 - 6         | Clayey Sand        | -                                     | $1.4 \times 10^{-6}$            | -            |                                             |
| 6 -12         | Soft<br>Silty Clay | $1.8 \times 10^{-3}$                  | $7.3 \times 10^{-8}$            | 0.43         |                                             |
| 12 -21        | Clayey Silt        | $6.8 \times 10^{-3}$                  | $2.4 \times 10^{-7}$            | 0.35         |                                             |
| AVERAGE       |                    |                                       |                                 | 0.40         | 1.20*                                       |

\* Note: The field settlement measurement was discontinued prematurely for accurately determining the secondary portion of the consolidation.

TABLE B-3

Arcata - 4th Street Interchange Sta. 23 + 25

| Depth<br>(Ft) | Soil Type               | From Laboratory Data                  |                                 |                       | Field<br>Settlement<br>Data |
|---------------|-------------------------|---------------------------------------|---------------------------------|-----------------------|-----------------------------|
|               |                         | $C_v$<br>( $\text{cm}^2/\text{Sec}$ ) | K<br>( $\text{cm}/\text{Sec}$ ) | C<br>(%) <sup>a</sup> |                             |
| 0-15          | Silty Sands             |                                       |                                 |                       | C<br>(%) <sup>a</sup>       |
| 15-27         | Silty Clay              | $6.3 \times 10^{-4}$                  | $4.2 \times 10^{-8}$            | 0.45                  |                             |
| 27-33         | Silty Clay<br>with Peat | $8.5 \times 10^{-4}$                  | $8.5 \times 10^{-8}$            | 0.86                  |                             |
| AVERAGE       |                         |                                       |                                 | 0.58                  | - *                         |

\* Note: The field settlement measurement was discontinued before the settlement-time curve reached into its secondary portion.

TABLE B-4

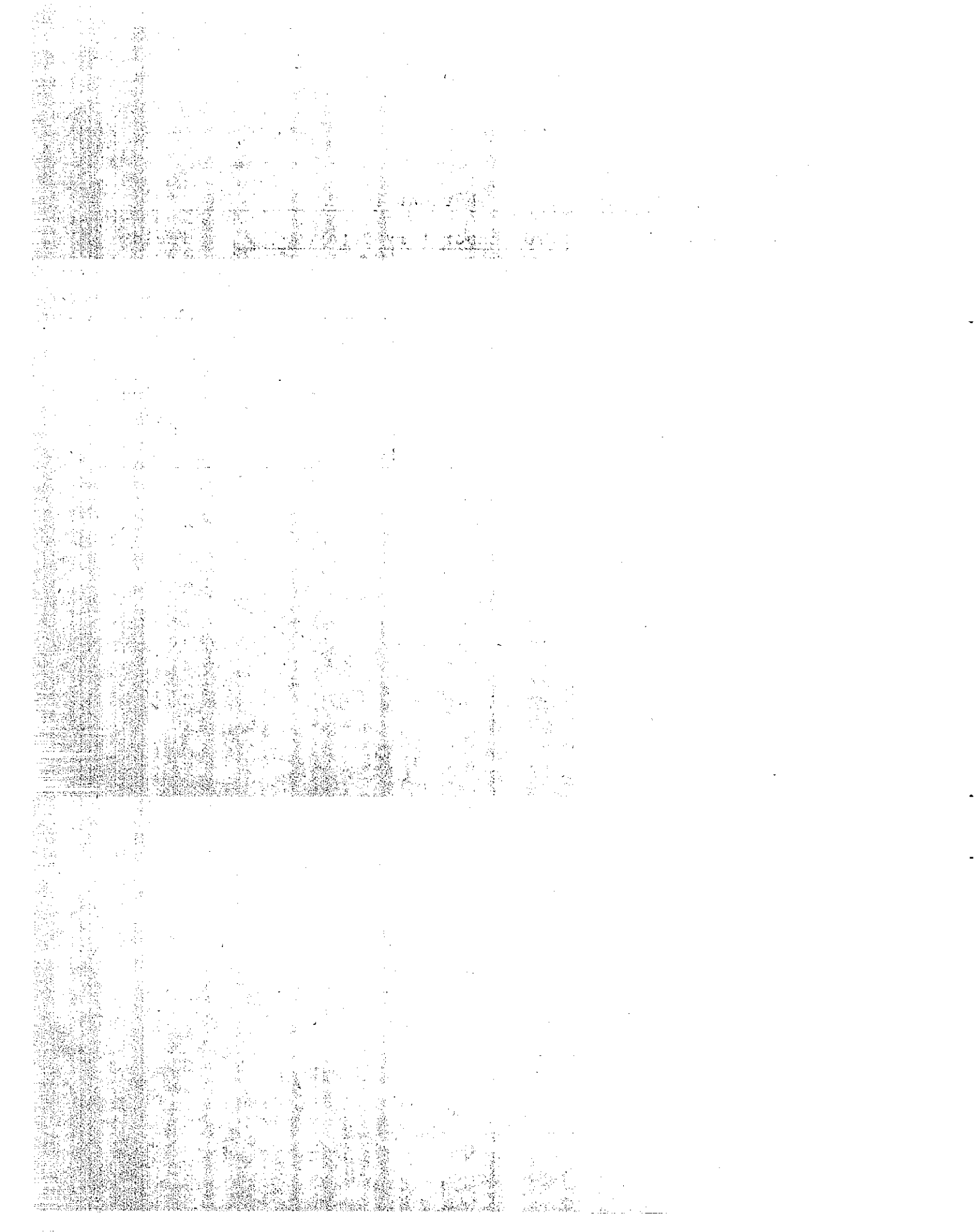
Lindsay Creek Bridge, Sta. 197 + 50

| Depth<br>(ft) | Soil Type    | From Laboratory Data                  |                                 |                       | Field<br>Settlement<br>Data |
|---------------|--------------|---------------------------------------|---------------------------------|-----------------------|-----------------------------|
|               |              | $C_v$<br>( $\text{cm}^2/\text{Sec}$ ) | K<br>( $\text{cm}/\text{Sec}$ ) | C<br>(%) <sup>a</sup> |                             |
| 0 - 8         | Clayey Silts | -                                     | -                               | -                     | C<br>(%) <sup>a</sup>       |
| 8 - 20        | Silty Clay   | $3.3 \times 10^{-3}$                  | $0.7 \times 10^{-7}$            | 0.2                   |                             |
| 20 - 27       | Clayey Silts | $8 \times 10^{-3}$                    | $1.8 \times 10^{-7}$            | 0.2                   |                             |
| 27 - 40       | Silty Clay   | $33 \times 10^{-3}$                   | $0.7 \times 10^{-7}$            | 0.2                   |                             |
| AVERAGE       |              |                                       |                                 | 0.2                   | 0.32                        |

TABLE B-5

San Ramon Rd. Overcross, Abutment 1

| Station | Soil Type       | From Laboratory Data                         |              | Field Settlement<br>(%)<br>$C_a$ |
|---------|-----------------|----------------------------------------------|--------------|----------------------------------|
|         |                 | $C_v$<br>( $\text{cm}^2/\text{Sec}$ )        | $C_a$<br>(%) |                                  |
| 28 + 90 | Soft Silty Clay | $2.2 \times 10^{-3} \text{ cm}^2/\text{Sec}$ | 0.20         | 0.30                             |
| 27 + 70 | Soft Silty Clay | $6.8 \times 10^{-4} \text{ cm}^2/\text{Sec}$ | 0.25         | 0.44                             |







APPENDIX C

WAHLS' METHOD OF TIME-SETTLEMENT  
CALCULATION

[The page contains extremely faint and illegible text, likely due to heavy noise or low resolution. No specific words or phrases are discernible.]

APPENDIX C

WAHLS' METHOD OF TIME-SETTLEMENT CALCULATION

In the formulation of the mathematical expression for the entire consolidation process, Wahls first expressed the total compression  $R_T$  as,

$$R_T = R_1 + R_2 \dots\dots\dots (C-1)$$

where  $R_1$  is the compression due to primary compression, and  $R_2$  is the compression due to secondary compression. Primary compression is represented by a Kelvin body exactly as that of Taylor's modified model (Figure C-1a). Secondary compression is represented by a viscous dashpot with a variable dashpot coefficient linked in series with each Kelvin body of the primary compression model (Figure C-1b). The total compression process is represented by an infinite series of these primary and secondary models as shown in Figure C-1c.

The above model of the consolidation process will yield the following relationships between the compressions and soil compressibilities. For an infinite series of Kelvin bodies, primary compression is given by,

$$R_1 = \sum_{n=0}^{\infty} R_n = A_p \Delta P \left[ 1 - \frac{1}{A_p} \sum_{n=0}^{\infty} A_n e^{-(B_n/A_n)t} \right] \dots\dots\dots (C-2)$$

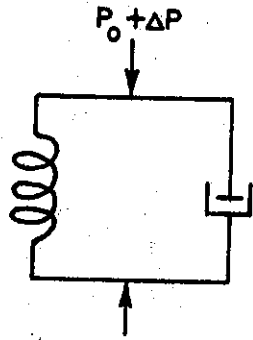
in which the coefficient of compressibility for the infinite series of Kelvin bodies is,

$$A_p = \sum_{n=0}^{\infty} A_n \dots\dots\dots (C-3)$$

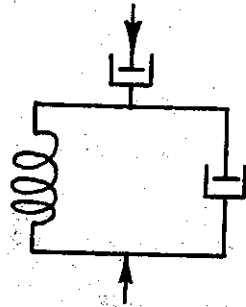
In Equation (C-2),  $A_n$  is the spring constant of the nth body and  $B_n$  is the dashpot constant of the nth viscous dashpot. Now, Terzaghi's theoretical equation of hydrodynamic consolidation may be written as,

$$\Delta e = a \Delta p \left[ 1 - \frac{8}{\pi^2} \sum_{n=0}^{\infty} \frac{1}{(2n+1)^2} e^{-\left(\frac{(2n+1)\pi}{2}\right)^2 T} \right] \dots\dots\dots (C-4)$$

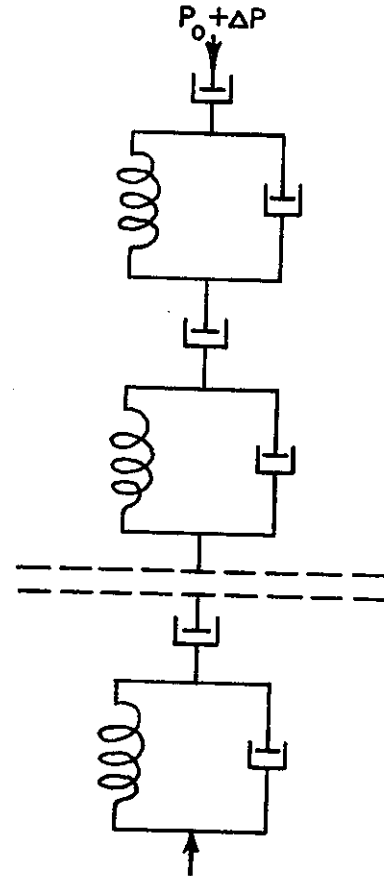
# RHEOLOGICAL MODEL IN WAHLS' METHOD



a. Kelvin Body of Primary Compression Only



b. Kelvin Body with Secondary Dashpot



c. Model for Consolidation Process

where  $a$  is the coefficient of compressibility and  $T$  is Terzaghi's time factor which is equal to  $(C_v t/H^2)$ . Since both equations C-2 and C-4 are expressions for primary compression, they may be compared to yield the expressions,

$$A_n = A_p \frac{\delta}{\pi^2 (2n+1)^2} \dots\dots\dots (C-5)$$

and

$$B_n = 2A_n \frac{T}{t} \dots\dots\dots (C-6)$$

therefore, Equation (C-2) may be rewritten as,

$$R_1 = A_p \Delta P \left[ 1 - \frac{\delta}{\pi^2} \sum_{n=0}^{\infty} \frac{1}{(2n+1)^2} e^{-\left[\frac{(2n+1)\pi}{2}\right]^2 T} \right]$$

$$= A_p \Delta P f(T) \dots\dots\dots (C-7)$$

in which  $f(T)$  is the time factor function for primary compression,

$$f(T) = 1 - \frac{\delta}{\pi^2} \sum_{n=0}^{\infty} \frac{1}{(2n+1)^2} e^{-\left[\frac{(2n+1)\pi}{2}\right]^2 T} \dots\dots\dots (C-8)$$

For the secondary compression, the deformation equation for the  $n$ th secondary dashpot is assumed to be,

$$\frac{dR_n}{dt} = \frac{C_n}{1 + \frac{B_n}{A_n} t} (P_0 + \Delta P) \dots\dots\dots (C-9)$$

in which  $C_n$  is the dashpot constant for the  $n$ th secondary dashpot. The total secondary compression,  $R_2$ , of the infinite series of secondary dashpots is,

$$R_2 = \sum_{n=0}^{\infty} R_n = C_f \sum_{n=0}^{\infty} A_n \log_{10} \left[ 1 + \frac{B_n}{A_n} t \right] \dots\dots\dots (C-10)$$

in which,

$$C_f = (P_0 + \Delta P) \ln 10 \sum_{n=0}^{\infty} \left( \frac{C_n}{B_n} \right) \dots\dots\dots (C-11)$$

The values of  $A_n$  and  $B_n$  may be substituted into Equation (C-10) so that,

$$R_2 = C_f \frac{8}{\pi^2} \sum_{n=0}^{\infty} \frac{1}{(2n+1)^2} \log_{10} \left[ 1 + \left( \frac{2n+1}{2} \pi \right)^2 T \right] \dots (C-12)$$

The time factor function in the above equation does not become linear with respect to the logarithm of  $T$  until  $T$  is greater than seven. However, primary compression is essentially completed before  $T$  is equal to two, and therefore, secondary compression should be linear with respect to logarithm of  $T$  when  $T$  exceeds two. When  $2 < T < 7$ , the compression determined from Equation (C-12) is closely approximated on a semi-logarithmic plot by a straight line with a slope equal to  $0.9215 C_f$ . Therefore, this slope is defined as the coefficient of secondary compression,  $C_d$ , and the extension of this slope is used to represent the secondary effect for  $T$  greater than seven. Therefore, using  $C_f = C_d / 0.9215$ , secondary compression may be written as,

$$R_2 = C_d h(T) \dots\dots\dots (C-13)$$

in which  $h(T)$  is the time factor function for secondary compression. For  $T < 7$ ,  $h(T)$  is given by,

$$h(T) = 1.08516 \frac{8}{\pi^2} \sum_{n=0}^{\infty} \frac{1}{(2n+1)^2} \log_{10} \left[ 1 + \left( \frac{2n+1}{2} \pi \right)^2 T \right] \dots\dots (C-14)$$

and for  $T > 7$ ,  $h(T)$  is given by,

$$h(T) = 0.8353 + \log_{10} T \dots\dots\dots (C-15)$$

Finally, the total compression  $R_T$  may be written as,

$$R_T = R_1 + R_2 = A_p \Delta P f(T) + C_a h(T)$$

$$= A_p \Delta P \left[ f(T) + \frac{C_a}{A_p \Delta P} h(T) \right] \dots\dots\dots (C-16)$$

In actual application of Wahls' method, only those time-compression curves which are representable by Type I curve in Figure 2 are considered in this investigation. The procedure for obtaining the time-compression relationship as expressed in Equation (C-16) involves the following steps:

- (1) Determine the value of  $C_a$ , coefficient of secondary compression, from the log time-compression plot. This value is taken as the magnitude of compression per log cycle in well-defined secondary range of compression.
- (2) Find the 100% primary compression point from the log time-compression plot of laboratory test. This is done by following Casagrande's construction. Also obtain theoretical zero compression and the 50% primary compression. These data will be used in the subsequent steps.
- (3) Obtain values for time factor functions  $f(T)$  and  $h(T)$  as expressed in Equations (C-8) and (C-14) or (C-15) for corresponding values of  $T$  (these values may be precalculated in a chart).
- (4) For large values of time (or  $T > 4$ ), and assuming the product  $A_p \Delta P$  as a combined constant, evaluate an average value of  $(A_p \Delta P)$  from the following equation:

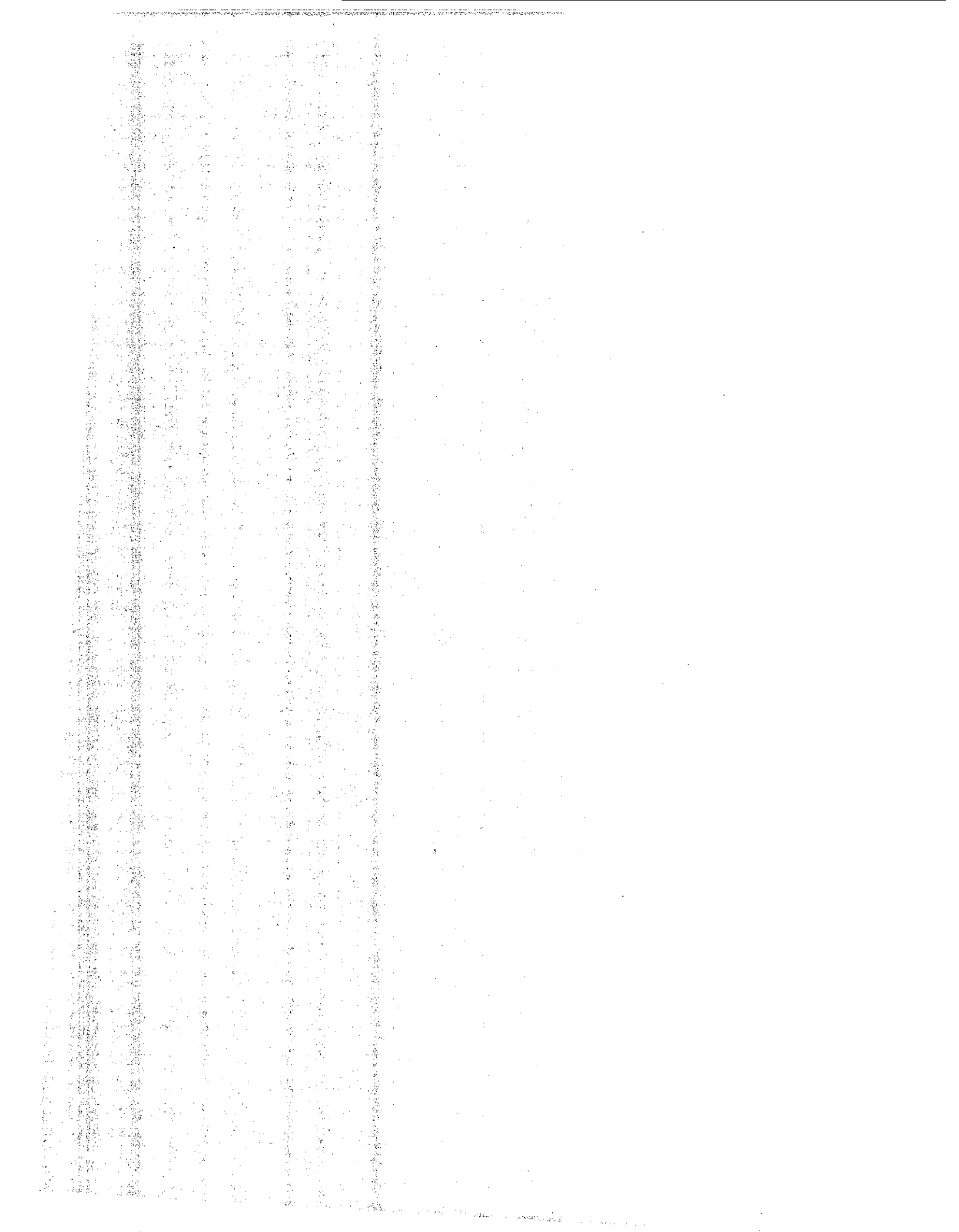
$$(A_p \Delta P) = \frac{R_t - C_a h(T)}{f(T)} \dots\dots\dots (C-17)$$

Where  $R_t$  is actual measured laboratory compression for a given time  $t$  ( $T > 4$ ). Obtain an average value of  $(A_p \Delta P)$  from several trials of large  $t$ .

- (5) The entire time-compression may then be calculated for various time using Equation (C-16). This time-compression relationship is then converted to obtain field time-settlement relationship knowing thickness of clay layer, drainage conditions, and coefficient of consolidation.

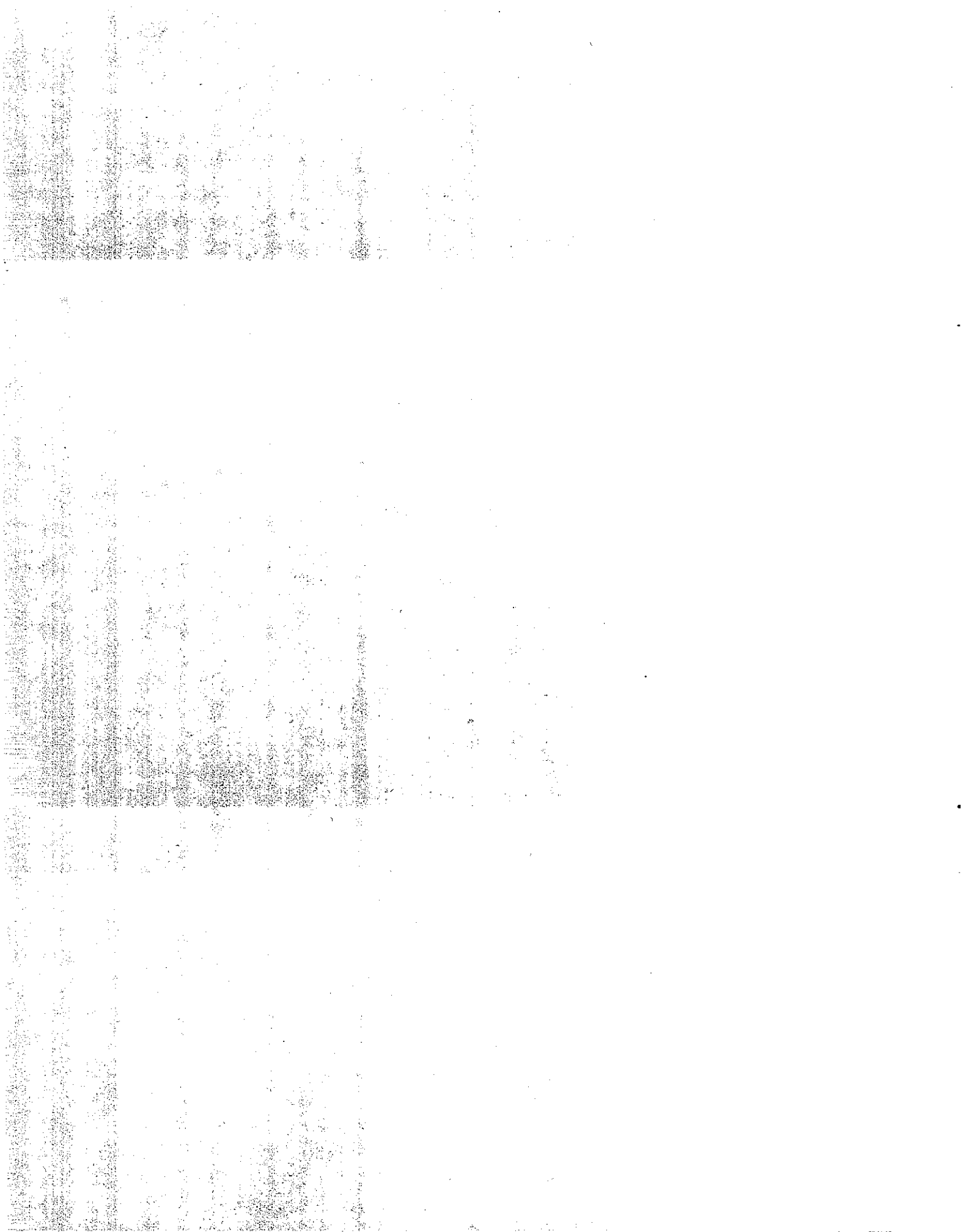
A computer program for this calculation as stated above is presented in Appendix E. Two examples of time-compression relationships calculated using Wahls' method are presented in Figure 16. It may be seen that the calculated curve generally agrees well with the laboratory curve especially within the secondary portion. When this method is applied to the field time-settlement relationship, the accuracy depends on, not only the accuracy of the laboratory data, but also how closely the field loading conditions are simulated in the laboratory. As shown in Figures 14 and 15, the time-settlement relationship is largely affected by the pressure-increment ratio.





APPENDIX D

HANSEN'S METHOD OF TIME-SETTLEMENT  
CALCULATION



APPENDIX D

HANSEN'S METHOD OF TIME-SETTLEMENT CALCULATION

Approximate equations of calculating the time-compression relationship of simultaneous primary and secondary compressions were developed in this method. The method involves first plotting the laboratory time-compression curve in a combined square-root time and logarithm of time plot. As shown in Figure D-1, the early part of the time-compression data is plotted on a square-root time scale so that an approximate linear relationship is established. Then the compression curve is continued to a logarithmic time scale to obtain an approximately linear relationship in the secondary range. These two parts are combined such that the two straight lines will intersect at, or at least in the vicinity of, the boundary line between the square-root time and the logarithm time scales.

The time-compression curve thus obtained will give three quantities,  $t_c$ ,  $E_c$ , and  $E_s$  as shown in Figure D-1 and are defined as below.

$t_c$  = time in minutes, at the intersection of two straight lines.

$E_c$  = compression in percent at  $t_c$ .

$E_s$  = compression in percent between  $t_c$  and the tangential intersection of the time-compression curve and secondary slope.

An approximate model law is proposed by Hansen for the whole process of primary and secondary compression based on the above quantities. The mathematical expression for this model law is,

$$E_t = \frac{E_s}{\left[ \frac{H^6/C_s^3}{(t \log_{10} \frac{t+5t_s}{5t_s})^3} + \frac{1}{(\log_{10} \frac{t+t_s}{t_s})^6} \right]^{1/6}}$$

in which  $E_t$  is the compression in percent at time  $t$  and  $H$  is the longest drainage path of compressible soil layer.

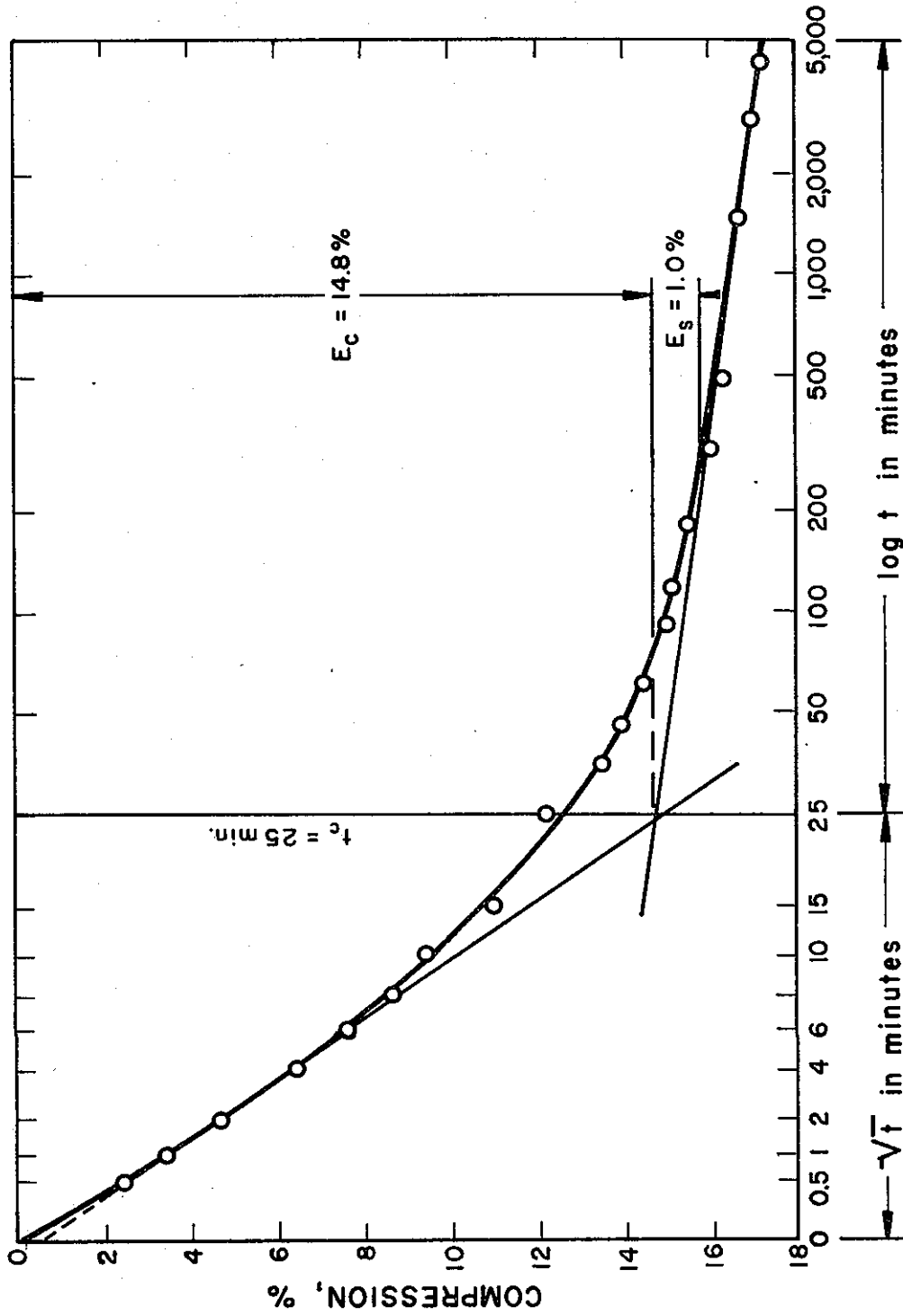
$$C_s \doteq \frac{A}{t_c} \left[ \frac{BH}{A + 0.297} \right]^2 \dots \dots \dots (D-2)$$

where

$$B \doteq \frac{E_c}{E_s} - \left[ \frac{1.1E_s}{E_c} \right]^2 - 0.13 \dots \dots \dots (D-3)$$

Figure D-1

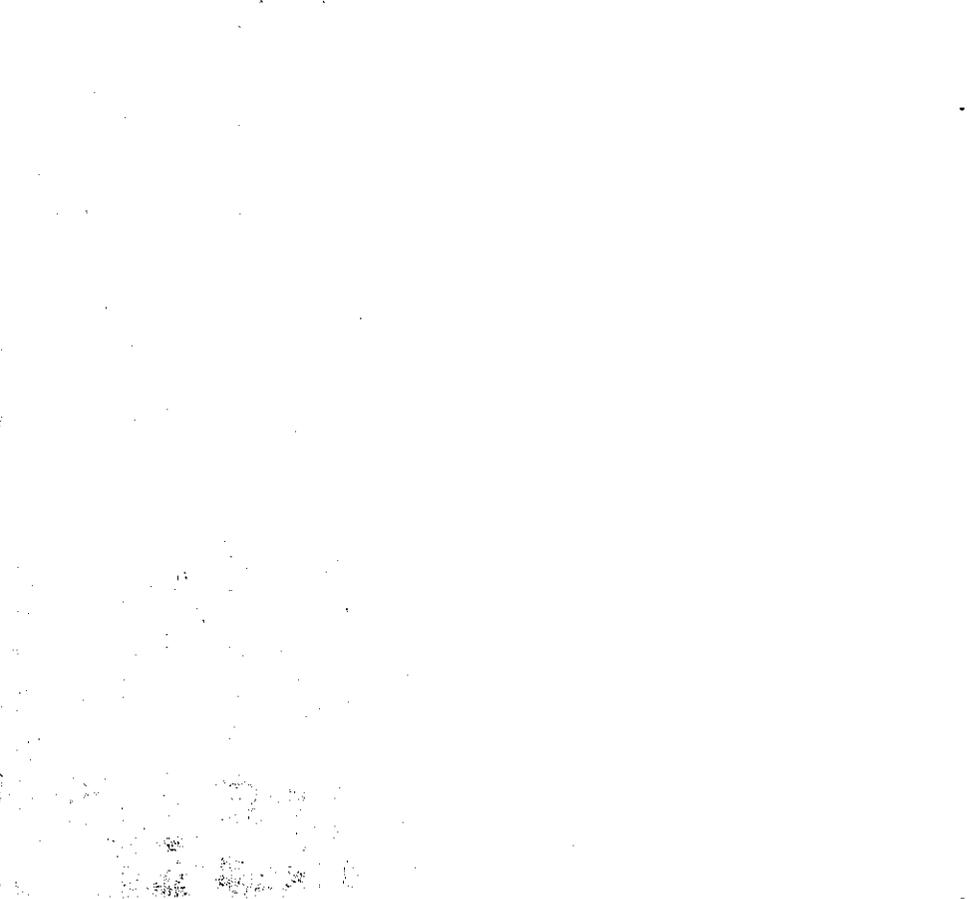
TIME-COMPRESSION PLOT IN HANSEN'S METHOD



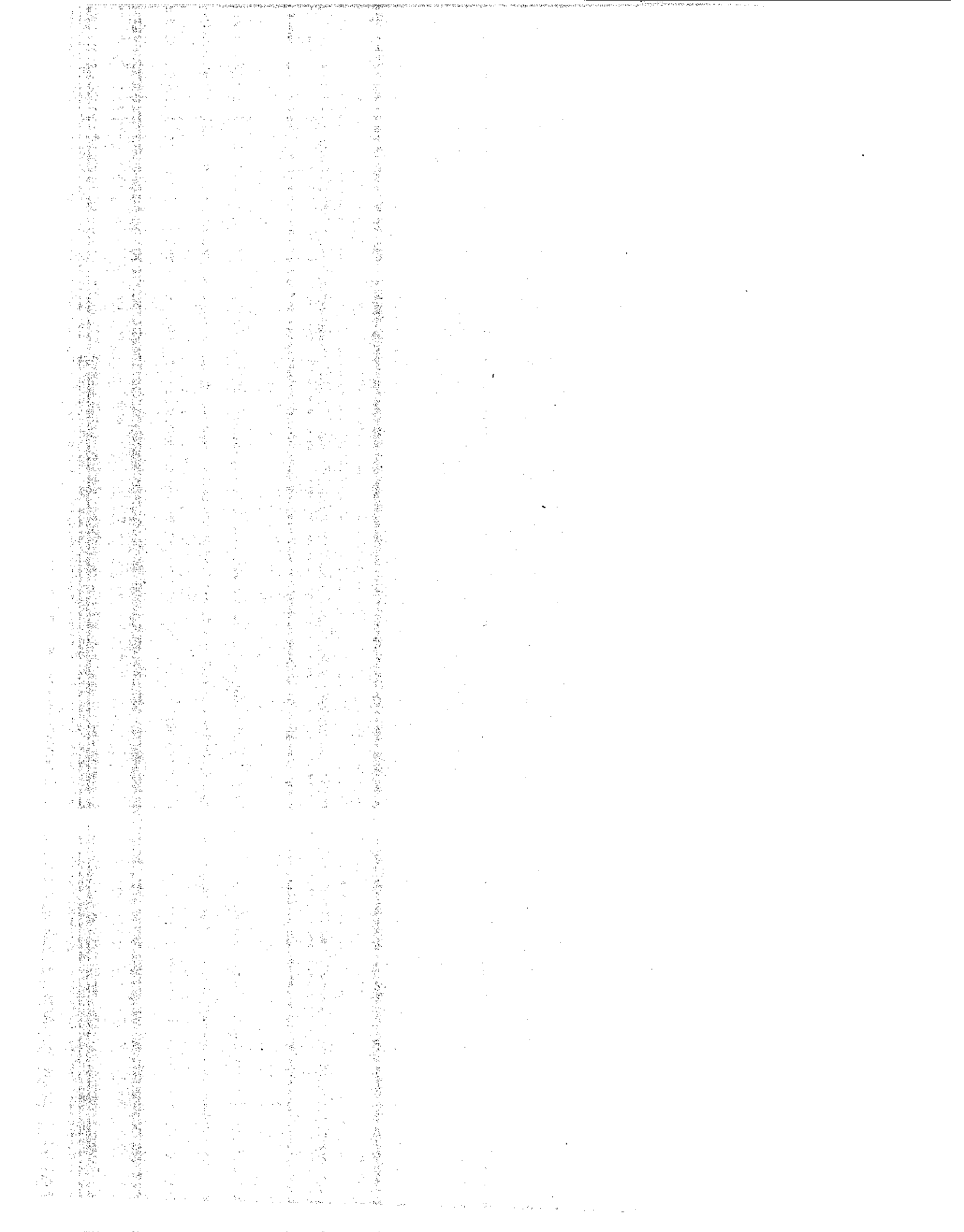
$$t_s = \frac{t_c}{10^B} \dots\dots\dots (D-4)$$

$$A = \log_{10} \left[ \frac{t_c + 50 t_s}{50 t_s} \right] \dots\dots\dots (D-5)$$

One of the basic assumptions in this method is that the compressions observed in a consolidation test will represent the actual properties of the compressible soil layer. Therefore, in applying this method to calculate the field time-settlement relationship, the actual field loading condition must be closely simulated in the laboratory to produce the type of time-compression curve that would represent the field behavior. In the curve fitting of laboratory data, the accuracy depends solely on the accuracy in determining the characteristic soil constants,  $E_s$ ,  $t_s$  and  $C_s$ . An example of this curve fitting is shown in Figure 16.







## APPENDIX E

### COMPUTER PROGRAM HONZ

#### 1. General

HONZ is a BASIC program that calculates field time-settlement relationship by Wahls' method, using laboratory consolidation data. This computer program is written for use in a General Electric Time Sharing system with a terminal directly connected to GE265 computer. HONZ reads from a BASIC file the input data including laboratory time-compression relationship, field data such as drainage condition, initial void ratio, total estimated change in void ratio due to the imposed load, and the total thickness of compressible clay layer. In its output, HONZ prints out the total estimated settlement, coefficient of secondary compression, and field time-settlement relationship. The required procedure to produce the computer input data and their entering in the analysis are described in the following sections. Sample input and output of the analysis and listing of the computer program are also included. The laboratory time-compression curve used in this sample analysis and the resulting field time-settlement curve are presented in Figure E-1 and Figure E-2, respectively.

#### 2. Laboratory Time-Compression Curve

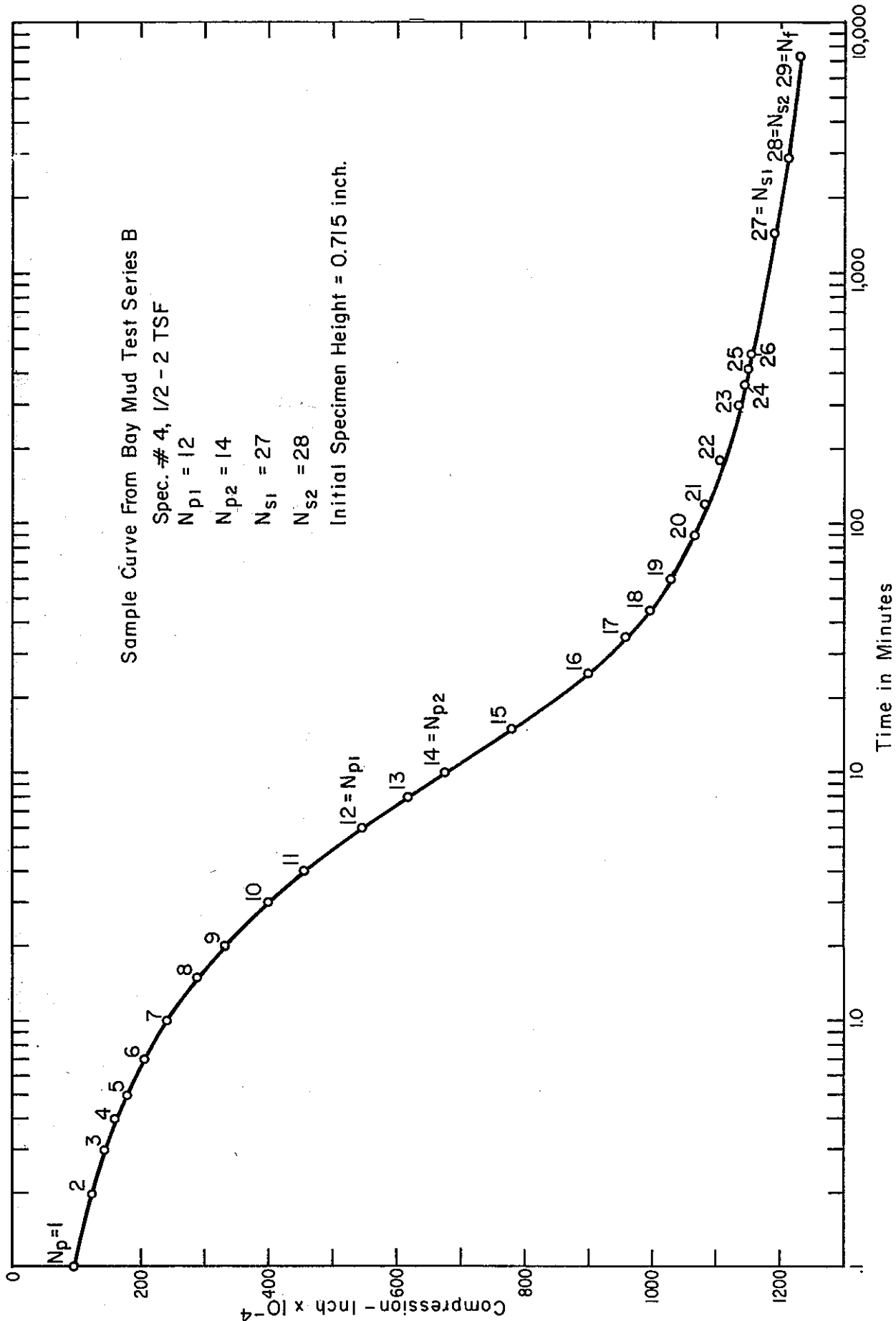
In proposed Wahls' method of settlement analysis, the laboratory time-compression relationship is used directly to predict the field behavior of settlement.

- (1) An undisturbed soil sample is subjected to a standard consolidation test up to the step where the effective pressure on the laboratory sample is equal to the effective overburden pressure in situ.
- (2) An incremental load equal to the field embankment loading is applied to the laboratory sample either instantaneously or in such a manner simulating the time-dependent field loading process. Sufficient time should be allowed for measurement of secondary compressions.
- (3) Plot laboratory time-compression curve in a five-cycle semi-log paper. A smooth log time-compression curve should be obtained from laboratory data such that linear portions of both primary and secondary ranges are defined. This time-compression curve at various time readings is then numbered for entering in the computer analysis (See Figure E-1). The following points are needed to be marked out.

$N_1 = 1$ , first point at time of 0.1 minute.

Figure E-1

LABORATORY TIME - COMPRESSION CURVE FOR WAHL'S METHOD COMPUTER ANALYSIS



$N_2 = 2$ , second point at time of 0.2 minute.

$N_3 = 3$ , third point at time of 0.3 minute.

$N_4 = 4$ , fourth point at time of 0.4 minute.

$N_{p1}$  = number indicating the first point in primary compression to be used in Casagrande construction.

$N_{p2}$  = number indicating the second point in primary compression to be used in Casagrande construction.

$N_{s1}$  = number indicating the first point in secondary compression to be used in Casagrande construction.

$N_{s2}$  = number indicating the second point in secondary compression to be used in Casagrande construction.

$N_f$  = total number of entry points in time-compression curve.

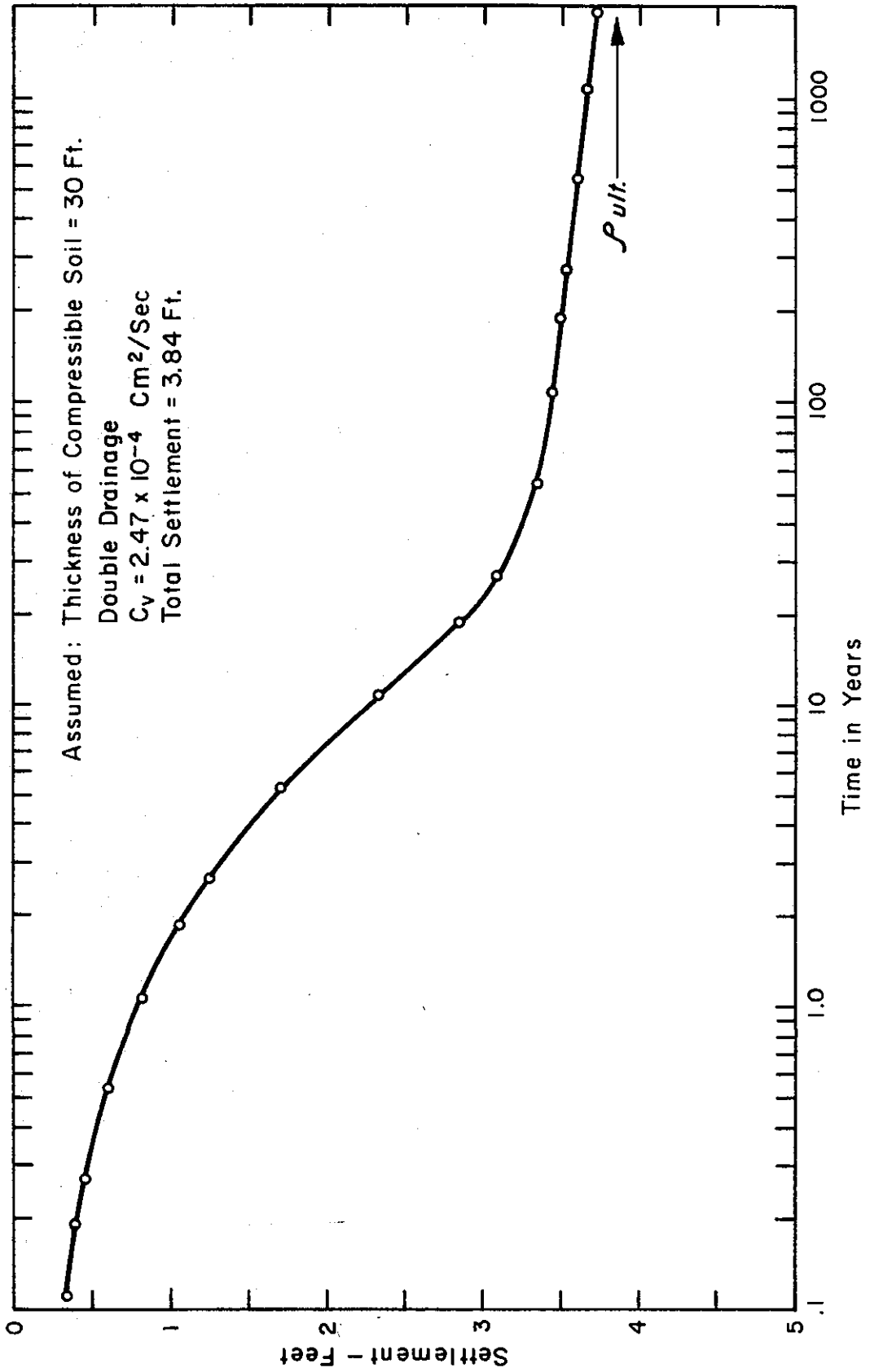
- (4) The maximum number of entries for the above time-compression relationship is 35.
- (5) The initial specimen thickness, and the coefficient of consolidation are required in the analysis. The value of  $C_v$  may be adjusted based on field conditions, such as layered system, before entry in the input. When more than one laboratory time-compression curve is available, an average time-compression curve and  $C_v$  value may be used.
- (6) Only those time-compression curves that resemble Wahls' type I curve may be used in this analysis. In a normally consolidated clay, a pressure-increment ratio of one or greater usually will give such a curve.

### 3. Evaluation of Field Data

- (1) The field drainage condition and layered system must be clearly defined to produce a reliable time-settlement prediction. If there exists a multiple-layer system for compressible soils, the time-settlement may be calculated for each layer separately using representative soil samples for consolidation test and the results superimposed.
- (2) The field void ratio change for the load increment is equal to the void ratio change in laboratory specimen in step (2) in the preceding section if the field loading is simulated in the laboratory test. The void ratio

Figure E-2

FIELD TIME-SETTLEMENT RELATIONSHIP  
CALCULATED USING WAHL'S METHOD, DATA IN FIGURE E-1





HONZ

1 DATA .197,0,.1975,.1,.198,.2,.2,.265,.202,.3,.205,.34,.209,.4  
2 DATA .212,.45,.2135,.55,.2125,.6,.21,.63,.205,.67,.195,.715,.18,.8  
3 DATA .001,.0357,.0221,.002,.0505,.0336,.004,.0735,.0502  
4 DATA .007,.0935,.0689,.01,.1114,.084,.02,.1598,.1225,.04  
5 DATA .2257,.1776,.07,.2985,.238,.1,.3562,.2867,.2,.5041,.4088  
6 DATA .4,.6973,.5756,.7,.8559,.7451,1,.9313,.8684,2,.9942  
7 DATA 1.1363,4,1,1.4307,7,1,1.6804,10,1,1.8353,20,1,2.1363  
8 DATA 40,1,2.4374,70,1,2.6804,100,1,2.8353,200,1,3.1363  
9 DATA 400,1,3.4353,700,1,3.67

100 FILES FIL1

| 110: | DAYS    | YEARS    | PERCENT<br>COMPRESSION | SETTLEMENT<br>IN FEET |
|------|---------|----------|------------------------|-----------------------|
| 130: | #####.# | #####.## | #####.##               | ###.##                |

| 140: | PTS | TIME<br>(MIN.) | COMP.<br>(.0001 INCH) |
|------|-----|----------------|-----------------------|
| 160: | ### | #####.##       | #####.##              |

170 DIMT(35),C(35),R(35),U(14),V(14),X(24),Y(24),Z(24),P(24)

180 DIMA(24),B(24)

190 READ#1,PS,DS,N1,N2,N3,N4,E1,H,C,E2,D,H1

200 FOR I4=1 TO 8

210 PRINT

220 NEXT I4

230 PRINT TAB(28);"\*\*\* INPUT DATA \*\*\*"

240 PRINT

250 PRINT

260 PRINT TAB(21);"PROJECT NAME : ";PS

270 PRINT TAB(26);"DATE : ";DS

275 PRINT

280 PRINT

282 PRINT TAB(10);"THICKNESS OF COMPRESSIBLE SOIL LAYER = ";

283 PRINT TAB(50);H;"FT"

284 PRINT TAB(10);"INITIAL VOID RATIO = ";TAB(50);E1

286 PRINT TAB(10);"CHANGE IN VOID RATIO = ";TAB(50);E2

290 IF D>0 THEN 296

292 LET S\$="DO NOT KNOW"

294 GOTO 304

296 IF D>1 THEN 302

298 LET S\$="SINGLE"

300 GOTO 304

302 LET S\$="DOUBLE"

304 PRINT TAB(10);"DRAINAGE CONDITION = ";TAB(51);S\$

306 PRINT TAB(10);"COEFF. OF CONSOLIDATION = ";TAB(50);C;"CM<sup>2</sup>/SEC"

307 LET C=C\*60/(2.54\*12)<sup>2</sup>

308 PRINT

310 PRINT

312 PRINT TAB(16);"CONSOLIDATION TEST TIME-COMPRESSION DATA"

314 PRINT

316 PRINT USING I40

318 PRINT USING I50

320 PRINT

HONZ CONTINUED

```
330LETI=I+1
340READ#1,T(I),C(I)
350PRINTUSING160,I,T(I),C(I)
360IFEND#1THEN380
370GOTO330
380FORN=1TOI
390LETR(N)=C(N)*100/C(I)
400NEXTN
410LETC1=(R(N4)-R(N3))/(LOG(T(N4)/T(N3))/LOG(10))
420LETM1=(R(N2)-R(N1))/(LOG(T(N2)/T(N1))/LOG(10))
430LETB1=R(N4)-(C1*(LOG(T(N4))/LOG(10)))
440LETB2=R(N1)-(M1*(LOG(T(N1))/LOG(10)))
450LETB3=(B2-B1)/(C1-M1)
460LETB3=10*B3
470LETB4=((C1*B2)-(M1*B1))/(C1-M1)
480LETR1=2*R(1)-R(4)
490PRINT
500PRINTTAB(10);"PRIMARY POINTS";TAB(45);N1;TAB(50);N2
510PRINTTAB(10);"SECONDARY POINTS";TAB(45);N3;TAB(50);N4
680LETC2=C1/(B4-R1)
690IFC2<.8THEN730
700PRINT
710PRINT"R A T I O I S G R E A T E R T H A N 0.8"
720GOTO1380
730LETR2=R1+(B4-R1)/2
740LETT2=(R2-B2)/M1
750LETT2=10*T2
760FORJ=1TO14
770READU(J),V(J)
780NEXTJ
790FORJ=2TO14
800IFC2>V(J)THEN870
810LETU1=U(J)-U(J-1)
820LETV1=V(J)-V(J-1)
830LETV2=V(J)-C2
840LETU2=U(J)-(V2*U1/V1)
850LETT9=T2/U2
860GOTO880
870NEXTJ
880LETL4=H*E2/(1+E1)
900LETC4=C1*C(N)/(H1*10000)
905LETC4=INT(C4*100+.5)/100
920FORJ=1TO24
930READX(J),Y(J),Z(J)
940NEXTJ
950LETI9=I9+1
960LETT5=T(N)/T9
970IFT5>=4THEN1010
980PRINT
990PRINT" T I M E C H O S E N I S L E S S T H A N 4"
```

HONZ CONTINUED

```
1000GOTO1330
1010LETR4=R(N)-R1
1020LETH3=.8353+LOG(T5)/LOG(10)
1030LETC6=C1*H3
1040LETA1=R4-C6
1050LETA2=A2+A1
1060IFI9=3THEN1035
1070LETN=N-1
1080GOTO950
1085LETA2=A2/3
1090FORM1=1T015
1100PRINT
1110NEXTM1
1120PRINTTAB(23);"*** OUTPUT OF RESULTS ***"
1122 PRINT
1124 PRINT
1126 PRINTTAB(21);"PROJECT NAME : "; P$
1128 PRINTTAB(26); "DATE : ";D$
1130 PRINT
1132 PRINT
1134PRINTTAB(10);"TOTAL ESTIMATED SETTLEMENT = ";
1135PRINTTAB(50);INT(L4*100+.5)/100;"FT"
1136PRINTTAB(10);"COEFF. OF SECONDARY COMPRESSION = ";TAB(50);C4;"PCT"
1138 PRINT
1140 PRINT
1142 PRINTTAB(22);"TIME SETTLEMENT RELATIONSHIP"
1144 PRINT
1146 PRINTUSING110
1150PRINTUSING120
1160PRINT
1180IFD<>0THEN1210
1190LETD1=1
1200GOTO1220
1210LETD1=D
1220FORJ=1T024
1230LETA5=A2*Y(J)
1240LETA6=C1*Z(J)
1250LETP(J)=R1+A5+A6
1260IFP(J)>=100THEN1320
1270LETA(J)=(H/D1)*2*X(J)/(C*1440)
1280LETA7=A(J)/365
1290LETB(J)=L4*P(J)/100
1300 PRINTUSING130,A(J),A7,P(J),B(J)
1310NEXTJ
1320IFD<>0THEN1350
1330LETD=2
1340GOTO1090
1350FORI4=1T06
1360PRINT
1370NEXTI4
1380END
```

\*\*\* INPUT DATA \*\*\*

PROJECT NAME : BAYMUD,B-4,.5-2  
 DATE : JUNE 1, 1970

THICKNESS OF COMPRESSIBLE SOIL LAYER = 30 FT  
 INITIAL VOID RATIO = 2.05  
 CHANGE IN VOID RATIO = .39  
 DRAINAGE CONDITION = DOUBLE  
 COEFF. OF CONSOLIDATION = .000247 CM<sup>2</sup>/SEC

CONSOLIDATION TEST TIME-COMPRESSION DATA

| PTS | TIME (MIN.) | COMP. (.0001 INCH) |
|-----|-------------|--------------------|
| 1   | .10         | 95.0               |
| 2   | .20         | 124.0              |
| 3   | .30         | 144.0              |
| 4   | .40         | 160.0              |
| 5   | .50         | 180.0              |
| 6   | .70         | 208.0              |
| 7   | 1.00        | 243.0              |
| 8   | 1.50        | 291.0              |
| 9   | 2.00        | 333.0              |
| 10  | 3.00        | 401.0              |
| 11  | 4.00        | 456.0              |
| 12  | 6.00        | 547.0              |
| 13  | 8.00        | 620.0              |
| 14  | 10.00       | 676.0              |
| 15  | 15.00       | 783.0              |
| 16  | 25.00       | 902.0              |
| 17  | 35.00       | 958.0              |
| 18  | 45.00       | 997.0              |
| 19  | 60.00       | 1028.0             |
| 20  | 90.00       | 1064.0             |
| 21  | 120.00      | 1082.0             |
| 22  | 180.00      | 1108.0             |
| 23  | 300.00      | 1134.0             |
| 24  | 360.00      | 1142.0             |
| 25  | 420.00      | 1150.0             |
| 26  | 480.00      | 1155.0             |
| 27  | 1440.00     | 1190.0             |
| 28  | 2880.00     | 1213.0             |
| 29  | 7220.00     | 1234.0             |

PRIMARY POINTS 12 14  
 SECONDARY POINTS 27 28

\*\*\* OUTPUT OF RESULTS \*\*\*

PROJECT NAME : BAYMUD, B-4, .5-2  
 DATE : JUNE 1, 1970

TOTAL ESTIMATED SETTLEMENT = 3.84 FT  
 COEFF. OF SECONDARY COMPRESSION = 1.02 PCT

TIME SETTLEMENT RELATIONSHIP

| DAYS     | YEARS   | PERCENT<br>COMPRESSION | SETTLEMENT<br>IN FEET |
|----------|---------|------------------------|-----------------------|
| 9.8      | .03     | 5.36                   | .21                   |
| 19.6     | .05     | 6.59                   | .25                   |
| 39.2     | .11     | 8.50                   | .33                   |
| 68.6     | .19     | 10.18                  | .39                   |
| 97.9     | .27     | 11.67                  | .45                   |
| 195.9    | .54     | 15.70                  | .60                   |
| 391.8    | 1.07    | 21.20                  | .81                   |
| 685.6    | 1.88    | 27.27                  | 1.05                  |
| 979.5    | 2.68    | 32.09                  | 1.23                  |
| 1959.0   | 5.37    | 44.42                  | 1.70                  |
| 3918.0   | 10.73   | 60.58                  | 2.32                  |
| 6856.5   | 18.78   | 74.04                  | 2.84                  |
| 9794.9   | 26.84   | 80.71                  | 3.10                  |
| 19589.9  | 53.67   | 87.29                  | 3.35                  |
| 39179.8  | 107.34  | 89.56                  | 3.44                  |
| 68564.6  | 187.85  | 91.11                  | 3.50                  |
| 97949.4  | 268.35  | 92.07                  | 3.53                  |
| 195898.8 | 536.71  | 93.93                  | 3.60                  |
| 391797.6 | 1073.42 | 95.80                  | 3.67                  |
| 685645.8 | 1878.48 | 97.30                  | 3.73                  |
| 979493.9 | 2683.55 | 98.26                  | 3.77                  |